National Library of Canada
Acquisitions and Bibliographic Services Branch
395 Wellington Street
Ottawa, Ontario
K1A 0N4

Bibliothèque nationale du Canada
Direction des acquisitions et des services bibliographiques
395, rue Wellington
Ottawa (Ontario)
K1A 0N4

Your file Votre référence

Our file Notre référence

NOTICE

The quality of this microform is heavily dependent upon the quality of the original thesis submitted for microfilming. Every effort has been made to ensure the highest quality of reproduction possible.

If pages are missing, contact the university which granted the degree.

Some pages may have indistinct print especially if the original pages were typed with a poor typewriter ribbon or if the university sent us an inferior photocopy.

Reproduction in full or in part of this microform is governed by the Canadian Copyright Act, R.S.C. 1970, c. C-30, and subsequent amendments.

AVIS

La qualité de cette microforme dépend grandement de la qualité de la thèse soumise au microfilmage. Nous avons tout fait pour assurer une qualité supérieure de reproduction.

S'il manque des pages, veuillez communiquer avec l'université qui a conféré le grade.

La qualité d'impression de certaines pages peut laisser à désirer, surtout si les pages originales ont été dactylographiées à l'aide d'un ruban usé ou si l'université nous a fait parvenir une photocopie de qualité inférieure.

La reproduction, même partielle, de cette microforme est soumise à la Loi canadienne sur le droit d'auteur, SRC 1970, c. C-30, et ses amendements subséquents.

Canada

Chemical Kinetics Analysis and Modelling of Hydrogen-Air Combustion Process in Supersonic Combustion Ramjet

Xia Chen

A Thesis

in

The Department

of

Mechanical Engineering

Presented in Partial Fulfillment of the Requirements
for the Degree of Master of Applied Science at
Concordia University
Montreal, Quebec, Canada

March 1996

National Library
of Canada

Acquisitions and
Bibliographic Services Branch

395 Wellington Street
Ottawa, Ontario
K1A 0N4

Bibliothèque nationale
du Canada

Direction des acquisitions et
des services bibliographiques

395, rue Wellington
Ottawa (Ontario)
K1A 0N4

Your file Votre référence

Our file Notre référence

ISBN 0-612-10830-9

Canada

ABSTRACT

Chemical Kinetics Analysis and Modelling of Hydrogen-air
Combustion processin Supersonic Combustion Ramjet
Xia Chen

An analytical study of H_2 - air combustion kinetic has been performed in this study. The study examines the effects of the initial conditions on the ignition time, reaction time and profiles of exhaust Calculations are made over a range of pressure from 0.2 to 10 atm, temperature from 850 to 2000K, Mach number from 0.1 to 10, and mixture equivalence ratio from 0 2 to 2.0. The detailed chemical reaction model includes 41 reactions with 8 species of the H_2 - air system The results indicate that the ignition time is nearly constant over a range of the equivalence ratio from 0.5 to 2.0. The change of Mach number makes the temperature - time history fall into two groups, one is supersonic combustion and the other is subsonic combustion In each group, the ignition time is independent of Mach number The effects of the initial temperature on the ignition time are indicated as a non - linear relation The results also indicate that the variation of the reaction time with the change of the initial temperature is nearly linear The relation between the reaction time and the initial pressure shows an exponential manner. This study also developed a quasi-global chemistry model of H_2-air system by using sensitivity analysis, and a global chemistry model of H_2-air system by using the steady-state approximations. By comparing the results of the detailed model, the quasi-global model is adequate for the calculation of the ignition time and reaction times by hydrogen - oxygen reactions in a constant pressure stream (about 0.5 to 6.0 atm at this study); and the errors for using this scheme to calculate the ignition and reaction times are about 10%. The global model developed in this study predicts the ignition and reaction times. Results obtained from the global model are in a reasonable agreement with those obtained from the detailed model and the quasi-global model.

ACKNOWLEDGEMENTS

The author would like to express her memory to her former supervisor Dr A J Saber for his constant encouragement, support, supervision and advice.

The author also wish to express her sincere gratefulness to her current supervisor Dr. S. Lin for his constant support, supervision at every stage of this study. The author would like to express her thanks to him for encouraging her to continuous her research after her former supervisor was killed.

The author would like to express her special thanks to Dr G. J. Gouw, Dr. G H Vatistas, Mr. P. Lawn, for their special support at the time she was in deep sorrow because of the tragedy of the death of her former supervisor.

The author acknowledges Dr. Hoa for his support and help. She also appreciates FCAR of Quebec government and CARA Committee of Concordia University for their financial support.

Finally, the author would like to express his heartfelt thankfulness to her husband, Zhenning Mao, for his constant source support, encouragement and pressure at the right moment.

TABLE OF CONTENTS

LIST OF FIGURES

LIST OF TABLES

NOMENCLATURE

A flow cross-sectional area.

A_j preexponential constant, cm^3-mol^{-1}-s^{-1} or cm^6-mol^{-2}-s^{-1}

$(A_j)_r$ value of A_j for a reference species as third body

a the speed of sound

a_{ij} relative third-body efficiency of species i in reaction j if the species is to be included as a third-body catalyst in the reaction

b_i body force of species i

c_p heat capacity of gas mixture at constant composition, energy/(mass-deg).

D diameter of cylindrical tube cross section, length units.

E flux vector in x coordinate direction

E_j activation energy of reaction j, cal/mole.

f fuel-air ratio

f_i mass fraction of species i

G_R Gibbs energy of reaction

G_i Gibbs energy of species i

H heat transfer coefficient, heat units/(length^2-sec-deg).

$(\Delta H_{298})_j$ molar heat of reaction at 298 K for the jth reaction proceeding in the forward direction, from left to right

h static enthalpy of gas mixture per unit mass, energy/ mass.

h_T total enthalpy per unit mass of flowing mixture, energy/mass.

K thermal conductivity of gas mixture heat units/(deg-length-sec).

K_j or K_{eq} equilibrium constant of reaction j

k_j forward reaction rate of reaction j

k_{bj} backward reaction rate of reaction j

L_w perimeter of flow cross section, length units.

l number of chemical reactions

M mixture Mach number.

M_e Mach number in the plane of exhaust

M_w mixture molecular weight, g/mole.

m mixture mass flow rate, mass/sec.

m_a air flow rate, mass/sec.

m_f fuel flow rate, mass/sec.

m_{ij} the third body efficiency factor for species i in reaction.

M_{wi} molecular weight of species i

N number of reacting species in mixture, not including inert.

n_j temperature exponent in reaction j

n^{equ}_k equilibrium value

nr number of chemical reactions

ns number of chemical species

Pr Prandtl number.

p static pressure, force/area or atm.

Q heat transfer rate from reacting system, heat units/(length-sec)

Q_R heating value of the fuel

q heat flux

Re Reynolds number.

R universal gas constant, energy/(mole-K).

R_j forward molar rates of reaction j as given by law of mass action

R_{-j} reverse molar rates of reaction j as given by law of mass action

r_d, r_c and r_n stagnation pressure ratio defined by Eqs. (2.7), (2.8), (2.9)

S^{Ψ}_j fit sensitivity

S^r_j rth response sensitivity

s_i represents the ith species

T gas mixture temperature, K.

T_o initial temperature, K.

T_f film temperature for heat transfer computations, K.

T_w wall temperature, K.

T_{ig} ignition temperature, sec.

T_{eq} equilibrium temperature, K

T_{TR} total reaction temperature, K.

t time, sec.

u flight speed, length/time

u_e exhaust velocity, length/time

V linear flow velocity, length/time

V_i diffusion velocity vector of species i

W_i net production rate of species i, moles/(volume-sec).

w_i species production rate of species i

w_{ij} net rate of formation of species i by reaction j, mole/volume-sec.

X_i molar density of species i, called the concentration

x distance, length units.

y_{ri} realization of the rth response in the ith observation.

Γ engine thrust

γ specific heat ratio

η_j a vector of l response for jth reaction, i.e. expectation value η_{1j}, η_{2j}, ...η_{lj}

η_{ri} a vector of rth response in the ith observation

θ_j parameter of fit sensitivity

μ gas mixture viscosity, g/(cm-sec).

μ_i chemical potential of each mixture component.

ρ gas mixture density, mass/volume.

σ_i concentration of species i, moles/mass of mixture.

τ shear stress

τ_{ig} ignition time, sec.

τ_R reaction time, sec.

τ_{TR} total reaction time, sec.

υ_{ij} forward direction stoichiometric coefficient for species i in reaction j.

υ'_{ij} reverse direction stoichiometric coefficient for species i in reaction j.

υ_{ik} the stoichiometric coefficient of species i in reaction k

Ψ_j net reaction conversion rate of reaction j, mole-volume/mass^2-sec

Ω_j the third body efficiency factor for jth reaction.

ω_i molecular weight of species i

$\acute{\omega}_{ri}$ statistical weight corresponding to the ith observation of rth repose

ω_k the reaction rate

CHAPTER 1. INTRODUCTION

1.1 CONTEXT AND MOTIVATION

This is a part of the undergoing project of hydrogen-fuelled supersonic combustion ramjets (scramjets) study in Dr. A.J. Saber's Aerospace Propulsion Research Laboratory. There is an increasing interest in using H_2 as a fuel in advanced air-breathing propulsion systems such as the aerospace plane, supersonic standoff missiles, air-to-ground missiles, and target vehicles because it has the lowest molecular weight, the highest exhaust velocity for a given maximum temperature and a short ignition and reaction time relative to conventional hydrocarbon fuels. Optimum performance of these advanced systems requires accurate combustor design, which in turn requires knowledge of the fluid dynamics and combustion processes in scramjets. The objective of the project is to simulate the process in scramjet engine, and to obtain a model for the purpose of the combustor design. As the part of this project, the study here is to predict a optimum H_2/air combustion models that can be used in the simulation of complex process in scramjet engine

In general, for establishing a combustion model, there are three main areas of interest in regarding to development of a reliable theory which would predict the flow properties of a reacting mixture of hydrogen and air. First is the establishment of the individual chemical reactions which are significant in describing the overall system. Second, an experimental evaluation of the reaction rates for the individual reactions is necessary, and third, a solution to the combined chemical kinetic and

fluid dynamics equations using the results of the investigations cited above, along with experimental verification, is required. Among these three areas, the third one is the most complex step. There are some work has been done regarding the fluid dynamics modelling. The numbers of reports [Law, 1992] [Warnatz, 1979] [Russin, 1974] have been published concerning the experimental investigations. These works included discovering the overall effects of fuel injection, mixing, and reaction on the flow in sub-scale engine components. This dependence on empirical results is due to the complexity of the flow around fuel injectors in three-dimensional geometries, which are not readily treated analytically.

Most numerical solutions are restricted to two- or three-dimensional parabolic flow with equilibrium or simple finite-rate chemistry models of the H_2-air system In general, combustion is a spatially three-dimensional, highly complex physical-chemical process of transient nature Models are therefore needed that simplify a given combustion problem to such a degree that it becomes amenable to theoretical or numerical analysis but that are not so restrictive as to distort the underlying physics or chemistry. In particular, in view of worldwide efforts to conserve energy and to control pollutant formation, models of combustion chemistry are needed that are sufficiently accurate to allow confident predictions of flame structure.

Historically combustion chemistry was first described as a global one-step reaction in which fuel and oxidizer react to form a single product Even when detailed mechanism of elementary reactions became available, empirical one-step kinetics approximations were needed in order to make problems amenable to theoretical analysis. This situation began to change in early 1970s when computing facilities

became more powerful and more widely available, thereby facilitating numerical analysis of relatively simple combustion problem, typically one-dimensional flames, with moderately detailed mechanisms of elementary reactions.

However, even on the fastest and most powerful computers available today, numerical simulations of, say, laminar, steady, three-dimensional reacting flows with reasonably detailed and hence realistic kinetic mechanism of elementary reactions are not possible. Even worse than for laminar reacting flows are the prospects for the numerical simulation of turbulent combustion problems with reasonably detailed kinetics mechanisms of elementary reactions. This is where systematically reduced kinetics mechanism come in.

Not only are these mechanisms useful for realizing numerical simulations of laminar and turbulent flows under the variety of practically relevant operating conditions of combustion systems, they also open avenues for new theoretical approaches to analysis of combustion problems Detail chemical kinetics analysis of H_2-O_2 reaction can reveal the relations between the species, reactions, third-body efficiency, and varying initial conditions & boundary conditions which all effect ignition and reaction time. Combustion model of H_2-O_2 system that is used in the simulation of pollutant formation and ignition phenomena and in the study of chemically controlled extinction limits often combine detailed chemical kinetics with complicated transport phenomena. As the number of chemical species and the geometric complexity of the computational domain increases, the modelling of such system becomes computational prohibitive on even the largest supercomputer. The difficulty canters primarily on the number of chemical species and on the size of the different length scales in the problem.

If one can reduce the number of chemical species in a reaction network while still retaining the predictive capabilities of the mechanism, potentially larger problems could be solved with existing technology. In addition, current large scale problems could be moved to smaller workstation computers. The objective of this thesis is to do this simplification.

1.2 OBJECTIVES

There are two main objectives for this study. The first one is to establish the model of chemical kinetic for H_2/O_2 combustion process in scramject combustion chamber. This model contains all the chemical reactions that possibly occur in the process, we, therefore, call this model as the detailed chemical reaction model. Then combining with one-dimensional fluid dynamic equations, the effects of initial conditions and boundary conditions to the ignition and the reaction time, also the effects of the combustor operates in a subsonic mode at low Mach number and in a supersonic mode at high Mach number, the profiles of chemical species of the exhaust have been investigated.

The second objective is to obtain a reduced chemical reaction model which still remain the predictive capabilities of the mechanism comparing what we have from the first objective, in order to be used in the complex, multi-dimensional fluid dynamics model. The simplification study includes:

1) By using sensitivity analysis, we simplified the detailed chemical reaction model to the quasi-global model. The quasi-global model is the simplest model that we can get from using sensitivity analysis method. The comparison of the detailed mechanism with the quasi-global model is also involved in this step

2) Since the most reduced chemical reactions model for H_2/air combustion is what we expect to obtain, the systematic reducing mechanism method can be used to simplify the quasi-global model to two steps global model. It is very important to compare the the global model with the quasi-global model and the detailed chemical reaction model.

3) The comparison of the global and quasi-global model with the detailed model give us an idea of the working errors for the global and quasi-global model. The criteria for the reduced models has been given.

1.3 ORGANIZATION OF THE THESIS

The successive chapters of this thesis are:

--- Review of the related literature of supersonic combustion ramjet engine.

--- Review of the related literature of chemical kinetics, ignition time and reaction time of combustion process, sensitivity analysis and steady state approximation.

--- Description of chemical kinetics and fluid dynamics simulation of the combustion process in scramjet combustor.

--- Establishment of the detailed chemical reaction model of H_2/O_2 combustion process and chemical kinetics analysis of detailed mechanism and the investigation of the effects of the initial conditions and boundary conditions on the ignition time, reaction time and the profiles of the exhaust.

--- The simplification of the detailed model to the quasi-global using sensitivity

analysis and the comparison of the detailed model and the quasi-global model.

--- The simplification of quasi-global model to global model, and the comparison of the detailed, quasi-global and global model. The comparison of the present results and the exiting results.

---Conclusions.

CHAPTER 2. LITERATURE REVIEW OF SUPERSONIC COMBUSTION RAMJETS (SCRAMJETS) ENGINE

2.1 INTRODUCTION

This chapter is confined to a review of the principle of scramjet engine and working conditions. First we describe the construction of ramjet, this is the essential principle of the scramjet The ideal ramjet concept has been introduced. The figure of thermodynamic path of the fluid in an ideal ramjet is very helpful to determine the fluid dynamic model, and to analysis chemical kinetics. Second, two concepts, ramjet in supersonic flight and supersonic combustion ramjet, have been brought out. All kinds of running conditions have been mentioned. T difference between these two types of ramjet operation is indicated. All these reviews concern the concept of scramjet, as well as the operation conditions of supersonic combustion and study interests.

2.2 RAMJET ENGINE

The simplest of all air-breathing engines is the ramjet, with no need for turbomachinery, and maximum tolerance to the high-temperature operation and minimum mass-per-unit thrust at suitable flight Mach numbers. The ramjet engine is used to power fast aircrafts operates on a constant pressure cycle similar to the gas turbine cycle. A ramjet is characterized, however, by the fact that the pressure is produced by the dynamic action of the airflow, often known as the ram effect of the speed of aircraft. As shown in Figure 2.1 [Hill & Peterson, 1992], the ramjet

consists of a diffuser, a combustion chamber, and an exhaust nozzle. Air enters a diffuser, where it is compressed before it is mixed with the fuel and burned in the combustion chamber. The hot gases are then expelled through the nozzle by virtue of the pressure rise in the diffuser as incoming air is decelerated from flight speed to a relatively low velocity within the combustion chamber.

The gas dynamic compression process of a ramjet is followed by injection of fuel into the air stream and burning the fuel-air mixture internally in a combustion chamber, thereby raising the temperature of the products of combustion. A ramjet does not have the compressor and turbine. Consequently, the products of combustion of a ramjet are led directly to an expansion nozzle, producing a high velocity jet stream.

To understand the performance of the ramjet, it is helpful to perform a thermodynamic analysis of a simplified model. We assume that the compression and expansion process in the engine are reversible and adiabatic, and that the combustion process takes place at constant pressure The ideal ramjet is a most useful concept, however, since its performance is the highest that the laws of thermodynamics will permit, and is the limit that real engines will approach it and the irreversibilities can be reduced Using the station numbers of Fig.2.1, Fig 2.2 [Hill & Peterson, 1992] shows, on a temperature-entropy diagram, the processes of the air goes through in an ideal ramjet. The compression precess takes the air from its condition at station (a) isentropically to its stagnation state (02) at station (2). The combustion process is represented by a constant-pressure heat and mass addition precess (02) to (04) up to the maximum temperature T_{04} The exit nozzle expands the combustion products isentropically to the ambient pressure With isentropic compression and expansion process, and low-speed constant-pressure

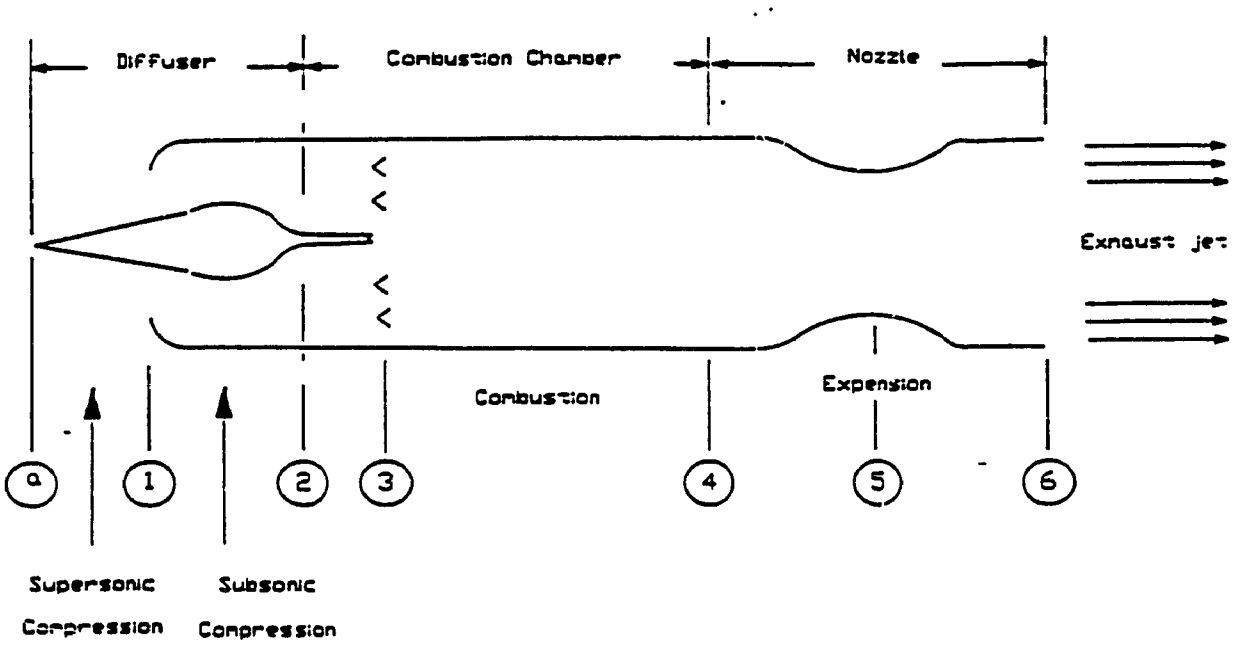

Figure 2.1 Schematic diagram of a ramjet engine

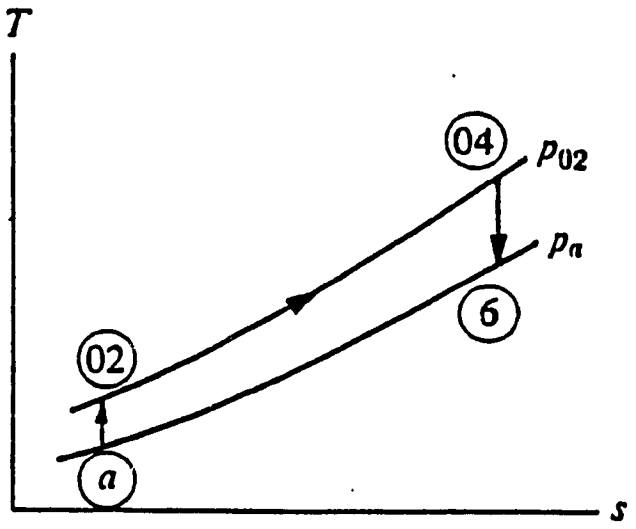

Figure 2.2 Thermal dynamic path of the fluid in an ideal ramjet

heat and mass addition, it follows that the stagnation pressure must be the constant throughout the engine. Therefore, $p_{0a} = p_{06}$. Here, P_{0a} and P_{06} are the stagnation pressure of state a and 6. The ideal engine thrust Γ may be obtained from Eq. (2.1):

$$\Gamma = m_a[(1+f)u_e - u)] \tag{2.1}$$

where m_a is air flow rate, f is the fuel-air ratio, u_e is exhaust velocity and u is the flight speed.

If we ignore the variations in fluid properties (R, γ) through the engine for this ideal case, then

$$\frac{p_{0a}}{p_a} = (1+\frac{\gamma-1}{2}M^2)^{\frac{\gamma}{(\gamma-1)}}, \frac{p_{06}}{p_e} = (1+\frac{\gamma-1}{2}M_e^2)^{\frac{\gamma}{(\gamma-1)}}$$

in which M is the flight Mach number and M_e is the Mach number in the plane of the exhaust.

Therefore, with the condition $p_e = p_a$, it is clear that

$$\frac{p_{0a}}{p_a} = \frac{p_{06}}{p_e}, M_e = M_a$$

Thus we can determine the exhaust velocity from

$$u_e = \frac{a_e}{a_a}u$$

where a is the speed of sound. Since $a = \sqrt{\gamma RT}$, then $a_e/a_a = \sqrt{T_e/T_a}$. However, for the case $M_e = M_a$, $T_e/T_a = T_{06}/T_{0a}$ and, since $T_{04} = T_{06}$, then

$$u_e = \sqrt{T_{04}/T_{0a}}\, u \tag{2.2}$$

The energy equation applied to the idealized combustion process, if we neglect the enthalpy of the incoming fuel, is

$$(1+f)h_{04} = h_{02} + fQ_R \tag{2.3}$$

where f is the fuel-air ration and Q_R is the heating value of the fuel. If the specific heat is assumed constant, then Eq. (2.3) may be solved for f in the form

$$f = \frac{(T_{04}/T_{0a}) - 1}{(Q_R/c_p T_{0a}) - T_{04}/T_{0a}} \tag{2.4}$$

Equations (2.1) and (2.2) may be combined to give the thrust per unit mass flow of air,

$$\frac{\Gamma}{m_a} = M\sqrt{\gamma R T_a}\,\left[(1+f)\sqrt{T_{04}/T_a}\,\left(1+\frac{\gamma-1}{2}M^2\right)^{-1/2} - 1\right] \tag{2.5}$$

where f is given by Eq. (2.4). The thrust specific fuel consumption is given by

$$TSFC = \frac{m_f}{\Gamma} = \frac{f}{\Gamma/m_a} \tag{2.6}$$

Figure 2.3 shows, for the ideal ramjet, the dependence of specific thrust and fuel-air ratio on flight Mach number and maximum temperature. The calculations are quite approximate, since:

1. The variations of the temperature of specific heat ratio have been neglected;
2. No frictional or shock losses have been allowed for;
3. No allowance has been made for dissociation of the combustion products.

Despite these approximations, however, Fig. 2.3 [Hill & Peterson, 1992] shows

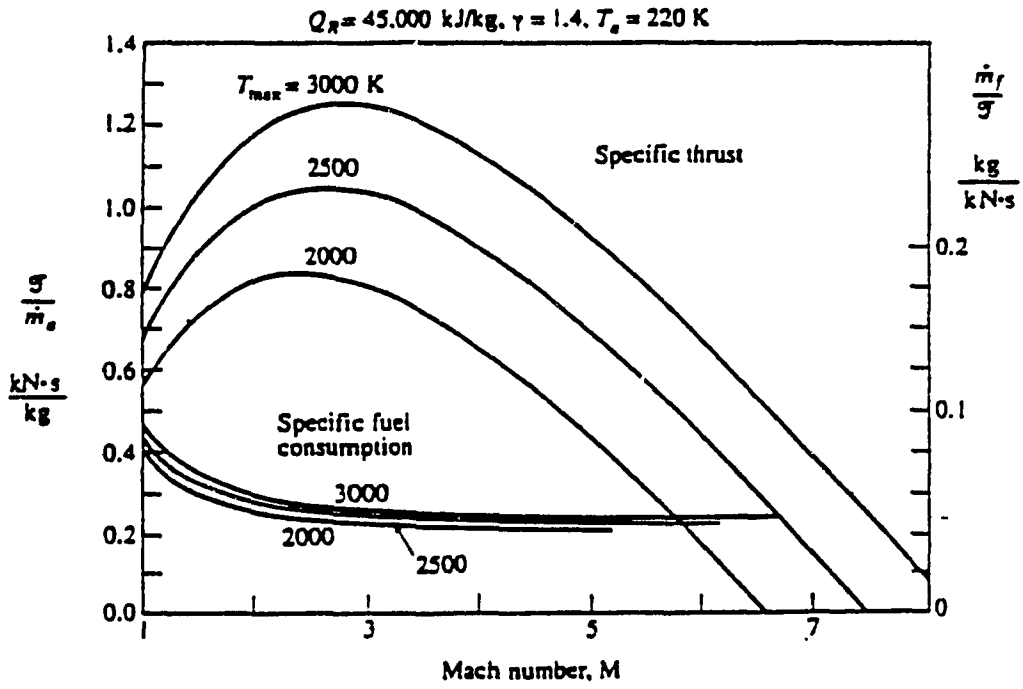

Figure 2.3 Ideal ramjet thrust and fuel consumption

qualitatively the same behaviour as that of the real ramjets, which require supersonic flight speed for acceptable specific thrust and reasonably low specific fuel consumption. Figure 2.4 [Hill & Peterson, 1992], which also applies to the ideal ramjet, shows that, though highest specific thrust is associated with a flight Mach number of about 2.6, Mach number well above 3 could provide much better range. Figure 2.4 shows the overall efficiency increasing sharply, while the specific thrust declines sharply, with increasing M. This is an example of a common result that the conditions of minimum fuel consumption (or maximum range) are quite different from those for which engine size per unit thrust is minimum. As the trends in Fig. 2.3 indicate, the thrust specific fuel consumption remains finite as the specific thrust approaches zero.

The propellant in a real ramjet, of course, suffers stagnation pressure losses as it flows through the engine. Figure 2.5 [Hill & Peterson, 1992] shows, on a T-s diagram, the effect of these irreversibilities on the processes of compression, burning, and expansion. The compression process, (a) to (02), is no longer isentropic, though the isentropic process is shown for comparison. The stagnation pressure at the end of the process is lower than it would be if the compression were isentropic. The performance of diffusers may be characterized by a stagnation pressure ratio r_d defined by

$$r_d = \frac{p_{02}}{p_{0a}} \tag{2.7}$$

It may be noted that a ramjet has no main engine rotating parts because neither a compressor nor a turbine are emplyed.

Similarly, the stagnation pressure ratio can be defined for the combustors r_c and

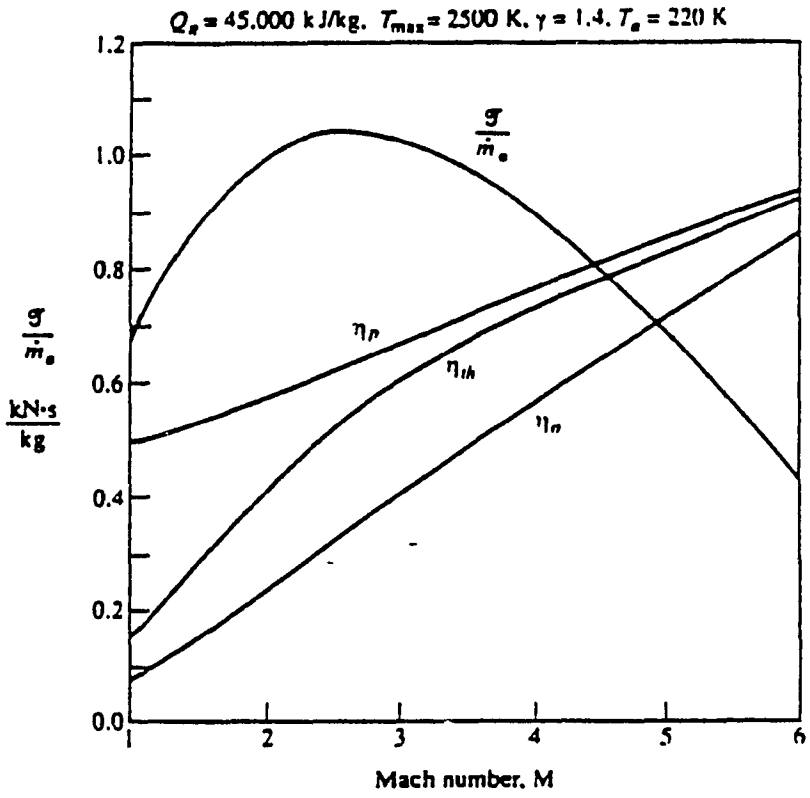

Figure 2.4 Ideal ramjet thrust and efficiencies

$$r_c = \frac{p_{04}}{p_{02}},$$

$$r_n = \frac{p_{06}}{p_{04}}.$$

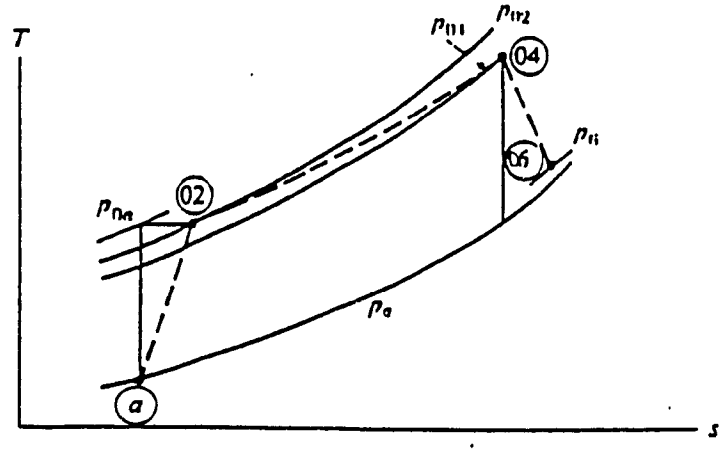

Figure 2.5 A T-s diagram showing aerodynamic losses incurred during ramjet processes

for the nozzle r_n as follows:

$$r_c = \frac{p_{04}}{p_{02}} \tag{2.8}$$

$$r_n = \frac{p_{06}}{p_{04}} \tag{2.9}$$

The overall stagnation pressure ratio is therefore

$$\frac{p_{06}}{p_{0a}} = r_d r_c r_n \tag{2.10}$$

Further, the actual exhaust pressure p_e or p_6 may not equal the ambient pressure p_a. However, for the isentropic flow, we have

$$\frac{p_0}{p} = \left(1 + \frac{\gamma - 1}{2} M^2\right)^{1/(\gamma - 1)} \tag{2.11}$$

$$M_e^2 = \frac{2}{\gamma - 1}\left[\left(1 + \frac{\gamma - 1}{2} M^2\right)\left(\frac{p_{06}}{p_{0a}}\frac{p_a}{p_e}\right)^{(\gamma-1)/\gamma} - 1\right]$$

where p_0 is the stagnation pressure. Thus, in terms of the component stagnation pressure ratios, we may write the exhaust Mach number as

$$M_e^2 = \frac{2}{\gamma - 1}\left[\left(1 + \frac{\gamma - 1}{2} M^2\right)\left(r_d r_c r_n \frac{p_a}{p_e}\right)^{(\gamma-1)/\gamma} - 1\right] \tag{2.12}$$

If heat transfer from the engine is assumed negligible (per unit mass of fluid), then the exhaust velocity is given by $u_e = M_e \sqrt{\gamma R T_e}$ or, in terms of the exhaust stagnation temperature,

$$u_e = M_e \sqrt{\gamma R T_{04} / \left(1 + \frac{\gamma - 1}{2} M_e^2\right)} \tag{2.13}$$

Since irreversibilities have no effect on stagnation temperatures throughout the engine, the fuel-air ratio necessary to produce the desired T_{04} is given by a modified form of Eq. (2.4):

$$f = \frac{(T_{04}/T_{0a}) - 1}{(\eta_b Q_R / c_p T_{0a}) - (T_{04}/T_{0a})}$$

where η_b is the combustion efficiency and $\eta_b Q_R$ is the actual heat release per unit mass of fuel. The thrust per unit airflow rate then becomes

$$\frac{\Gamma}{m_a} = [(1 + f) u_e - u] + \frac{1}{m_a}(p_e - p_a) A_e \tag{2.14}$$

or, if we use Eqs. (2.13) and (2.14),

$$\frac{\Gamma}{m_a} = (1 + f) \sqrt{\frac{2\gamma R T_{04}(m - 1)}{(\gamma - 1) m}} - M\sqrt{\gamma R T_a} + \frac{p_e A_e}{m_a}\left(1 - \frac{p_a}{p_e}\right), \tag{2.15}$$

in which

$$m = \left(1 + \frac{\gamma - 1}{2} M^2\right)(r_d r_c r_n \frac{p_a}{p_e})^{(\gamma - 1)/\gamma}$$

Again, the thrust specific fuel consumption is given by

$$TSFC = \frac{m_f}{\Gamma} = \frac{f}{\Gamma / m_a} \tag{2.16}$$

Figures 2.6 and 2.7 [Hill & Peterson, 1992] provide the result of the effects of aerodynamic losses by assuming loss coefficients $r_d = 0.7$, $r_b = 0.95$ and $r_n = 0.98$.

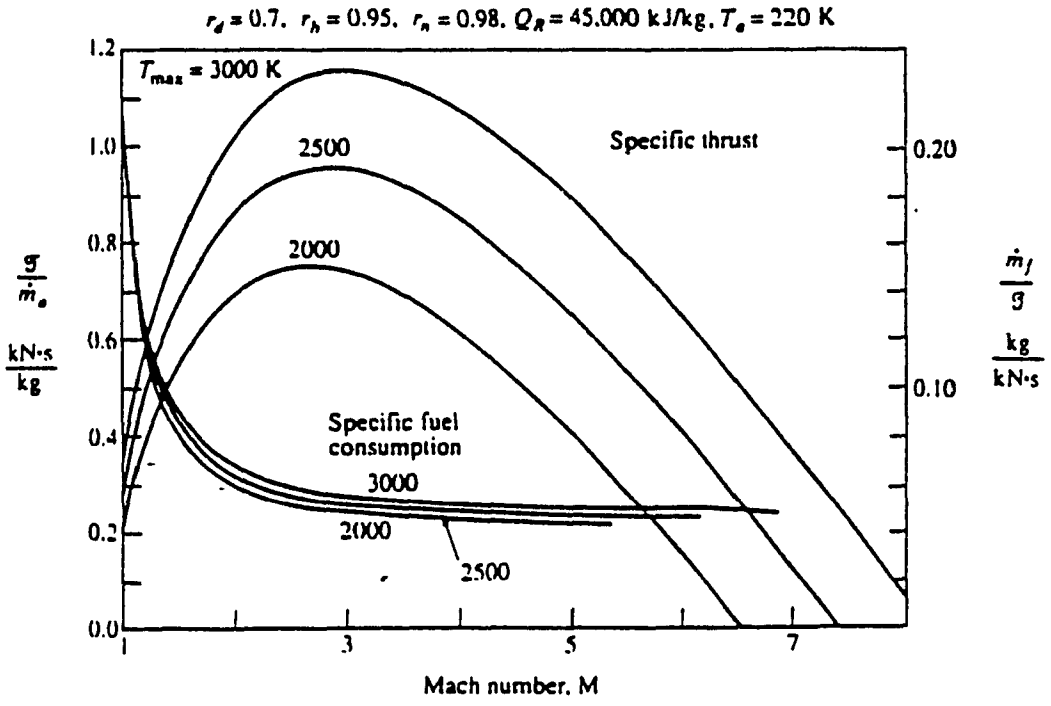

Figure 2.6 Ramjet thrust and fuel consumption

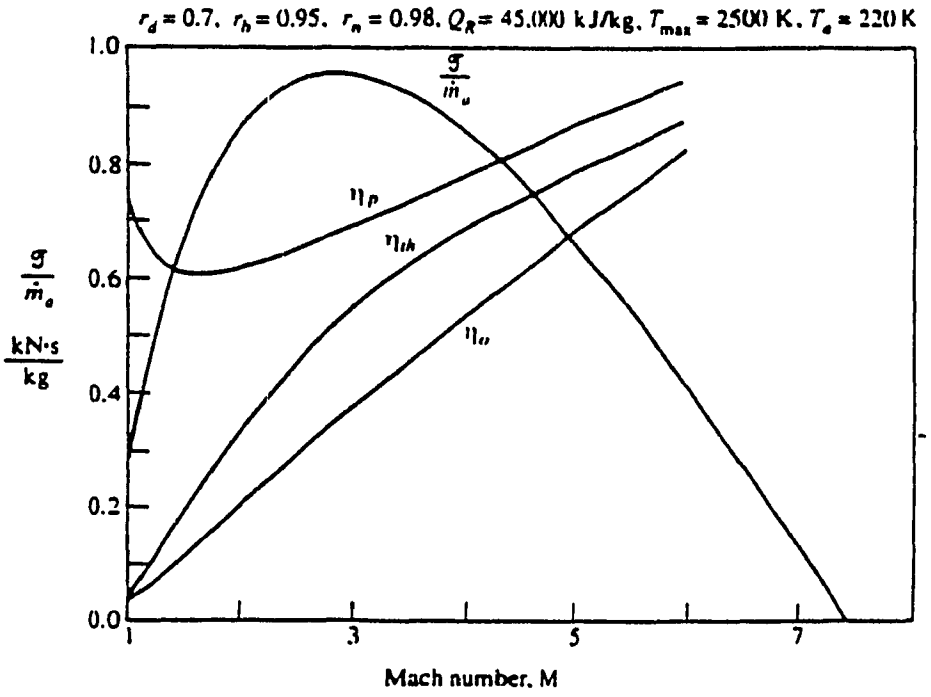

Figure 2.7 Ramjet thrust and efficiencies

Comparison of these with Figs. 2.3 and 2.4 shows less than 10% reduction in the maximum specific thrust and also in the specific fuel consumption.

It may be noted that a ramjet has no main engine rotating parts because neither a compressor nor a turbine are employed. There are some advantages gained by elimination of the rotating parts of an engine, most important of which is the limitation imposed on the maximum temperature of the cycle after the combustion. Higher temperatures are usually accompanied by an increase in thrust and efficiency. The significant drawback of a ramjet, however, is the complete dependability of the system on the ram air to produce the necessary compression, and consequently the engine can operate only if the aircraft maintains a sufficient flight speed.

2.3 SUPERSONIC COMBUSTION RAMJET (SCRAMJET) ENGINE

As we mentioned last section, the ramjet is most suitable for supersonic flight. Figure 2.1 is typical of supersonic ramjets that employ partially supersonic diffusion through a system of shocks. Since the combustion chamber requires an inlet Mach number of about 0.2 to 0.3, the pressure rise at supersonic flight speeds can be substantial. For example, for isentropic deceleration from $M = 3$ to $M = 0.3$, the static pressure ratio between the ambient and the combustion chamber would be about 34. The temperature in combustion chamber will be raised to perhaps 3000 K before the products of combustion expand to high velocity in the nozzle.

The materials used at present for the walls of combustion chambers and nozzles cannot tolerate temperature much above 1200 K, but they can be kept much cooler

than the main fluid stream by a fuel-injection pattern that leaves a shielding layer of relatively cool air next to the wall. This relatively high peak-temperature limit of the scramjet allows operation at high flight Mach number. As the Mach number is increased, however, the combustion chamber inlet temperature also increases, and at some limiting Mach number it will approach the temperature limit set by the wall materials and cooling methods. For example, at a flight Mach number of 8 in an atmosphere at 225 K, the stagnation temperature is about 2500 K.

At temperatures above 2500 K, dissociation of the combustion products may be significant [Hill & Peterson, 1992]. At high temperature the major effect of further fuel addition is further dissociation rather than actual temperature rise.

For the conventional ramjet of supersonic flight, there is a limiting Mach number about 6, above which the temperature of the air entering the combustor is so high that combustion cannot be completed. Most of the chemical energy of combustion is no useful transferred into dissociation reactions that an expansion do not provide the exhaust velocity needed for satisfactory ramjet performance. To avoid this problem, substantial research has been, and is still being, focused on supersonic combustion ramjet (scramjet). The difference between this and conventional ramjet of supersonic flight is that combustion is to take place in a supersonic steam. Fuel must be injected in supersonic air stream and must mix and burn in a millisecond or so. Conventional fuels do not ignite quickly enough, and gaseous hydrogen seems the most likely candidate

For ramjet there is no such limitation based on compressor aerodynamics Also it is possible to have the combustion in a supersonic stream without prohibitive aerodynamics losses. The SCRAMJET denotes the supersonic combustion ramjet,

a concept that has been under study for flight Mach number so high that the ramjet should be superior to the turbojet in propulsion efficiency. The SCRAMJET concept has not yet found application in a flight

As we have seen, the losses associated with subsonic ramjet combustion can be substantial. If ramjets are to be applied to supersonic or hypersonic flight, additional problems arise because of extremely high temperature at the entrance to the combustion chamber. This not only makes vehicle cooling very difficult, but it leads to severe combustion loss due to dissociation. Figure 2.8 [Hill & Peterson, 1992] shows the air temperature reached after adiabatic deceleration from a high-altitude ambient temperature of 220 K and from flight Mach number M to a chamber pressure of either 1 or 10 atm. For hypersonic flight (e.g , for M > 8) the temperature of the air in the chamber is quite dependent on the pressure: for the higher pressure, there are the less dissociation and the higher temperature of the mixture. The temperature of the combustion products is likewise pressure dependent For a combustion pressure of 10 atm and a flight Mach number of 10, there is no temperature rise due to combustion; all of the combustion energy, so to speak, is absorbed by dissociation One sees the strange result that, at sufficiently high Mach number, the temperature of the combustion products can be lower than that of the incoming air. Consideration of the speed with which the fuel and air can be converted into dissociation products may show that there is sufficient residence time in the combustion chamber to approach equilibrium [Billig, 1971]

The balance between a conventional ramjet and supersonic combustion ramjet (scramjet) lies in the efficiencies of the processes and the initial temperature level (i.e., Mach number). Also at these high temperatures, the degree of equilibrium

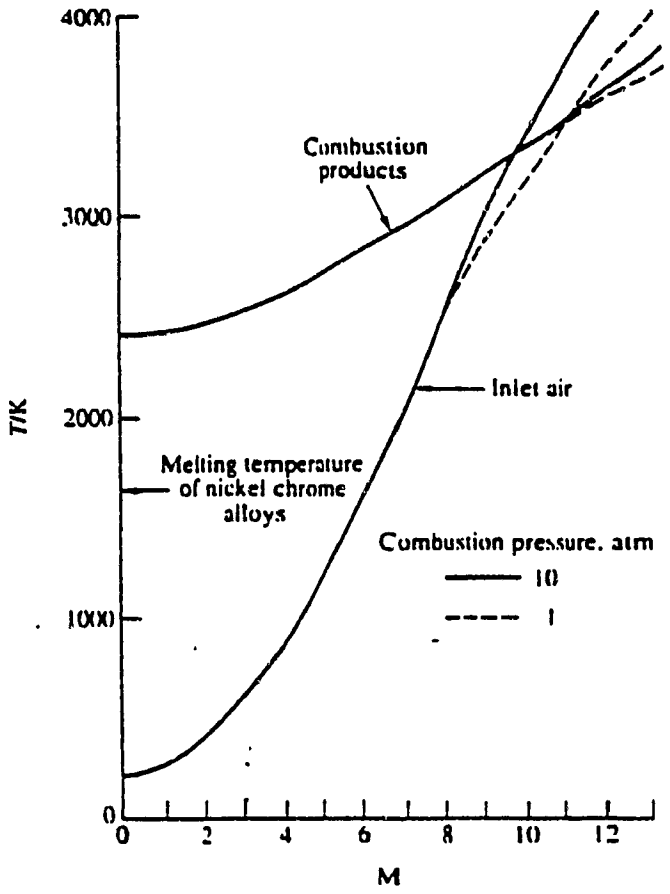

Figure 2.8 Hypersonic ramjet with kerosine fuel; adiabatic compression and combustion, equivalence ratio, ϕ=1.0

flow can have a considerable effect and this is dependent on the fuel. It should be noted that subsonic combustion necessitates a decrease of static pressure (for acceleration of the flow) and that the supersonic combustion implies an increase of static pressure (deceleration of the flow) but both are accompanied by loss of stagnation pressure. The stagnation pressure and the temperature at the beginning of expansion then indicate the output available. The temperature is very much higher, which promotes very fast combustion. The pressures too are high, again helpful. Nevertheless, a fuel like hydrogen is almost a necessity and so is a flow situation which permits some stability.

2.4 CONCLUSION

This chapter introduces the principle of the ramjet, and supersonic flight ramjet and supersonic combustion ramjet. Some important working conditions had been indicated. Some researchers have proposed the concept of the supersonic combustion ramjet as a way to avoid the dissociation loss as well as the stagnation pressure losses associated with deceleration in supersonic-to-subsonic inlets. With supersonic combustion, fluid temperature is relatively low, and this decreases the dissociation loss because dissociation depends on static rather than stagnation temperature. Wall heat transfer, in contrast, depends essentially on the stagnation temperature, so the wall-cooling problem is not removed by employing supersonic combustion. All those discussions reminded in this study specially the effects of Mach number range and effects of high temperature for the dissociation must be tested very carefully.

CHAPTER 3. LITERATURE REVIEW

3.1 INTRODUCTION

The principle of the supersonic combustion ramjet has been presented in the last chapter. The operating conditions of supersonic combustion have been indicated. In this chapter, the review concerns the chemical kinetics analysis and modelling of combustion processes, especially some publications with H_2/air combustion and supersonic combustion.

Chemical kinetic modelling is an important tool in the analysis of many combustion systems. The use of detailed kinetic models in the interpretation of fundamental kinetics experiments in the reactors is widespread. Recently these models, coupled with fluid mechanical models, have become valuable in helping to understand complex phenomena in practical combustion devices. One-dimensional models can be the best used to look in detail at the coupling of a very large number of species interactions in a geometry that is an approximation to reality. So the first review is the principle of chemical reaction mechanisms and kinetics. Also the governing equations for fluid dynamics and thermodynamics model have been reviewed.

The chemical kinetics analysis for combustion system concerns the ignition and reaction time study. The review of the different definitions of the ignition and reaction time have been introduced from the previous research. Because of the increasing interest in using H_2 as a fuel in advanced air-breathing propulsion systems, some aspects of H_2/air combustion have been extensively studied. The reviews summarize those studies.

The last, and also most important part of this reviews are reduced kinetic mechanisms for combustion system. While the kinetics of combustion are relatively well established, incorporation of full kinetic schemes in multidimensional flow models is computational prohibitive. Therefore, a systematically simplified model of kinetics is needed that retains the important kinetic steps. The sensitivity analysis and steady state approximations as the asymptotic limit methods have been introduced.

3.2 CHEMICAL KINETICS AND MODELLING OF COMBUSTION PROCESSES

Detailed study of the rates and mechanisms of combustion reactions has not been in the mainstream of combustion research until the recent recognition that further progress in the optimizing combustion performance can only be done with fundamental understanding of combustion kinetics and chemistry. This has become apparent at a time when our understanding of the kinetics, at least of small-molecule combustion, and our ability to model combustion processes on large computers have developed to the point that real confidence can be placed in the results.

3.2.1 CHEMICAL KINETICS

Given that combustion reactions occur as a consequence of a number of elementary reactions taking place in the burning gas, how does one identify these and find out how each of them contributes to the progress of the reaction? These questions

belong to the area of chemistry known as reaction kinetics [Gardiner, 1984].

Chemical kinetics involve knowing how fast each elementary reaction proceeds. In kinetics one defines the rate of a chemical reaction as the derivative of the concentration of a product species with respect the reaction involved. Each chemical reaction can be written in the general form

$$\sum_{i=1}^{N} \upsilon_{ij} S_i \underset{k_{-j}}{\overset{k_j}{\rightleftharpoons}} \sum_{i=1}^{N} \upsilon'_{ij} S_i \qquad (3.1)$$

where υ_{ij} is the forward direction stoichiometric coefficient for species i in reaction j. υ'_{ij} is the reverse direction stoichiometric coefficient for species i in reaction j, s_i represents the ith species. The forward reaction rate k_j is given by

$$k_j = A_j T^{n_j} \exp\left(\frac{-E_j}{RT}\right) \qquad (3.2)$$

where n_j is the temperature exponent in reaction j. E_j is the activation energy for reaction j. The backward reaction rate is determined from k_j and the equilibrium constant K_j:

$$k_{bj} = \frac{k_j}{K_j} \qquad (3.3)$$

The total molar species formation rate W_i is defined as

$$W_i = \sum_{j=1}^{J} W_{ij} = \sum_{j=1}^{J} (\upsilon'_{ij} - \upsilon_{ij})(R_j - R_{-j}) \qquad (3.4)$$

where W_{ij} is the net rate of formation of species i by reaction j (moles/volume-sec). R_j and R_{-j} are the forward and reverse molar rates of reaction j as given by law of

mass action. We shall now define a net reaction conversion rate Ψ_j [Bittker et al, 1971] as an indication of the amount of change due to each reaction that occurs in the mixture. The form of Ψ_j depends on the type of reaction.

$$\Psi_j = \frac{R_j - R_{-j}}{\rho^2}$$

Then

$$W_{ij} = \rho^2 (\nu'_{ij} - \nu_{ij}) \Psi_j \tag{3.5}$$

Three types of reversible chemical reactions are considered in general computer program [Oran & Boris,1981]. Type 1 - Bimolecular shuffle reaction:

$$S_1 + S_2 \rightleftharpoons S_3 + S_4 \tag{3.6}$$

with

$$R_j - R_{-j} = k_j \rho^2_{molar} \left(\sigma_1 \sigma_2 - \frac{\sigma_3 \sigma_4}{K_j} \right)$$

Then

$$\Psi_j = k_j \left(\sigma_1 \sigma_2 - \frac{\sigma_3 \sigma_4}{K_j} \right) \tag{3.7}$$

Type 2 - Three-body recombination:

$$\Omega + S_1 + S_2 \rightleftharpoons S_3 + \Omega \tag{3.8}$$

(where Ω can be any species present in the scheme)

For some problems the heat release is an important consideration. In these

$$\Psi_j = k_j \Omega_j (\rho \sigma_1 \sigma_2 - \frac{\omega_3}{K_j}) \tag{3.9}$$

In this equation, Ω_j is the third-body efficiency factor for the jth reaction defined as

$$\Omega_j = \sum_{i=1}^{N} m_{i,j} \sigma_i \tag{3.10}$$

and $m_{i,j}$ is the third-body efficiency factor for species i in reaction j. This factor is a correction to the preexponential factor A_j in the rate

$$m_{i,j} = \frac{(A_j)_{s_i}}{(A_j)_r} \tag{3.11}$$

where $(A_j)_r$ is the value of A_j for a reference species as third body. The calculations presented in this thesis, all third-body efficiencies are referenced to N_2. Except as listed at the bottom of Table 5.2, all third-body efficiencies are 1.0.

Type 3 - Two-body dissociation:

$$\Omega + s_3 \underset{k_{ij}}{\overset{k_j}{\rightleftharpoons}} s_1 + s_2 + \Omega \tag{3.12}$$

with

$$\Psi_j = k_j \Omega_j (\sigma_3 - \frac{\rho \sigma_1 \sigma_2}{K_j}) \tag{3.13}$$

situations a useful quantity is the net energy conversion rate for the jth reaction defined as

$$(\Psi_R)_j = \Psi_j (\Delta H_{298})_j \qquad (3.14)$$

where $(\Delta H_{298})_j$ is the molar heat of reaction at 298 K for the jth reaction proceeding in the forward direction, from left to right.

In combustion processes, the concentration of a given species may be affected by a large number of elementary reactions. The rate of change of each species concentration must therefore be found by adding up the effects of all elementary reactions producing the species and subtracting the effects of all elementary reactions that consume it. Thus the solution we arrive at are restricted and depended on both the time and the physical conditions. A model of combustion system may serve as an excellent way to test our understanding of the interactions of the individual physical processes which control the behaviour of a reactive flow system

3.2.2 DETAILED MODELLING OF SUPERSONIC REACTING FLOW

Modelling supersonic combustion system has its own particular problems because of the strong interaction between the energy released from chemical reactions and the dynamics of fluid motion. Release of chemical energy generates gradients in temperature, pressure, and density. These gradients in turn influence the transport of mass, momentum, and energy in the system. Currently, one-dimensional models can be best used to look in detail at the coupling of a very large range number of species interactions in a geometry that is an approximation to reality.

Governing Equations

A common feature of all combustion calculations summarized in this thesis is the use of essentially the same governing equations. They are the one-dimensional balance equations for continuity, momentum, energy and the chemical species. The Navier-Stokes, energy, and species continuity equations governing multiple species undergoing chemical reaction have been derived by Williams [1978]. The terms used in these and subsequent equations are defined in the Nomenclature. The governing equations are given by

Continuity:

$$\frac{\partial \rho}{\partial t} + \nabla \cdot (\rho V) = 0 \tag{3.15}$$

Momentum:

$$\frac{\partial (\rho V)}{\partial t} + \nabla \cdot (\rho V V) = \nabla \cdot \tau + \rho \sum_{i=1}^{ns} f_i b_i \tag{3.16}$$

Energy:

$$\frac{\partial (\rho E)}{\partial t} + \nabla \cdot (\rho V E) = \nabla \cdot (\tau \cdot V) - \nabla \cdot q + \rho \sum_{i=1}^{ns} f_i b_i (V + V_i) \tag{3.17}$$

Species continuity:

$$\frac{\partial (\rho f_i)}{\partial t} + \nabla \cdot (\rho V f_i) = w_i - \nabla \cdot (\rho f_i V_i) \tag{3.18}$$

If there are ns chemical species, then i = 1, 2, ..., (ns - 1) and (ns - 1) equations must be solved for the species f_i . The final species mass fraction f_{ns} can be found by conservation of mass since

$$f_{ns} = \sum_{i=1}^{ns} f_i = 1$$

Thermodynamics Model

To calculate the required thermodynamic quantities, the specific heat for each species is first defined by a fourth-order polynomial in temperature:

$$\frac{c_{pi}}{R} = a_i + b_i T + c_i T^2 + d_i T^3 + e_i T^4 \qquad (3.19)$$

The coefficients are found by a curve fitting of the data tabulated in [McBride et all, 1963]. Knowing the specific heat of each species, the enthalpy of each species is then found [Drummond, 1982], also the total internal energy is computed.

To determine the equilibrium constant for each chemical reaction being considered, first, the Gibbs energy of each of the species must be found. For a constant-pressure process, first, c_p/T from Eq. (3.19) is integrated over temperature to define the entropy of the species and then resulting expression is integrated again over temperature to obtain a fifth-order polynomial in temperature for the Gibbs energy of each species. The Gibbs energy of reaction is then calculated as the difference between the Gibbs energy of the product and reactant species:

$$\Delta G_{R_j} = \sum_{i=1}^{ns} \nu'_{ji} G_i - \sum_{i=1}^{ns} \nu_{ji} G_i \qquad j = 1,2,...,nr \quad (3.20)$$

The equilibrium constant for each reaction can then be found from [Kanury, 1982]

$$K_{eq_j} = (1/(RT))^{\Delta n} \exp[-\Delta G_{R_j}/(RT)] \qquad (3.21)$$

where Δn is the change in the number of moles when going from reactants to

products. R is the universal gas constant.

Chemistry Models

The reacting gas system is assumed to contain j finite-rate reactions, all of which may be expressed as Equation (3.1). The rate of chemical reactions is often defined by using the Arrhenius law. A modified form of the Arrhenius law usually is employed when modelling supersonic combustion. It is given by Equation (3.2). The rate of change of the mass fraction of the ith chemical species in the jth reaction, represented by Eq. (3.1), can be expressed as [Kanury, 1982]:

$$\left(\frac{dw_i}{dt}\right)_j = K_j \frac{\omega_i}{\rho}(\nu'_{i,j} - \nu_{i,j}) \prod_{i=1}^{I} \left(\frac{w_i \rho}{\omega_i}\right)^{\nu_{ij}} \left(\rho \sum_{i=1}^{I} \frac{a_{i,j} w_i}{\omega_i}\right)^{\nu_{I+1,j}} \qquad (3.22)$$

The last term in this equation accounts for the homogeneous catalysts, say M, in third-body reactions. The index $a_{i,j}$ is the relative third-body efficiency of species i in reaction j if the species is to be included as a third-body catalyst in the reaction, but is zero if that species is to be excluded. The quantity $\nu_{I+1,J}$ is also an index and is equal to unity for all third-body reactions. For bimolecular reactions, $\nu_{I+1,j}$ is zero for all values of $a_{i,J}$ set equal to unity.

The total rate of change of the mass fraction of the ith species in the reacting gas mixture is obtained by summation over all j reactions; that is,

$$\frac{dW_i}{dt} = \sum_{j=1}^{j} \left(\frac{dw_i}{dt}\right)_j \quad (i = 1, 2, \ldots I) \qquad (3.23)$$

where the summation includes both forward and reverse reactions. The set of equations to be solved includes the I differential equations indicated by Equation (3.23), along with Equations (3.15)-(3.22) and (3.2). The unknowns are reduced to

W_1, W_2, .. W_I and T, ρ, K_j. The initial values of the mass fractions and temperature are specified at the entrance of the combustor so that a forward integration of this set of equations can be carried out along the length of the combustor by use a modified Runge-Kutta scheme.

3.3 CHEMICAL KINETIC SCHEME OF H_2/AIR COMBUSTION

The elementary reactions in the mechanism of H_2 oxidation have been extensively studied and documented. Although the more detail studies are hydrocarbon oxidation system. The H_2 oxidation system, in fact, is much smaller than the hydrocarbon oxidation one, but the same reaction steps are also essential for the combustion of the hydrocarbon oxidation. [Smooke,1991].

Initially, there are some studies concerning the different scale of H_2/air chemical kinetic scheme, such as Pergament [1963] described the H_2/O_2 combustion system with 8 reactions involving 6 species. Erickson and Klieb [1970] studied H_2/O_2 constant pressure combustion and established a chemical kinetics model including 13 reactions with 8 species. Evans and Schexnayder [1986] also established the chemical kinetics model for H_2/O_2 combustion with 18 reactions and 7 species, and Correa and Mani [1980] studied H_2/O_2 chemical kinetics model with 9 reactions and 7 species.

Based on the chemical kinetic theory, for a chemistry reaction scheme, more reactions it contains, more precise the model is. Baulch et al [1972] had introduced most detailed scheme for H_2/O_2 and $H_2/O_2/N_2$ kinetics. These two tables have been listed in Appendix 1, Table I and Table II, respectively.

3.4 IGNITION TIME AND REACTION TIME OF SUPERSONIC COMBUSTION

For supersonic combustion engine design, the ignition and reaction time of H_2 /air combustion are very important parameters. The studies aims to get these values, and analysis the effects for these two values.

Ignition time

The ignition time, also known as ignition delay or induction time τ_{ig} is the time required for rapid build up of the free radicals and atoms with very little heat release. Three definitions of ignition time have been used in previous research [Schott, 1960] [Momtchiloff et al, 1962]:

(1) the time for concentration of OH to reach 5×10^{-9} mol/cm3,

(2) the time at the end of the constant exponential growth of OH mass fraction,

(3) the time taken to reach a temperature at ignition Tig of

$$T_{ig}=0.05(T_{eq}-T_o)+T_o \tag{3.24}$$

The ignition time given by definition (1) was used only for comparison with the experimental data by Slack, and Grillo [1977]. It was observed that the ignition times given by definition (2) and (3) are approximately the same over a wide range of pressure and temperature.

Reaction time

The total reaction time τ_{TR} is defined as the time taken to reach a temperature T_{TR} where [Schott. 1960],

$$T_{TR}=0.95(T_{eq}-T_o)+T_o \tag{3.25}$$

Reaction time is then defined as,

$$\tau_R = \tau_{TR} - \tau_{ig} \tag{3.26}$$

The ignition-time results from this calculation are therefore presented using equation (3.24).

3.5 SYSTEMATICALLY REDUCTION OF KINETIC MECHANISMS

As the number of chemical species and reactions of the computational domain increases, the modelling of detailed chemical kinetics with complicated transport phenomena becomes computational prohibitive on even the largest supercomputer. If one can reduce the number of species in a reaction network while still retaining the predictive capabilities of the mechanism, potentially larger problems could be solved with existing technology. Reduced mechanisms for combustion modelling are useful for at least two applications:

1. they reduce the computational effort in numerical calculations of flames by replacing a number of differential equations for intermediate species- those that are assumed as being in steady state-by algebraic relations;
2. they allow to study the flame structure by asymptotic methods and by that help to identify the relatively few kinetic parameters that mainly influence global properties such as the burning velocity or extinction strain rates.

Although the concept of reducing a chemical reaction mechanism (both in the number of species and reaction) has been known by chemists for some time , it is only within the last few years that it has been applied with considerable success to combustion systems As discusses by Peters [1991], the first applications of

these ideas were surprisingly, not to hydrogen-air systems which is considered a much simpler flames that first showed the full potential of the methodology, but rather to hydrocarbon flames. Previous attempts for hydrogen flames had been discouraging mainly for two reasons: first, the level of radicals as candidates for the steady state approximation in these flames is too high to justify such an assumption. Secondly, since only a small portion of the total number of species in the hydrogen-air system could be assumed in steady state, the gain in reducing the numerical effort out rules the algebraic and numerical complications involved.

Since the mid-1980s research in this area has increased dramatically. However, not only are these mechanisms useful for realizing numerical simulations of laminar and turbulent flows under the variety of practically relevant operating conditions of small-scale and large-scale combustion systems, they also open avenues for new theoretical approaches to analysis of combustion problems. The first mechanisms were published in the 1980s for pre-mixed and non-premixed methane flames [Peters, Kee, 1987] [Bilger et al, 1990], and, shortly thereafter, they were used in asymptotic and numerical analysis [Williams, 1988]. In these "early years" from 1985 to 1988 a number of research groups focused attention on methane flames because these flames provided a good testing ground for the development of strategies that are useful in the systematic reduction of detailed kinetic mechanisms to only a few kinetic steps. In particular, workshops on the derivation of reduced kinetic mechanisms for methane flames were held in Sydney in 1987, in Yale in 1988, and in La Jolla at UCSD in 1989. During the 1990 workshop in Cambridge (HK) it emerged that the first "learning period" was over [Peters, 1991].

For entering these details, some general aspects of reduction strategy shall be presented. These concern the basis of sensitivity analysis that for simplifying the

[illegible] those which contribute the most for the system, and the basis of the steady state assumption in terms of the magnitude of the formation and consumption rates, the choices that lead to a particular global reaction mechanism, and the consequences of a truncation of some steady state relations will be addressed below.

3.5.1 SENSITIVITY ANALYSIS

In a detailed chemistry model not all the reactions "contribute' equally to the chemical history, and hence to the model fit. On the contrary, some of them may contribute significantly, some marginally, and some not at all. To indicate which reaction contributes significantly, and remove the irrelevant reactions from the detailed chemistry model, the sensitivity analysis will be used.

Frenklach [1984] has described the sensitivity analysis in combustion system. In order to do this systematically, the parameter (θ_j) of fit sensitivity has been introduced;

$$S^{\Psi}_{j}=\frac{\partial\Psi(\theta)}{\partial\theta_j} \quad (3.27)$$

and the rth response sensitivity of parameter θ_j

$$S^{r}_{j}=\frac{\partial\eta_j}{\partial\theta_j} \quad (3.28)$$

Note that the fit sensitivity and response sensitivity are interrelated, as can be demonstrated in the case of the weighted least squares, when

$$\Psi(\theta)=\sum_{r,j}\omega_{rj}(y_{rj}-\eta_{rj})^2 \quad (3.29)$$

repose, and y_{ri} is realization of the rth response in the ith observation.

$$\frac{\partial \Psi(\theta)}{\partial \theta_j} = -2\sum_{r,i} \omega_{ri}(y_{ri} - \eta_{ri})\left(\frac{\partial \eta_r}{\partial \theta_j}\right)_i \tag{3.30}$$

These sensitivities provide numerical measures for the contribution of the jth reaction when θ_j is associated with the parameter of the corresponding rate expression, namely, with rate constant K_j for the isothermal case or with the preexponential factor A_j for the nonisothermal model. It is more convenient to deal with non-dimensional, or logarithmic, measures of sensitivities [Bukhman, 1969; Frank, 1978; Gardiner, 1977]. Thus the rth logarithmic response sensitivity of rate constant K_j is given by

$$LS^r_j = \frac{\partial \ln \eta_r}{\partial \ln K_j} = \frac{k_j}{\eta_r}\frac{\partial \eta_r}{\partial K_j} \tag{3.31}$$

which measures the relative change in response η_r with respect to the relative change in rate constant K_j.

The evaluation of sensitivities can be approached in the number of ways. The simplest, so-called "brute force" method, consists of the computation of the response at distinct values of the parameter considered while keeping the others constant. Assuming that

$$\frac{\partial \ln \eta_r}{\partial \ln k_j} \approx \frac{\Delta \ln \eta_r}{\Delta \ln k_j} \tag{3.32}$$

we obtain an "interval" or integral sensitivity. Another method, called the direct method, have been introduced in Bukhman et al., [1969] and Dickinson & Gelinas, [1976]. A newcomer to kinetic modelling is well advised to begin, and the seasoned modeller to remain, with the "brute force" method for the following

reasons. First, it is easy to use since hardly any additional programming is required. Second, the interpretation of sensitivities is direct and any conceivable response can be considered, whereas state sensitivities cannot be easily related, if they can be related at all, to such characteristic combustion measures as induction times. Third, the approximation involved in expression Eq. (3.32) is harmless, since for the purpose of sensitivity analysis only relative comparison of sensitivities is of interest.

The set of logarithmic response sensitivities for all rate constant is referred to as a sensitivity spectrum. The highest absolute values of the sensitivities in the spectrum pinpoint the most important reactions in kinetic scheme for determining the chosen set of responses. The lowest absolute values of sensitivities, however, do not necessarily identify unimportant reactions. The reactions having the smallest absolute values are removed from the scheme and the new responses are computed and compared to the initial ones. If no change is detected, further reactions are removed and the procedure continued until the difference in responses becomes larger than the computational errors. The removed reactions constitute the least important ones, within the range of sensitivity tests.

3.5.2 STEADY STATE APPROXIMATIONS

Steady state approximations for intermediate species can be justified in many different ways. [Peters, 1991]. They first were derived for zero dimensional homogeneous systems that depend only on time, and the term "steady state" was introduced because the time derivative of these species is set to zero.

$$\frac{d[X_i]}{dt}=0=\sum_{k=1}\upsilon_{ik}\omega_k \qquad (3.33)$$

Here, $[X_i]$ denotes the molar density of species i, called the concentration, t, the time, υ_{ik}, the stoichiometric coefficient of species i in reaction k and ω_k, the reaction rate. The justification for this approximation is generally provided in physical terms by stating that the rate at which species i is consumed is much faster than the rate by which it is produced. Therefore its concentration always stays much smaller than those of the initial reactants and the final products. Since the concentration always small, its time derivative also stays small compared to the time derivatives of the other species, as Eq. (3.33) implies

As an example, one may look at the well-known mechanism for thermal production of NO

A $\quad O + N_2 \rightarrow N + NO$

B $\quad N + O_2 \rightarrow O + NO$

Here, we assume that the level of atomic oxygen O is given as result of oxidation reactions in a combustion system. Now we assume that the atomic nitrogen N is in steady state because reaction B is faster than reaction A. One than can add both reactions, and cancel N to obtain the global reaction

(I) $\quad N_2 + O_2 \rightarrow 2NO$

The rate of the overall reaction is that of the first reaction that is slow and therefore rate-determining. Since two moles of NO are formed according to reaction I, the time change of NO is

$$\frac{d[X_{NO}]}{dt}=2k_A(T)[X_{O_2}][X_{N_2}] \qquad (3.34)$$

This shall now be derived in a more systematic way. The balance equations for NO and N are

$$\frac{d[X_{NO}]}{dt} = k_A[X_o][X_{N_2}] + k_B[X_N][X_{O_2}] \tag{3.35}$$

$$\frac{d[X_N]}{dt} = k_A[X_o][X_{N_2}] - k_B[X_N][X_{O_2}] \tag{3.36}$$

These equations will be non-dimensional by introducing reference values for all concentrations and the temperatures. Peters [1991] defined

$$c_{NO} = \frac{[X_{NO}]}{[X_{NO}]_{ref}} \tag{3.37}$$

$$c_N = \frac{[X_N]}{[X_N]_{ref}} \tag{3.38}$$

and non-dimensional time as

$$\tau = \frac{t k_A(T_{ref})[X_O]_{ref}[X_{N_2}]_{ref}}{[X_{NO}]_{ref}} \tag{3.39}$$

For simplicity, we assume the temperature and the concentrations of O_2, O and N_2 to be constant equal to their reference value. Then the reference value for N must be chosen as

$$[X_N]_{ref}=\frac{k_B(T_{ref})[X_O]_{ref}[X_{N_2}]_{ref}}{k_A(T_{ref})[X_{O_2}]_{ref}} \tag{3.40}$$

in order to obtain the non-dimensional equations, Peters (1991) defined:

$$\frac{dc_{NO}}{d\tau}=1+c_N \tag{3.41}$$

$$\epsilon\frac{dc_N}{d\tau}=1-c_N \tag{3.42}$$

Here ε denotes a small parameter defined by [Peter,1991]:

$$\epsilon=\frac{[X_N]_{ref}}{[X_{NO}]_{ref}}=\frac{k_A(T_{ref})[X_O]_{ref}[X_{N_2}]_{ref}}{k_B(T_{ref})[X_{O_2}]_{ref}[X_{NO}]_{ref}} \tag{3.43}$$

The two parts of this equation suggest that ε may be assumed small based on two different kinds of reasoning:

1. The concentration of the intermediate species in Eqs.(3.41) and (3.42) is small compared to the typical concentration of products, which is NO in this case, or

2. the rate constant k_A by which the intermediate N is formed is much smaller than the rate constant k_B at which it is consumed. The solution of the system Eqs. (3.41) and (3.42) had been given in [Peters, 1991].

This example illustrates that the steady state assumption may be analyzed rigorously by asymptotic methods In a more complicated chemical system, where many steady state assumptions applied, this methodology can become cumbersome,

since many small parameters that relate rate constants to each other, will appear. These parameters then must be ordered in a specific way to obtain a reasonable and self-consistent result. Very often it is easier to analyze numerical results from a complete solution and compare the magnitude of the concentration of intermediates to the concentration of the initial reactants or the final products. This corresponds to the reasoning associated with Eq.3.33. The error introduced by each steady-state assumptions is then typically of the order of concentration ratio. For many engineering purposes, it will be acceptable to assume those intermediate species in steady-state, whose concentration is significantly less than 10% of the initial fuel concentration. The reaction rates must be expressed in terms of the rate constants and the concentrations. Some concentrations are those of steady state species. The most important step in reducing mechanisms is a systematic truncation of some steady state relations such that system of no-linear algebraic equations becomes explicit.

3.6 KINETIC MECHANISMS STUDY FOR PREMIXED HYDROGEN COMBUSTION

There have been a number of studies of structures and propagation velocities of premixed hydrogen-oxygen flames through numerical integrations of one-dimensional, adiabatic conservation. Especially notable among these are the very extensive and pioneering works of Dixon-Lews [1975] [1979] and the more recent thorough studies of Warnatz [1979] [1981]. These references should be consulted for additional literature on the subject. These cited works accomplished more than merely the computation of flame structures. They helped to improve knowledge of rates of important elementary steps and also identified accuracies of various steady-

state and partial-equilibrium approximations throughout the flames. Moreover, they reviewed and evaluated available experimental results sufficiently thoroughly, so that in the present study it will be adequate to focus attention on theoretical and numerical comparisons with the more recent experimental data presented in [Law, 1992].

Although the earlier work produced a fairly good understanding of the chemistry in H_2-O_2-N_2 mixtures, it is the development of simplified descriptions and reduction of the chemistry to the smallest number of global steps from which burning velocities can reasonably be calculated that can further improve understanding of these flames Derivation of such reduced mechanisms has been achieved recently for methane, methanol and propane flames [Paczko et al.,1988] for example, through systematic development of reduced kinetic mechanisms, using sensitivity analysis and steady state assumptions. Since the full kinetics of methane flames are considerably more complicated than those of hydrogen flames, the hydrogen-flame problem might be thought to be the simpler and therefore more readily solvable. However, the larger numbers of steps in hydrocarbon flames can contribute to accuracy of simplified approximations for radical pools by keeping radical concentrations sufficiently low. This is not the case for the hydrogen flame and, therefore, in many respects the hydrogen flame has been found to be the more difficult one for which to obtain asymptotic descriptions [Williams, 1985]. Some progress in this direction has been made for hydrogen-air diffusion flames [Gutheil et al., 1991] but no results have been made for the premixed flame The intent of the present investigation is to present a sufficiently accurate 2-step reduced mechanism suitable for numerical calculations of premixed hydrogen flames. The mechanism will form the basis of the asymptotic analysis of the flame structure to be developed in the future.

CHAPTER 4. FORMULATION OF PREMIXED H_2-AIR FLOW IN SUPERSONIC COMBUSTION SYSTEM

4.1 INTRODUCTION

The study of the fluid dynamics and combustion processes of hydrogen-fuelled scramjets concerns the overall effects of the fuel injection, mixing, reaction on the flow as well as the heat lose from the system Most of these studies have been, of necessity, experimental investigations in pilot-scale engine components The dependence on empirical results is due to the complexity of the flow around fuel injection in three-dimensional geometries, which are not readily treated analytically So the numerical calculation of the turbulent mixing and reaction of fuel in the supersonic flow through a scramjet combustor is a necessary supplementary means, in somehow, is an only feasible method.

In addition to the usual complexities involved in numerical integration of the parabolic Navier-Stokes equations, it is necessary to include the finite-rate chemical kinetic mechanisms of the fuel-air reactions (both the detailed or reduced) The introduction of the detailed or reduced chemical mechanisms into theoretical analysis of complex turbulent mixing flows results a chemical kinetics model. To begin the calculation therefore requires a prior knowledge of the extent of fuel mixing, ignition and reaction. A sufficient data base has been established to define a scramjet engine concept

The present analytical study uses a computer code, called General Chemical Kinetics Code for Gas-Phase Flow Processes (GCKP84) [David et al. 1984], for solving chemical kinetics problems in one-dimensional flow, with an hydrogen-air

chemistry model consisting of a numbers of reactions involving several species

Because the computer code is for one-dimensional flow, the effects of fuel injection and mixing cannot be included However, the present finite-rate calculation of premixed hydrogen-air flows are considered important in predicting ignition and reaction in the recirculating zones near the fuel injectors In analysis of scramjet combustors, where the reaction may be limited by the mixing, these results for premixed reactants provide a lower limit of the times required for reaction.

4.2 DIFFERENTIAL CONSERVATION EQUATIONS FOR ONE-DIMENSIONAL FLOW REACTIONS IN SUPERSONIC COMBUSTION SYSTEM

The computer code used for this analysis of a complex reacting gas mixture flowing through an arbitrarily assigned area employs the conservation equations for one-dimensional flow. The flow is assumed to be isobaric, premixed, invisid, and adiabatic.

These equations can be derived under the assigned area profile for the flow, and the pressure profile is determined by the ideal-gas law. In this case, we have N+3 variables, the N species concentrations plus ρ, T, and velocity V We assume, as before, a homogeneous, frictionless gas in one-dimensional flow with velocity V and constant mass flow rate m. Global continuity is then represented by the equation:

$$\frac{d(\rho AV)}{dt} = \frac{dm}{dt} = 0 \qquad (4.1)$$

or

$$\rho AV = m \qquad (4.2)$$

where A is the flow cross-sectional area at any point. The individual species continuity equations are now written as:

$$\frac{d}{dt}(\sigma_i m) = W_i AV \qquad i = 1, 2, \ldots, N \qquad (4.3)$$

here σ_i is the number of moles of species i per unit mass of mixture. Because m is constant mass flow rate , equation (4.3) becomes:

$$\frac{d\sigma_i}{dt} = \frac{W_i}{\rho} \qquad i = 1, 2, \ldots, N \qquad (4.4)$$

Now we need derive new differential equations for V, ρ, and T. These are obtained from the momentum and energy conservation equations. The momentum equation

$$\frac{\partial(\rho V)}{\partial t} = -[\nabla \cdot \rho V^2] - \nabla p \pm \nabla \cdot \tau + \rho g \qquad (4.5)$$

where "p" is the thermodynamic gas pressure inside the system

Since we neglect viscous stress ($\nabla \cdot \tau$) and gravity force (ρg), and examine only one-dimensional flow, the momentum equation can be expresses as:

$$\rho \frac{dV}{dt} + \frac{1}{V}\frac{dp}{dt} = 0 \qquad (4.6)$$

and from the definition of total enthalpy, the energy conservation equation:

$$h+\frac{V^2}{2}=h_T \qquad (4.7)$$

where

$$h=\Sigma\sigma_i h_i \qquad i = 1,2,\ldots,N \qquad (4.8)$$

here h_T is the total enthalpy of the flowing gas per unit mass Equation (4.8) is differentiated with respect to time by using

$$\frac{dh_T}{dt}=\frac{dh_T}{dx}\frac{dx}{dt}=-\left(\frac{Q}{m}\right)V \qquad (4.9)$$

where Q is now defined as the (positive) instantaneous heat loss rate per unit length of flow (heat units lost per unit length and time). The resulting enthalpy differential equation is:

$$\frac{dh}{dt}+V\frac{dV}{dt}+\frac{QV}{m}=0 \qquad (4.10)$$

The dependence of Q on temperature, mass flow rate, and flow geometry has been discussed in the previous section.

Also we can have the molecular weight of the gas mixture

$$M_w=\frac{1}{\Sigma\sigma_i} \qquad i = 1,2,\ldots,N \qquad (4.11)$$

and the equation of state

$$p=\frac{\rho RT}{M_w} \qquad (4.12)$$

then Equations (4.1), (4.7), (4.11), and (4.12) are differentialed and combined with equation (4.6) to get the flowing differential equations [David, 1984]

$$\frac{dV}{dt} = \frac{V}{M^2-1}\left[\frac{1}{A}\frac{dA}{dt} - \alpha + \Phi\right] \qquad (4.13)$$

$$\frac{d\rho}{dt} = -\rho\left[\frac{M^2}{M^2-1}\left(\frac{1}{A}\frac{dA}{dt} - \alpha + \Phi\right) + \alpha - \Phi\right] \qquad (4.14)$$

$$\frac{dT}{dt} = -T\left[\frac{(\gamma-1)M^2}{M^2-1}\left(\frac{1}{A}\frac{dA}{dt} - \alpha + \Phi\right) + \beta + \Phi\right] \qquad (4.15)$$

In these equations, the following auxiliary definitions have been made [David, 1984]

$$\alpha = \frac{RT}{p}\sum W_i - \beta \qquad i = 1, 2, \ldots N \qquad (4.16)$$

$$\beta = \frac{1}{p}\left(\frac{\gamma-1}{\gamma}\right)\sum h_i W_i \qquad i = 1, 2, \ldots N \qquad (4.17)$$

$$\Phi = \frac{VM_w}{RT}\frac{Q}{m}\left(\frac{\gamma-1}{\gamma}\right) \qquad (4.18)$$

and the Mach number M is defined by

$$M^2 = \frac{V^2 M_w}{\gamma RT} \qquad (4.19)$$

where

$$\gamma = \frac{Cp}{Cp - \frac{R}{M_w}} \qquad (4.20)$$

here Cp is the heat capacity of the mixture per unit mass assuming fixed

$$Cp=\Sigma\sigma_i (Cp)_i \qquad (4.21)$$

composition and $(Cp)_i$ is the heat capacity of species i

The reacting gas also be described by equations that use distance x as the independent variable. The relationship

$$V\frac{dZ}{dx}=\frac{dZ}{dt}$$

is used to rewrite equations (4.13, 14, 15), where Z represents any of the dependent variables V, ρ, T, and the σi's. The distance equations are [David, 1984]

$$\frac{d\sigma_i}{dx}=\frac{W_i}{\rho V} \qquad (4.22)$$

$$\frac{d\rho}{dx}=-\rho\left[\frac{M^2}{M^2-1}\left(\frac{1}{A}\frac{dA}{dx}-\alpha^*+\Phi^*\right)+\alpha^*-\Phi^*\right] \qquad (4.23)$$

$$\frac{dV}{dx}=\frac{V}{M^2-1}\left(\frac{1}{A}\frac{dA}{dx}-\alpha^*+\Phi^*\right) \qquad (4.24)$$

$$\frac{dT}{dx}=-T\left[\frac{(\gamma-1)M^2}{M^2}\left(\frac{1}{A}\frac{dA}{dx}-\alpha^*+\Phi^*\right)+\beta^*+\Phi^*\right] \qquad (4.25)$$

where

$$\alpha^* = \frac{\alpha}{V}$$

$$\beta^* = \frac{\beta}{V}$$

$$\Phi^* = \frac{\Phi}{V}$$

The equations form a system of N+3 equations for N+3 unknowns. This equation system is solved by numerical integration with time or distance for a specified area distribution.

4 3 CHEMICAL EQUILIBRIA OF THE REACTIONS

The code solves the one-dimensional reacting flow with the finite-rate chemical reactions. The reactions are considered to get the chemical equilibria at every calculation steps The traditional thermodynamic description of each equilibrium state is based on the pertinent Gibbs functions of the system.

In continuous system, such as being considered here, one normally assumes that enthalpy (h) as Gibbs function is known; it depends on the entropy s, pressure p, and the chemical potentials of the reaction:

$$dh = Tds + V_s dp + \sum_i \mu_i M_{w_i} dn_i \qquad (4.26)$$

where V_s is the volume of the system, μ_i is the chemical potential of each mixture component, and M_{wi} is the molecular weight of species i

In the isobaric combustion, the energy G in the system is used as

$$dG=-sdT+V_s dp+\sum_i \mu_i M_{w\,i} dn_i \qquad (4.27)$$

Eq.4.27 identifies that G is the dependent of the variables T, P, and n_i

We acknowledge that the chemical equilibrium is the set of values n_k^{equ} at given values of T and P. This is established by the extra condition

$$\left[\frac{\partial G}{\partial n_k^{equ}}\right]_{T,p,n_i} = 0 \qquad (4.28)$$

It is well-known that the free enthalpy is minimized

The equilibrium values n_k^{equ} needed to satisfy the mole balance equation and must be established The solution to this constrained minimization function is obtained by the method of Lagrange multipliers, thus

$$\mathcal{L}(n,\lambda,T) = -G+\sum_i M_{wi}\mu_i n_i+\sum_i \lambda_j [b^{\Phi}{}_j-\sum_i a_{ji} n_i] \qquad (4.29)$$

with constructs

$$\left[\frac{\partial \mathcal{L}}{\partial n_i}\right]_{n_i,\lambda,T} = 0$$

$$\left[\frac{\partial \mathcal{L}}{\partial \lambda_j}\right]_{\lambda_i,n,T} = 0$$

$$\left[\frac{\partial \mathcal{L}}{\partial T}\right]_{n_i, \lambda_j} = 0$$

This creates a set of (i+j+1) equations for the (i+j+1) unknowns, n_k^{equ} and T Thus, the state function at each stage is prescribed

4 4 NUMERICAL INTEGRATION PROCEDURE

The computer code of GCKP84 [David, 1984] for solving the one-dimensional flow with finite-rate chemical reactions uses a new implicit numerical integration procedure for sets of "stiff" differential equations developed by Zeleznik [Zeleznik et al, 1984] This property of stiffness often arises in the differential equations of chemical kinetics because of widely varying rates of relaxation of the fluid dynamics and chemical processes toward the equilibrium conditions This can cause an integration algorithm to take excessively small steps, out of proportion to the rate change of the dependent variables Zeleznik developed a generalized theory of implicit numerical integration that includes the methods of Gear [Gear et al, 1971] and Nordsieck [Hindmarsh, 1972] as special cases It also describes a practical computer code applying the theory to the solution of equations very similar to those presented in this thesis This variable-order, predictor-corrector method selects the largest step size consistent with the gradients of the unknowns and with the accuracy requirements

Input to the computer program is user oriented This allows for easy modification to the chemical reaction system, reaction-rate parameters, thermodynamic properties and general problem specification Additional details of the input specification are given by

CHAPTER 5. DETAILED CHEMICAL KINETIC MECHANISM OF H_2/AIR SUPERSONIC COMBUSTION SYSTEM

5.1 INTRODUCTION

As we discussed in past chapters, most of the studies of fluid dynamics and the combustion processes in supersonic combustion ramjet have been, of necessity, experimental investigations of the overall effects of the fuel injection, mixing, and reaction on the flow in sub-scale engine components. The dependence on empirical results is due to the complexity of the flow around fuel injectors in three-dimensional geometries, which are not readily treated analytically. Most numerical solutions are restricted to two or three-dimensional parabolic flow with equilibrium or simple finite-rate chemistry models of the H_2/air system. Such numerical solution schemes are applicable only in the parabolic flow region well down-stream of the disturbance caused by the transverse fuel injection Scramjet combustor relys on transverse injection of the fuel in order to achieve rapid mixing and reaction To begin the calculation therefore requires a prior knowledge of the extent of fuel mixing, ignition and reaction.

All this information, particularly the ignition/reaction state, may not even be available from experimental data because of the difficulty of freezing the reaction in a sample extracted by a probe from the high-velocity, high-temperature combustor flow. So building a detailed kinetic model is the first step for analysis the reaction mechanisms.

An important goal of modelling of H_2/air combustion system is to develop a computational model with a well-understood range of validity. This model can then

be used in a predictive role to evaluate the facility and validity of new concepts. It can also be used to interpret experimental measurements, the design of combustion chamber of scramjet Throughout these applications, the model may serve us an excellent way to test our understanding of the interactions of H_2/air combustion in scramjet.

This chapter describes a detailed chemical reaction scheme for H_2/air combustion system. An analytical study of the chemical mechanism involved in the ignition and reaction of H_2/air system is also performed in this chapter at the conditions representative of a scramjet combustor. The calculations are made with a one-dimensional kinetics program. The objective of these calculations is to provide information for an assessment of the conditions at which kinetics are important in scramjet combustors. Specifically, the study considered how ignition times and reaction times are affected by the initial temperature, initial pressure, fuel equivalence ratio, and Mach number.

5.2 THE DETAILED CHEMICAL KINETIC SCHEME OF H_2/AIR COMBUSTION

As we indicated in section 3.3, initially, a detailed mechanism is constructed by including all possibly relevant, known reactions as well as some that may be completely hypothetical. Rate constant expressions for these reactions are selected from literature sources.

Based on the chemical kinetics theory, for a chemistry reaction scheme, more reactions it contains, more precise the model is. Here we select reactions, that possibly happen for the H_2/air combustion process while the N_2, AR and CO_2 are

kinetic scheme. This scheme is listed in Table 5.1. It consists of 41 elementary reactions involving 8 (N = 8) species;

H_2, O_2, H_2O, H,
O, OH, HO_2, H_2O_2

These reactions are compilations from the recent literatures. We assume the third-body efficiency are 1.0 except those are listed in Table 5.2.

Reaction-rate data were taken from references [Baulch et al.,1973] [Warnatz, 1984] [Bahn, 1972] [Slack, 1977] [Jensen, 1978] [Brokaw,1973] [Lloyd, 1974]. There are two type of reactions. One is the bimolecular, or "shuffling" reactions which, when proceeding in the forward direction, consume the molecular species and form H_2O and the O, H, and OH radicals, such as Reaction (1-3). Other reactions are the recombination reactions which produce the major portion of the energy release in the hydrogen-oxygen reaction. The symbol "M" in the equations represents a third body. The temperature range for this scheme is up to 2500-3000 K. The data are of the latest available for the hydrogen oxidation mechanisms provided improvements to the reaction-rate parameters and third-body efficiency for certain key reaction such as

$$H+O_2 \rightarrow HO_2+M$$

$$NO+HO_2 \rightarrow OH+NO_2$$

and

$$H+OH+M(H_2O) \rightarrow H_2O+M(H_2O)$$

The impact of the reaction rates on the ignition and reaction will be discussed later.

TABLE 5.1. DETAILED CHEMICAL KINETIC SCHEME WITH THIRD-BODY EFFICIENCIES FOR HYDROGEN-OXYGEN COMBUSTION

[Rate constant is given by $k = AT^N \exp(-\text{Activation-energy}/1.987T)$]

No	Reaction	CONST		
		A	N	E
1	$M + O_2 \rightarrow O + O$	6.81E+18	-1.	118848
2	$M + H_2 \rightarrow H + H$	2.20E+14	0.	95151
3	$M + H_2O \rightarrow OH + H$	2.20E+16	0.	104213
4	$H + O_2 \rightarrow OH + O$	2.00E+14	0.	16859
5	$OH + O \rightarrow H + O_2$	2.30E+13	0.	0.
6	$H_2 + O \rightarrow OH + H$	1.80E+10	1.	8826
7	$H + OH \rightarrow O + H_2$	8.30E+09	1.	6895
8	$H_2 + OH \rightarrow H_2O + H$	2.20E+13	0.	5102
9	$H_2O + H \rightarrow OH + H_2$	9.30E+13	0.	20193
10	$OH + OH \rightarrow H_2O + O$	6.30E+12	0.	1084
11	$H_2O + O \rightarrow OH + OH$	6.80E+13	0.	18203
12	$H + H \rightarrow H_2 + M$	6.40E+17	-1.	0.
13	$H + OH \rightarrow H_2O + M$	1.40E+23	-2.	0.
14	$O + O \rightarrow O_2 + M$	2.90E+17	-1.	0.
15	$H + O_2 \rightarrow HO_2 + M$	1.50E+15	0.	-985
16	$M + HO_2 \rightarrow H + O_2$	2.10E+15	0.	45310
17	$HO_2 + H \rightarrow OH + OH$	2.50E+14	0.	1872
18	$OH + OH \rightarrow HO_2 + H$	1.20E+13	0.	39794
19	$HO_2 + H \rightarrow H_2 + O_2$	2.50E+13	0.	690
20	$H_2 + O_2 \rightarrow HO_2 + H$	5.50E+13	0.	57327
21	$HO_2 + H \rightarrow H_2O + O$	3.00E+13	0.	1727
22	$H_2O + O \rightarrow HO_2 + H$	2.98E+13	0.	58657
23	$HO_2 + O \rightarrow OH + O_2$	1.80E+13	0.	407
24	$OH + O_2 \rightarrow HO_2 + O$	2.30E+13	0.	55564

25	$HO_2 + OH \rightarrow H_2O + O_2$	6.00E+13	0.	0.
26	$H_2O + O_2 \rightarrow HO_2 + OH$	7.61E+14	0.	72950
27	$HO_2 + HO_2 \rightarrow H_2O_2 + O_2$	2.00E+12	0.	0.
28	$M + 2\ OH \rightarrow H_2O_2 + M$	9.10E+15	0.	5024
29	$M + H_2O_2 \rightarrow 2\ OH + M$	1.20E+17	0.	45113
30	$H + H_2O_2 \rightarrow HO_2 + H_2$	1.70E+12	0.	3743
31	$H_2 + HO_2 \rightarrow H_2O_2 + H$	7.30E+11	0.	18518
32	$H + H_2O_2 \rightarrow H_2O + OH$	1.00E+13	0.	3597
33	$OH + H_2O \rightarrow H_2O_2 + H$	3.39E+12	0.	74892
34	$O + H_2O_2 \rightarrow HO_2 + OH$	2.80E+13	0.	6427
35	$OH + HO_2 \rightarrow H_2O_2 + O$	9.53E+12	0.	20791
36	$OH + H_2O_2 \rightarrow H_2O + HO_2$	1.00E+13	0.	1793
37	$H_2O + HO_2 \rightarrow H_2O_2 + OH$	2.80E+13	0.	32505
38	$O + H \rightarrow OH + M$	7.10E+18	-1.	0.
39	$H_2 + O_2 \rightarrow OH + OH$	1.00E+13	0.	43000
40	$H_2 + O_2 \rightarrow H_2O + O$	4.10E+13	0.	50470
41	$H_2 + HO_2 \rightarrow H_2O + OH$	2.00E+13	0.	25000

*The t hird body efficiency M is given in Table 5.2

TABLE 5.2. THIRD-BODY EFFICIENCY FOR TABLE 5.1.

M (Third-body) = Efficiency	M (Third-body) = Efficiency
M (O_2 , No. 1 reaction) = 4.0	M (O_2 , No. 13 reaction) = 1.6
M (H_2 , No. 2 reaction) = 2.0	M (O_2 , No. 15 reaction) = 2.6
M (O_2 , No. 12 reaction) = 2.0	M (H_2 , No. 29 reaction) = 2.0
M (H_2 , No. 13 reaction) = 4.0	M (H_2O , No. 3 reaction) = 6.0
M (H_2 , No. 15 reaction) = 5.0	M (H_2O , No. 1 reaction) = 2.0
M (O_2 , No. 29 reaction) = 0.78	M (H_2O , No. 2 reaction) = 8.0
M (H_2O_2 , No. 29 reaction) = 6.6	M (H_2O , No. 12 reaction) = 15.0
M (O , No. 1 reaction) = 10.0	M (H_2O , No. 12 reaction) = 20.0
M (H , No. 2 reaction) = 5.0	M (H_2O , No. 15 reaction) = 32.5
M (H_2 , No. 12 reaction) = 5.0	M (H_2O , No. 29 reaction) = 6.0

5.3 THE SCOPE OF PRESENT CALCULATION

Equations (4.1 - 4.29) will be supplemented with a set of initial conditions and a description of the pressure along a streamline. The initial conditions required are the complete chemical composition, pressure and temperature.

For parameter variation, the principal parameters of these calculations are the initial static pressure and initial temperature and the hydrogen /air mixture composition. Initial pressure were varied between 0.2 and 10.0 atm; the initial temperatures were

between 850 K and 2000 K. The range of Mach number is 0.1 to 10. The amount of hydrogen in the initial mixture was varied corresponding to equivalence ratios between 0.2 and 2.0. The equivalence ratio is an indication of the relation stoichiometry of the mixture based on the global reaction for the oxidation of hydrogen

$$2H_2 + O_2 \rightarrow 2H_2O$$

For this reaction the stoichiometric mass ratio of hydrogen to oxygen is:

$$\phi^* = \frac{(H_2 moles)(MW)_{H_2}}{(O_2 moles)(MW)_{O_2}} = \frac{2(2.16)}{1(32)} = 0.126$$

For an arbitrary mixture of hydrogen and air (or other species) with a mass ratio of hydrogen ϕ, the equivalence ratio is defined as:

$$\Phi = \frac{\phi^*}{\phi}$$

where Φ is equivalence ratio, ϕ is local hydrogen-oxygen ratio and ϕ^* is stoichiometric hydrogen-oxygen ratio. Most of the calculations were made for Φ = 1.0.

The chemistry model is as same as in section 5.2, given in Table 5.1, consistent of 41 reactions and 8 species. The ignition-time is presented by Equation (3.24), and the reaction-time is calculated by Equations (3.25 - 3.26).

5.4 RESULTS AND DISCUSSION FOR USING DETAILED CHEMICAL KINETIC SCHEME AS THE CHEMICAL MODEL OF H_2/AIR SUPERSONIC COMBUSTION

5.4.1 GENERAL DISCUSSION

A series of calculations were made after last section for the conditions similar to those existing in the combustion chamber of scramjet. A range of the initial pressures, initial temperatures, equivalence ratios, and Mach number were studied to determine their quantitative effects on the results.

Typical output of the computer code [Bittker, 1984] is presented in Figures 5.1(a-c) in the form of the time variation of species mass fractions through the ignition and reaction zones. Results are given for a stoichiometric H_2/air mixture (ϕ = 1)at an initial temperature of 1000K and the initial pressures of 0.5, 1.0 and 2.0 atm in Figures 5 1(a),5.1(b) and 5.1(c), respectively, and the Mach number equals to 5. The ignition time and total reaction time are noted on each figure by τ_{ig} and τ_{TR} which calculated by Equations (3.24-3.26). Comparing these three figures, a very remarkable effects by the increased initial pressure have been indicated. The effect of the increased pressure between 0.5 to 1.0 to shorten total reaction time can be seen by much smaller different between τ_{TR} and τ_{ig} in Figure 5.1(b) at 1.0 atm when compared with the different indicated in Figure 5.1(a) at 0.5 atm. Contrary to this, when the initial pressure changed from 1.0 to 2.0, the total reaction time increased between the Fig.5.1(c) and Fig.5.1(b). These effects are the same for the ignition time, but for the reaction time, the increase is only the direction from those figures. The more details about this we will discuss later.

The bimolecular reactions are faster than the recombination reactions and thus

dominate the early part of the combustion process. An examination of the production terms for any species would indicate that, in this period, the Reactions, like Reaction (1)-(3), make important contributions, the other reactions contributing terms which are less by many orders of magnitude. As process continues, the free radical concentrations increase and the contributions from the other reactions start becoming more important. There is however, a significant time delay before any appreciable temperature rise is observed. This period is called here the ignition delay period, during which little change occurs in the molecular species, large changes in H_2O, O and OH concentrations are noted, and the hydrogen radical reaches its peak value.

In Chapter 3, we already discussed the definitions of ignition time. It was found from our results that the definition used here closely corresponds to the time at which a peak occurs in the atomic hydrogen concentration [Eq.(3.24)] since the increase in temperature usually associated with the formation of water is energetically balanced by the dissociation of oxygen and hydrogen molecules. Thus the ignition delay period represents, in effect, a prelude to the recombination of atomic hydrogen and oxygen which releases most of the energy to the flow and causes the increase in temperature. Because of its large heat of formation the atomic hydrogen plays the most important role during this period. The time for the process to proceed from the end of the ignition delay to an equilibrium state is referred here is the reaction time [Eq.(3.25)]. An equilibrium state is assumed to be reached when the temperature increases by an amount equal to 95% of the total temperature rise [Momtchiloff, 1962].

5.4.2 IGNITION-TIME DISCUSSION

Temperature/Time History

Figures 5.2 (a)-(c) show the temperature-time histories for a wide range of the initial pressure, initial temperature, Mach number and equivalence ratio.

The Figure 5.2(a) indicates the effects of the initial pressure to the temperature-time history. When the initial pressure increases between 0.5 to 4.0 atm, the ignition-time decreases sharply, but after 6 atm, as the initial pressure increases, the ignition-time slightly increases. This effects are also shown in Figure 5.3. This presentation indicated that the initial pressure affects the reaction rates for the recombination reactions is considerable. Figure 5.2(a) also indicates the equilibrium temperature slightly increases with the initial pressure rising.

Figure 5.2(b) indicates the effects of the initial temperature to the temperature-time history. The ignition-time decreases clearly when the initial temperature rises, but the reduction of the ignition-time decreases too as the initial temperature increases. The equilibrium temperature is weakly dependent of the initial temperature, because the temperature rising causes more dissociation reactions.

A comparison of the effects of the equivalence ratio to the temperature-time history is shown in Figure 5.2(c). The interest results show the weak dependence of ignition-time on equivalence ratio change for the rich hydrogen fuel ($\phi >$ or $= 1$). This observation has been confirmed in the reference [Momtchiloff, 1962]. But in dilute hydrogen fuels, the results as we expected, the clearly reducing of ignition-time is shown when the ratio increases. Furthermore, a charge in the equivalence ratio is seen to indicate a change of the equilibrium temperature, as expected.

From the beginning of this thesis, we always talk about the advantages of supersonic combustion comparing with subsonic combustion. Figure 5.2(d) give us this clearly idea. The Figure has been divided to two parts, one is Mach number over 1 (4 to 10), the other is Mach number iess than 1 (0.2 to 0.5). In each part, the ignition time and equilibrium temperature are nearly the same. Between the two parts, supersonic combustion have shorter ignition-time, shorter total reaction-time and higher equiiibrium temperature than the subsonic one.

Initial Pressure and Initial-Temperature Affect Ignition-Time

Figure 5.3 and Figure 5.4 show the effects of the initial pressure and temperature on the ignition time of a stoichiometric H_2/air mixture. The igniti. n-time vs the initia pressure history at different initiai temperature, and the ignition-time vs initial temperature history at different initial pressure are shown in those two figures, respectively. Figure 5.3 indicates a drastic non-linearity in the pressure dependence, particularly at values of initial tempe.ature below 1250K. The constant pressure curves of ignition-time as a function of the initial temperature in Figure 5.4 indicate that the ignition-times decreases as the initial temperature increases These effects produced by the present chemical mechanism are primarily due to the formation of the HO_2 molecule through the reaction

$$H + O_2 + M\ (N_2) \rightarrow HO_2 + M\ (N_2)\ .$$

This reaction is a pressure- and temperature-dependent, highly exothermic chain propagating step. Because of the reactivity of HO_2, this reaction behaves effectively as a chain terminating step, especially at high temperature Furthermore, this reaction is important because a considerable part of heat of combustion may be released in this step This is also conformed from sensitivity analysis in Chapter 6. At high pressure, the reaction is more important because it produces HO_2 as a second chain carrier, leading back to H atoms less efficiently via

$$H + HO_2 \rightarrow OH + OH$$

and

$$OH + H_2 \rightarrow H_2O + H.$$

Equivalence Ratio and Mach Number Affect Ignition-Time

The effects of the equivalence ratio and Mach number to the ignition-time are presented in Figures 5.5 and 5.6, respectively. The ignition-time is nearly independent of the fuel equivalence ratio for range of 0.5 to 2.0. As we expected, for the low ratio hydrogen fuel, the ignition-times are longer. The effect of Mach number on ignition-time is illustrated in Fig. 5 6, the variation of τ_R is also nearly independent of Mach number, both for lower and higher Mach number. From Fig. 5 2(d), Mach number does affect the ignition and total reaction-time. It made temperature-time history fall into two groups, one is for supersonic reaction, another one is for subsonic reaction, but the ignition-time is independence of M in each group Figure 5 6 shows the clear relation between τ_{ig} and M.

Mass Fraction/Time History

It is instructive to compare the temperature-time histories with the corresponding mass fraction-time histories as shown in Figures 5.7(a-f) and 5.8(a-f) with initial pressure change and initial temperature change, respectively. The rapid change of the molecular species to approximately the equilibrium values is noted, once the ignition delay period is ended. During the ignition delay the H_2O and free radical concentrations are seen to increase rapidly. As stated previously the ignition delay time, as defined by Equation (3-24), closely corresponds to the peak in the atomic hydrogen concentration This can be confirmed by an examination of Figures 5.7(d) and 5 8(d) It is clear from the examinations of the composition histories that the recombination of atomic hydrogen is the rate controlling step in the

approach to an equilibrium state. In fact, during the reaction period the bimolecular reactions are nearly in equilibrium so that the equilibrium of the mixture can only be reached when the slower three body reactions equilibrate. This is the basis for the reducing mechanisms for chemical kinetics analysis as we prepared to study in next two chapters. The "slower" reactions consist of the main chemical kinetic mechanisms The effects of the initial temperature and pressure on the ignition-time are reflected by the changes in the composition history. A comparison in Fig.5.8 shows the results of increase the initial temperature from 1250K to 2000K at an initial pressure of one atmosphere.

5.4.3 REACTION-TIME DISCUSSION

In the present analysis the reaction-time is defined as the time difference between the ignition-time and total reaction time required to achieve 95 percent of the equilibrium temperature rise (see Eqs (3.25) and (3.26))

The effects of the initial pressure and the initial temperature on the variation of reaction time are presented in Figure 5.9 and 5 10 respectively for stoichiometric mixtures of H_2/air. In the semi-log of Figure 5 9, the variation of τ_R with the initial pressure seems on an exponential relation and shows a strong dependence on initial pressure. This is because of the influence of the three body recombination reactions to determine the reaction-time. It is expected that the initial pressure would have a greater effect in this period than in the induction period. The variation of τ_R with initial temperature is nearly a linear relation, this result conforms to the experimental data by Pergament H.S.[1963].

The comparison of the effects of equivalence ratio and Mach number on the reaction time are indicated in Figures 5.11 and 5.12 respectively. From Figure 5.12, the weak dependence of the reaction time on Mach number at the high and low values of M The reaction-times are almost constant but fall into two groups of M<1 and M>1. These effects are confirmed by Figure 5.2(d) too. It means that there is longer total reaction-time for subsonic combustion. The variation of reaction-time with the fuel equivalence ratio is significant, for the range of ϕ from 0.2 to 0.8, the reaction-time is reduced with the ratio increase. And between the range of ϕ from 1 to 1.6, the reaction time is the weak dependence of the equivalence ratio which shown in Fig 5.11 In range of ϕ from 1.8 to 2.0, the reaction-time is slightly increased with the ratio rise.

5.4 4 CONCLUSIONS

An analytical study of the chemical mechanism involved in the ignition and reaction of the H_2/air system has been performed at conditions representative of the scramjet combustor. The calculations are made for a one-dimensional kinetics program with H_2-O_2 (N_2 considered inert) chemistry model consisting of 41 reactions in 8 species. An objective of the calculations in this chapter is to provide information for an assessment of the conditions at which kinetics are important in scramjet combustor Specifically, the study considered how the ignition and reaction times are affected by the initial temperature, initial pressure, fuel equivalence ratio, Mach number and the reaction rate of key reactions.

Results of the calculations indicate that, within a 15% percent error, the ignition-time is nearly constant over a range of the equivalence ratios from 0.5 to 2.0. The Mach number change make the temperature-time history fall into two groups, one

is for supersonic combustion and the other is for subsonic combustion But the ignition-time for supersonic combustion is shorter than for the subsonic combustion. The effects of the initial temperature and initial pressure on the ignition-time are indicated a non-linear relation. The constant-pressure curves of τ_{ig} as a function of the initial temperature in Fig.5.3 indicated very long ignition times as T_0 decreases. These effects produced by the present chemical mechanism are primarily due to the formation of the HO_2 molecule through the reaction $H + O_2 + M - HO_2 + M$, which was included in the kinetics model of 41 reactions.

The present calculations indicate that the reaction-time, defined as the time from the onset of the ignition to attainment of 95 percent of the equilibrium temperature, is independent of Mach number in two different ranges, $M>1$ and $M<1$. The advantages of supersonic combustion are obviously in short ignition and reaction-time and high equilibrium temperature. They also indicated that the variation of the reaction-time with the initial temperature is nearly linear, and that the relation of the reaction-time change with the initial pressure is nearly an exponential manner.

The present calculations also indicate the reducing mechanism is possible and necessary This conclusion is through out by the discussion of mass fraction histories. It shows that some very fast reactions are not important for chemical mechanism The next two chapters will describe of studies about reducing mechanisms.

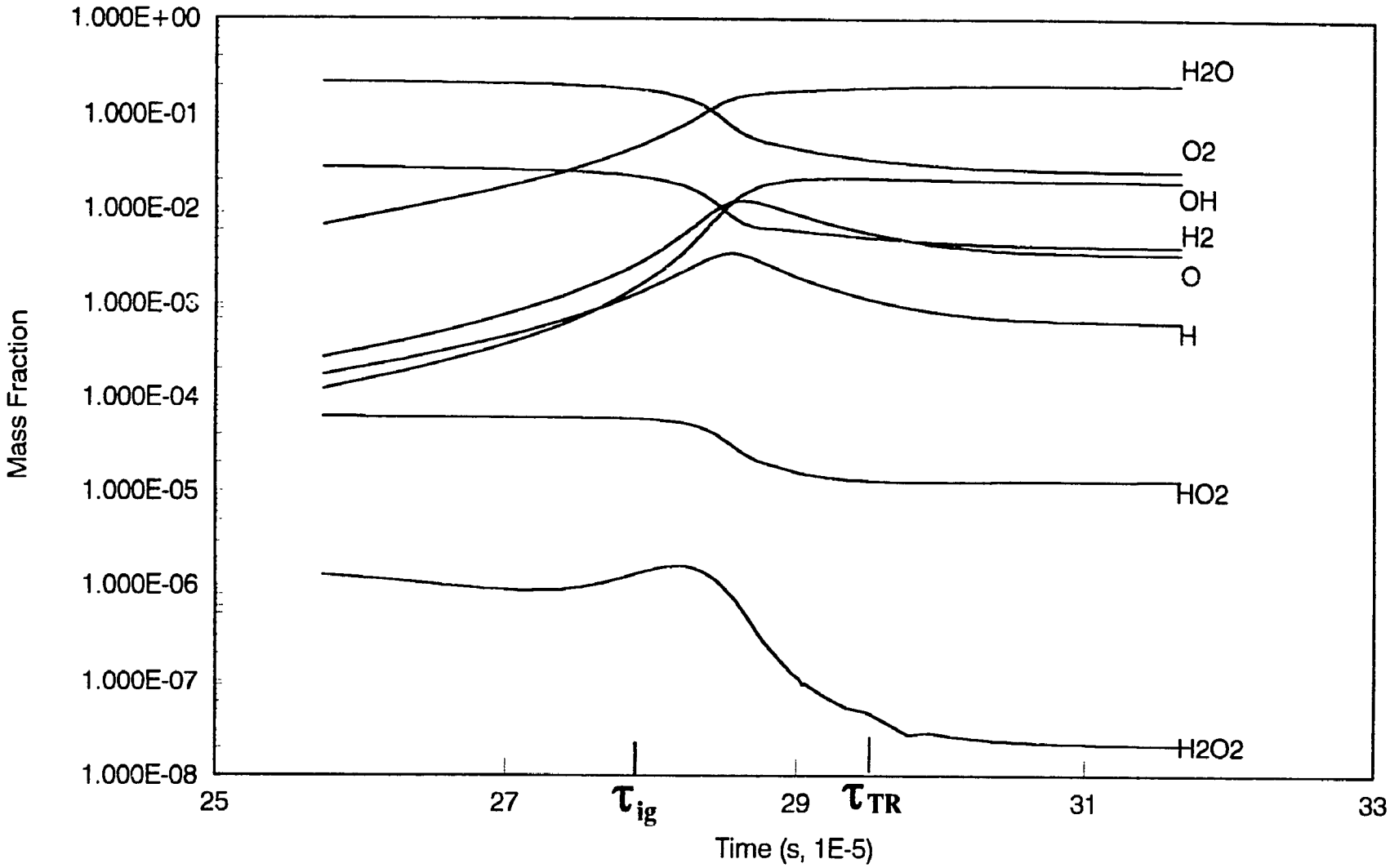

Figure 5.1 (a) Species mass fraction as function of time.
Po = 0.5 atm, To = 1000K , ϕ = 1.0, M = 5.0

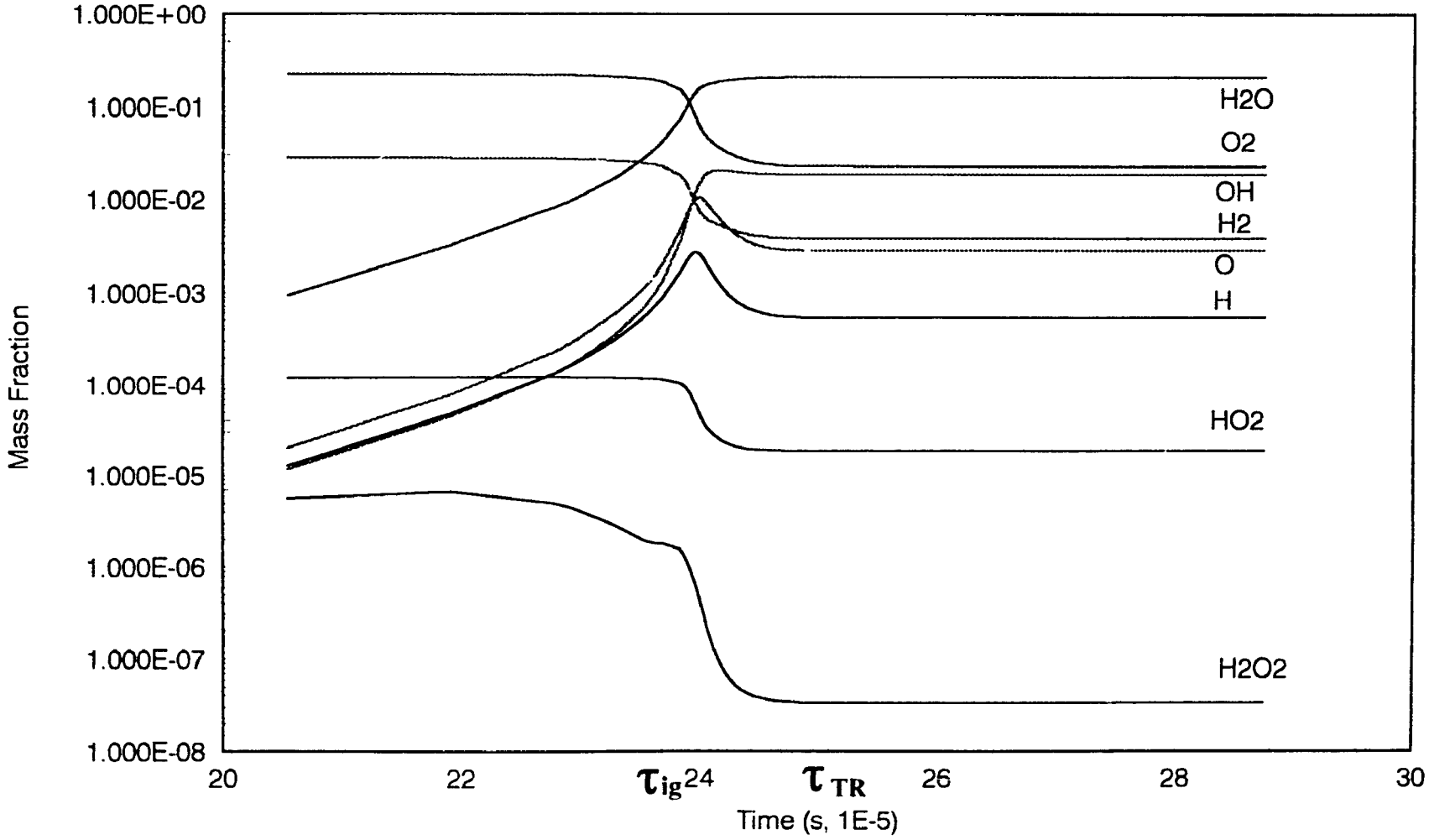

Figure 5 1 (b) Species mass fraction as function of time.
Po = 1.0 atm, To = 1000K, ϕ = 1.0, M = 5.0

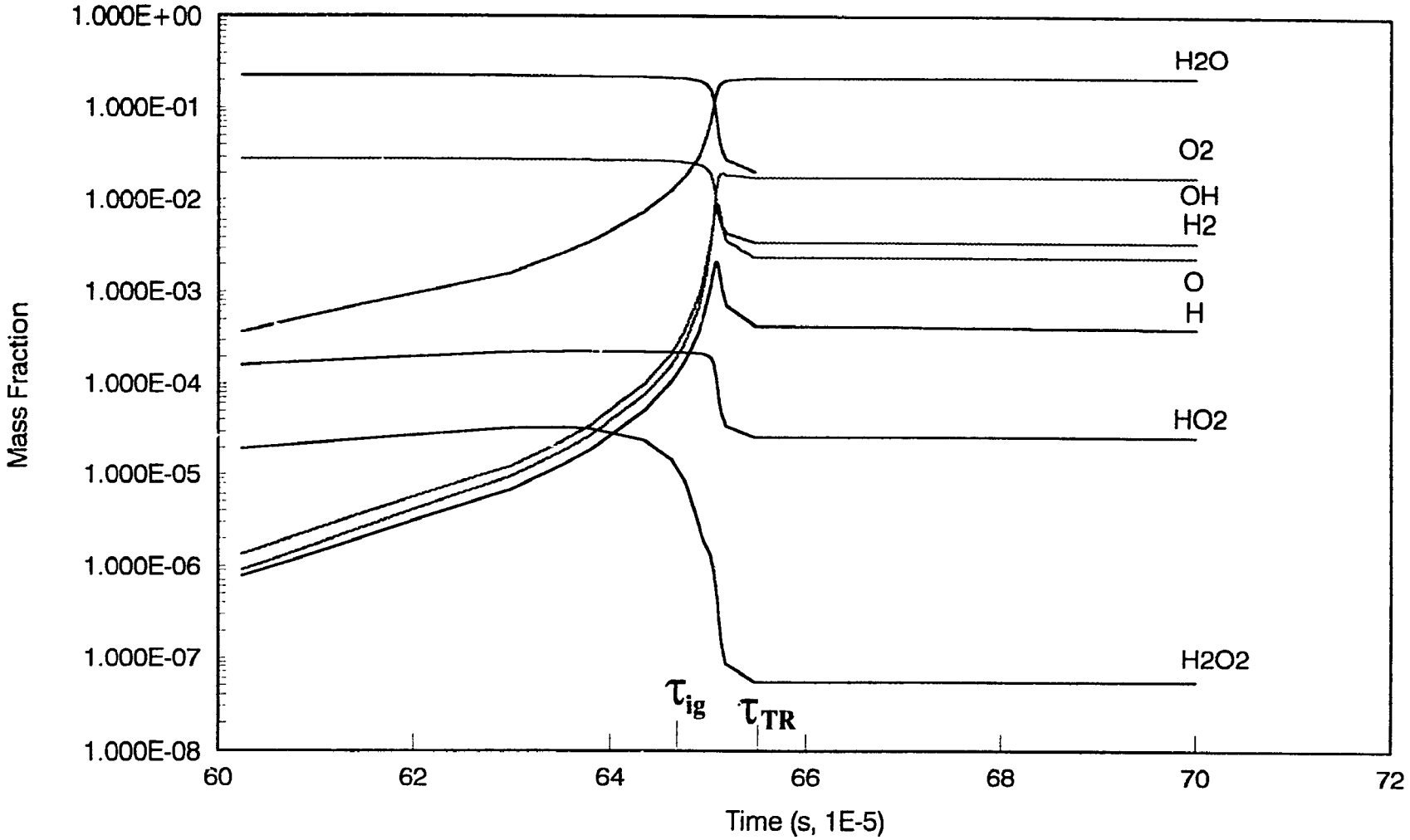

Figure 5.1 (c) Species mass fraction as function of time
Po =2.0 atm, To = 1000K, $\phi = 1.0$, M = 5.0

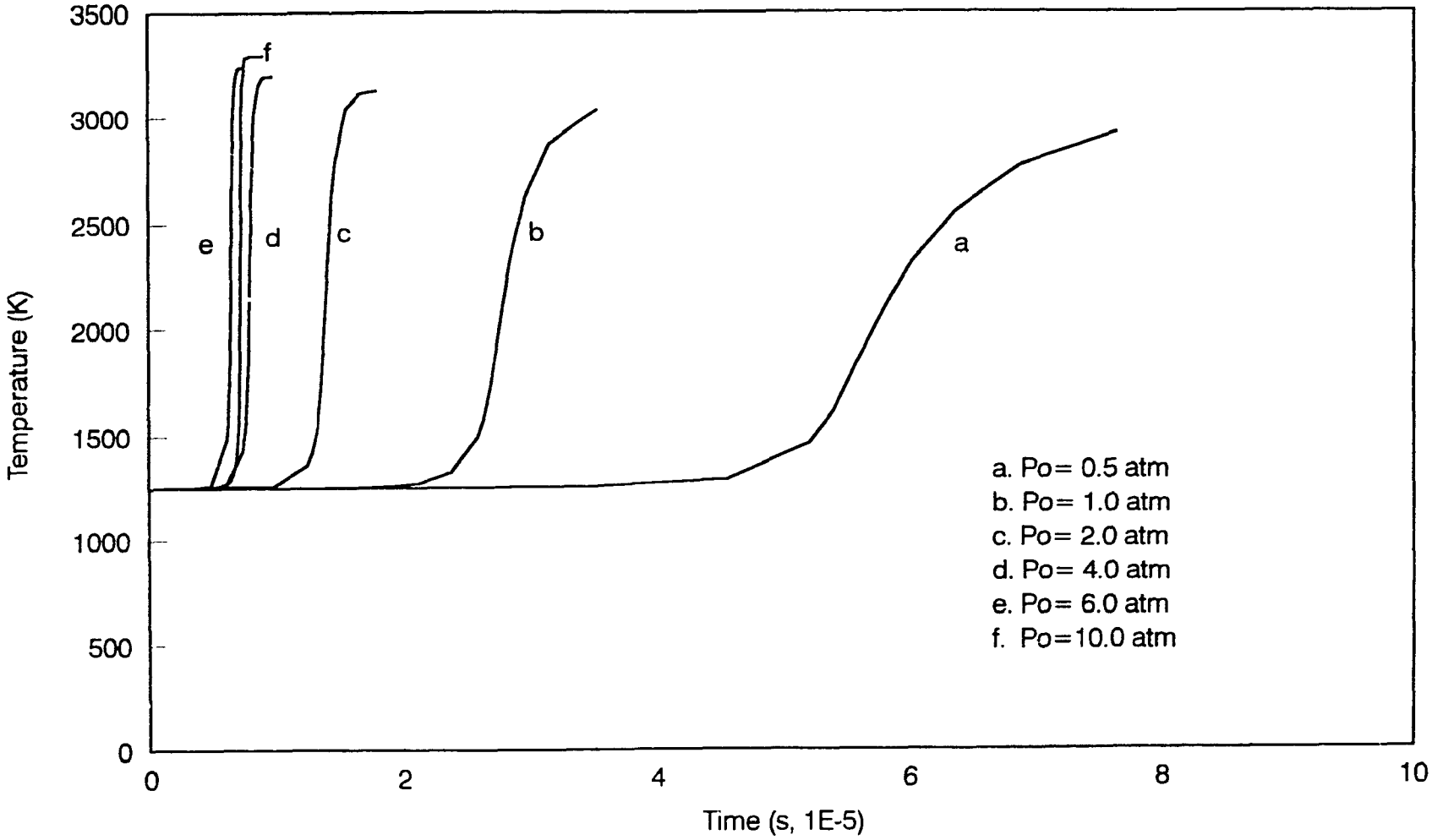

Figure 5.2 (a) Temperature - time histories at T_i =1250K, ϕ=1.0, M = 5.0

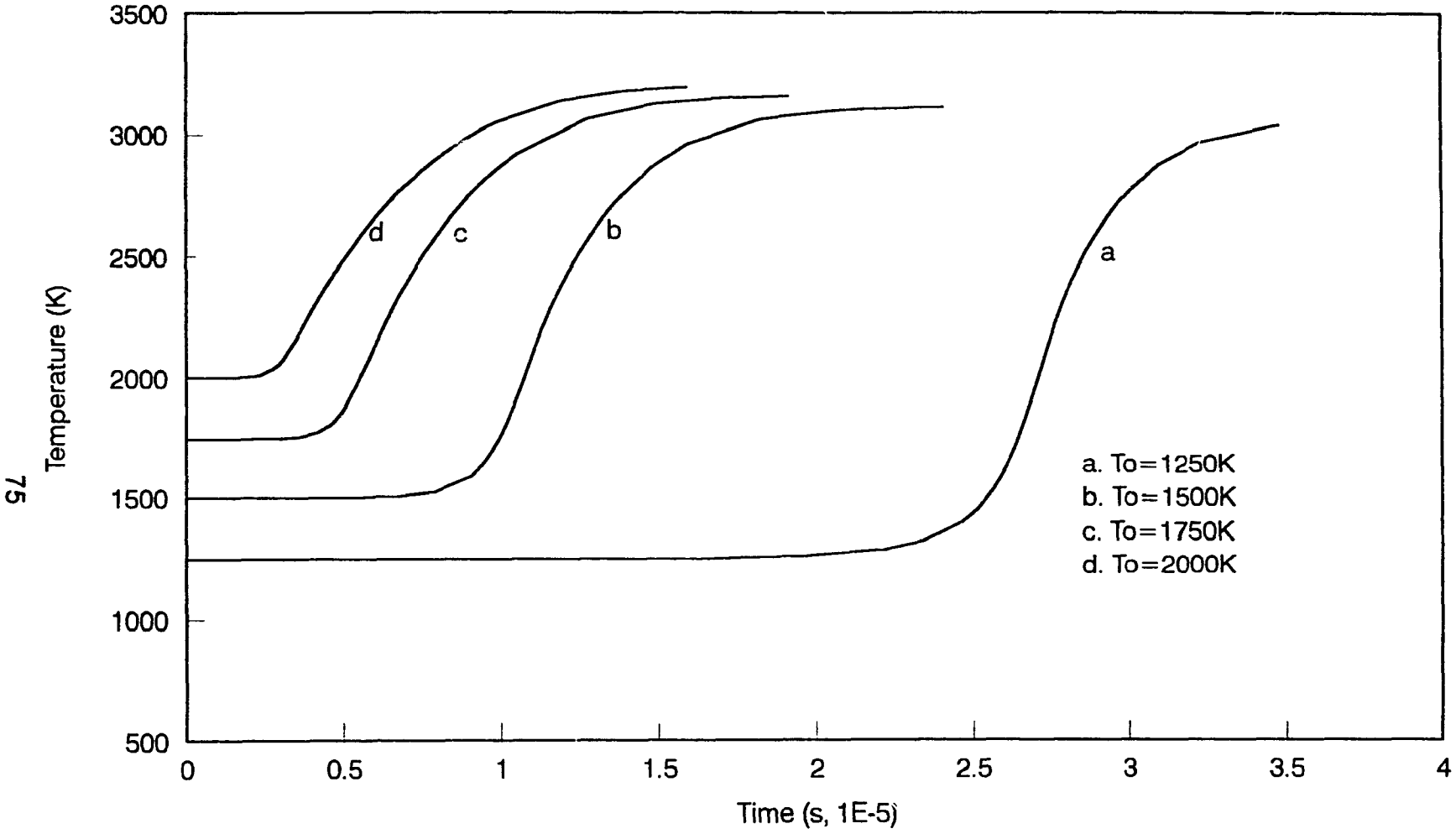

Figure 5.2 (b) Temperature - time histories at Po=1.0 atm, ϕ=1.0, M = 5.0

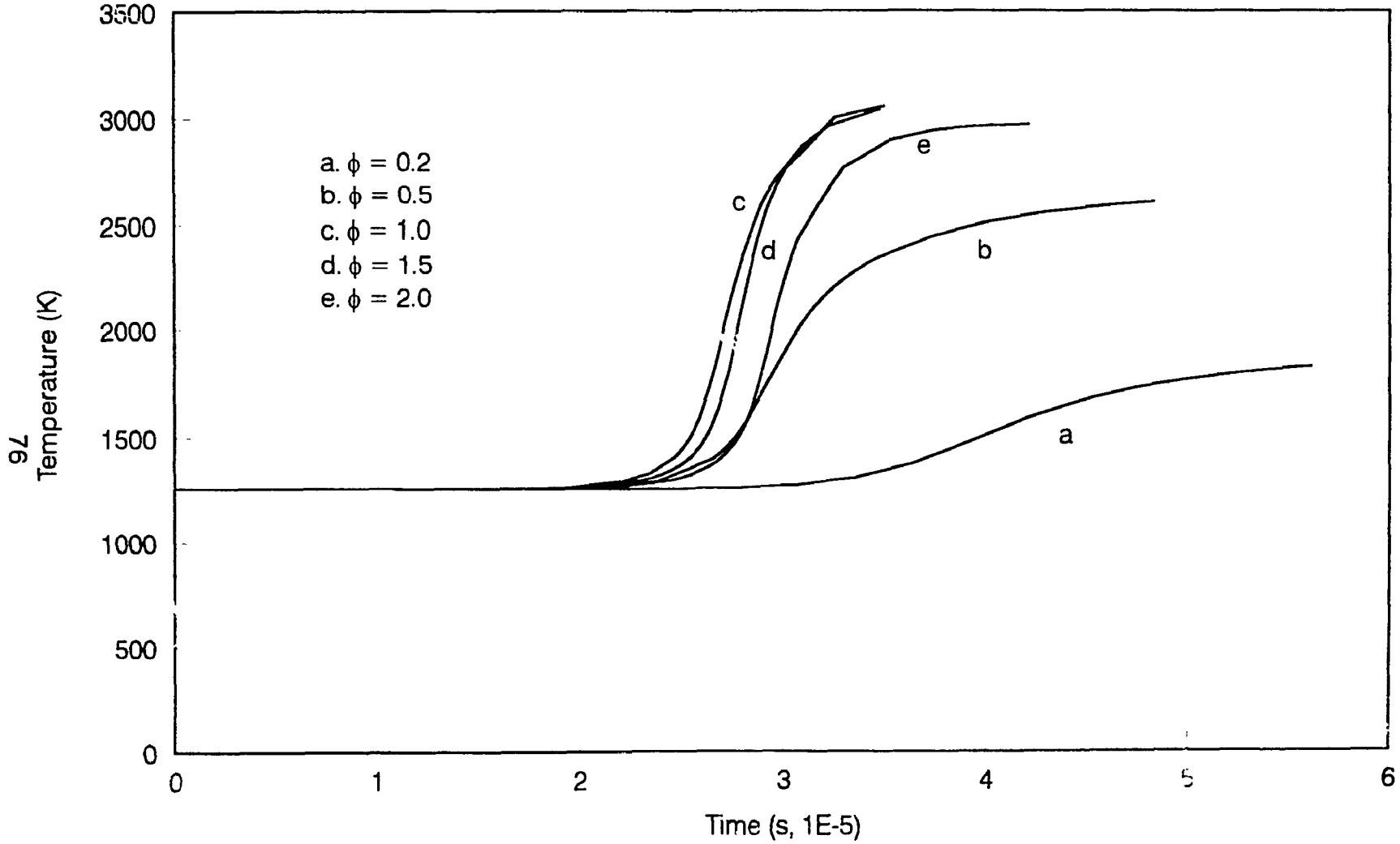

Figure 5-2 (c) Temperature - time histories at Po= 1atm, To= 1250K, M= 5.0

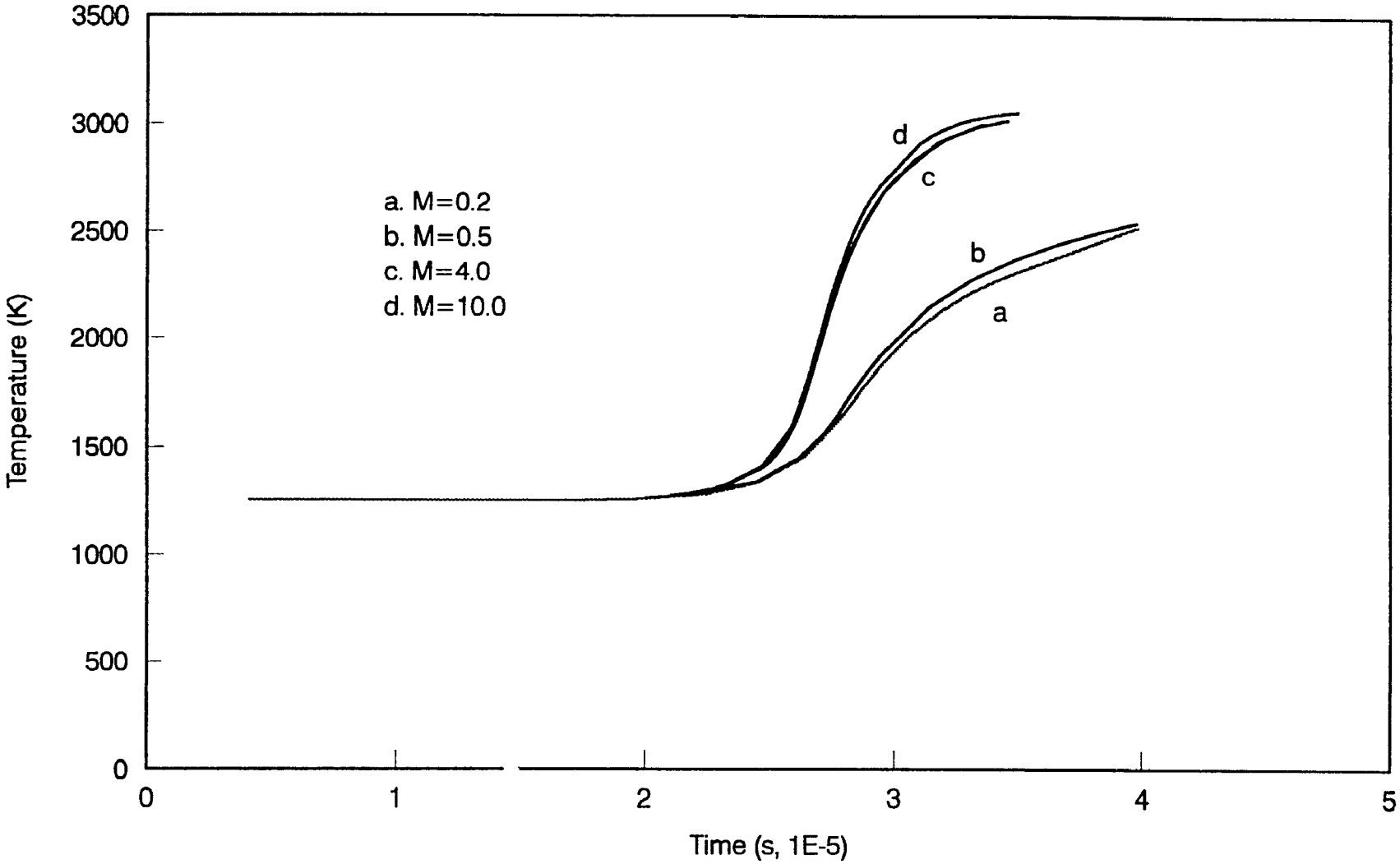

Figure 5-2 (d) Temperature - time histories at P.,= 1.0atm, To= 1250K, ϕ= 1 0

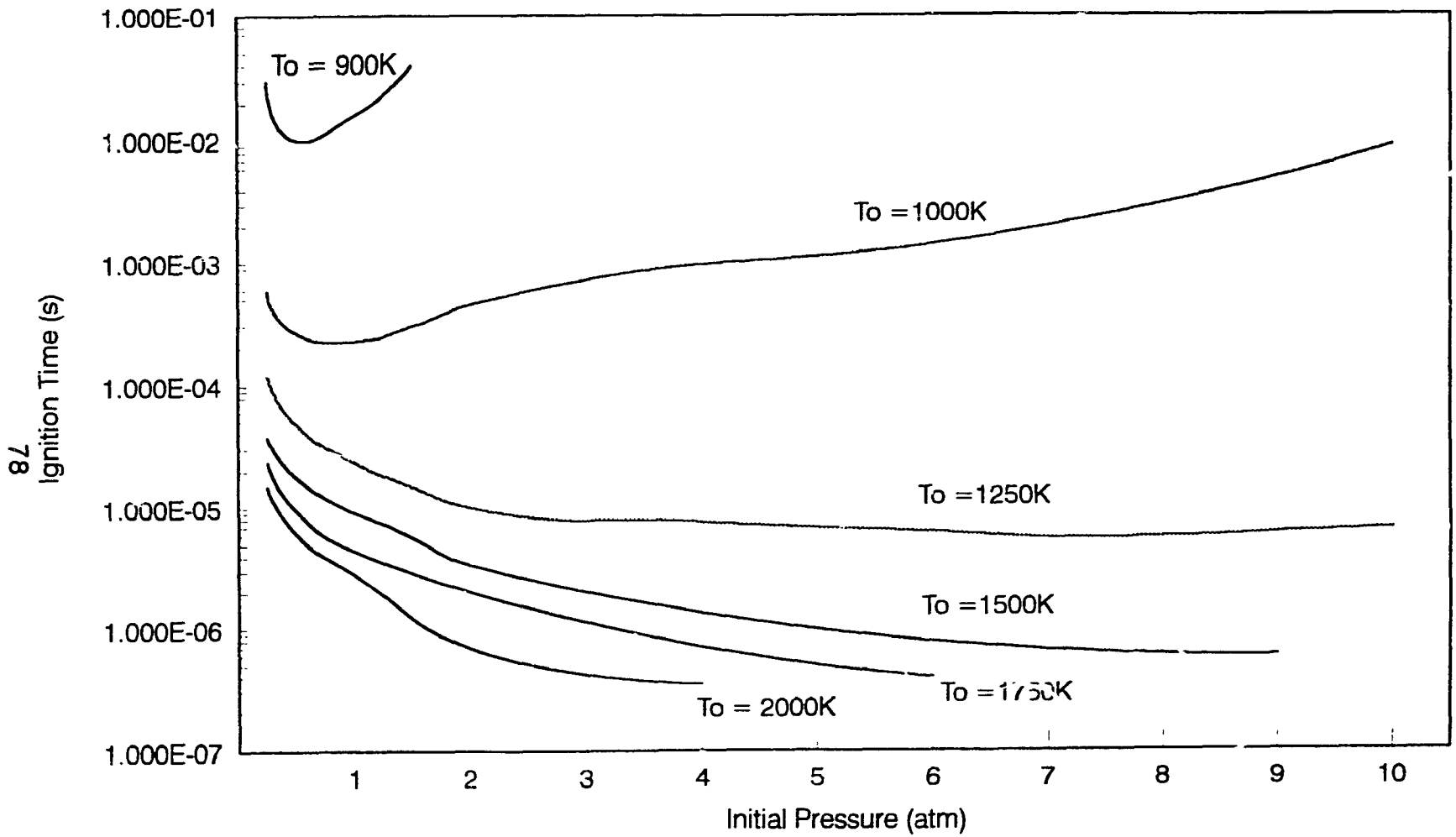

Figure 5-3 The effects of initial pressure on ignition time, ϕ=1.0, M = 5.0

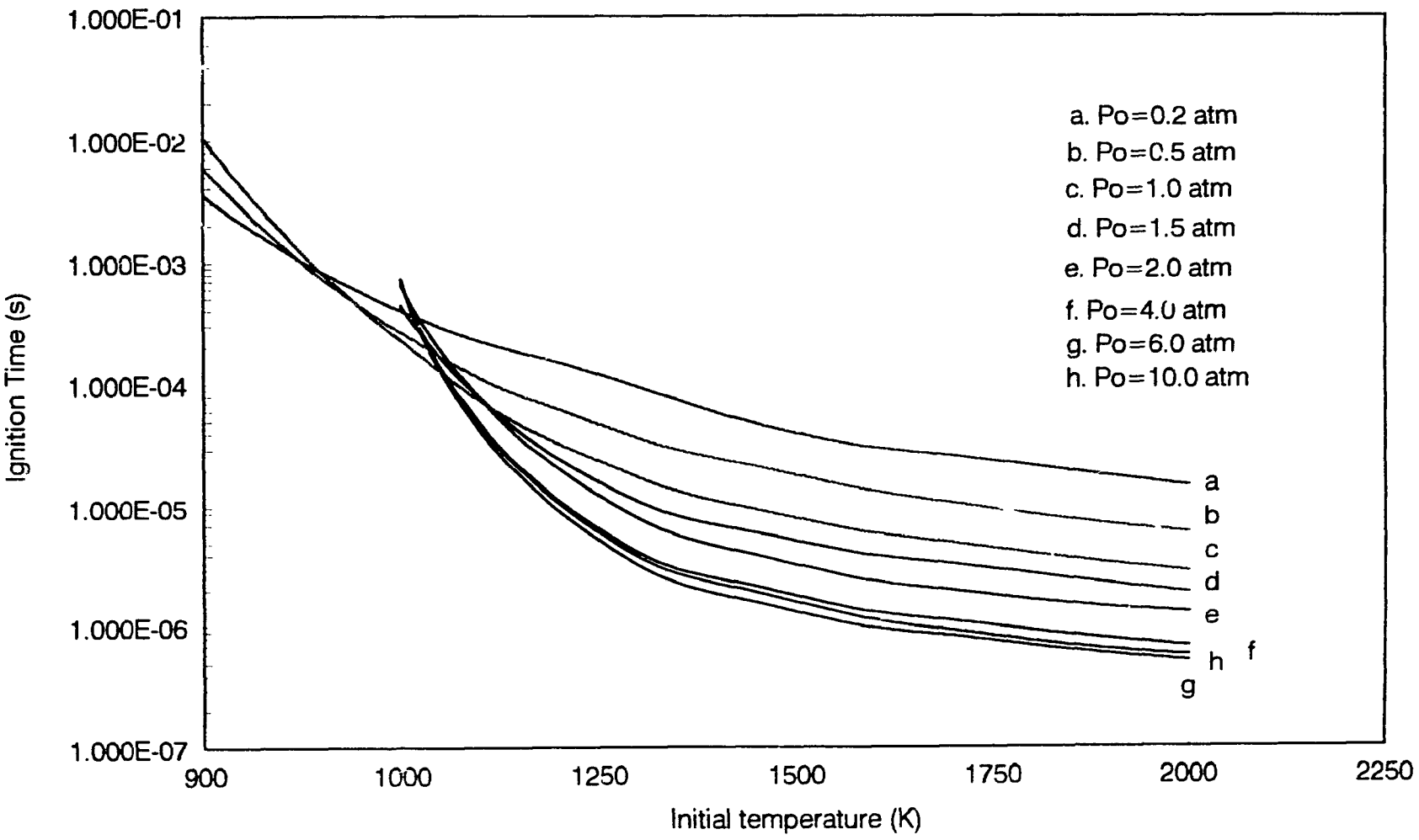

Figure 5.4. The effects of initial tepmerature on ignition time. ϕ = 1.0, M = 5.0

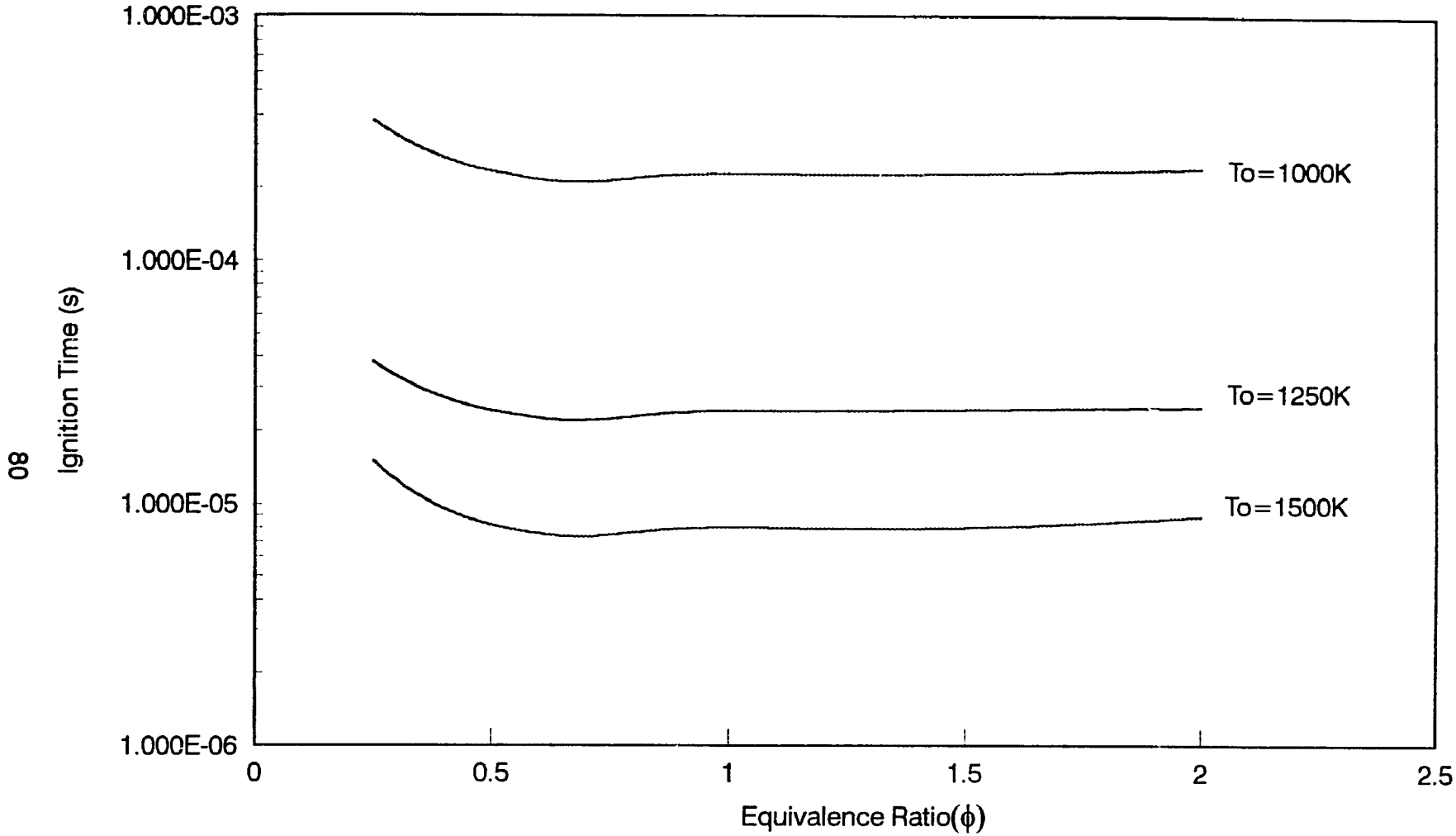

Figure 5.5 Effects of equivalence ratio on ignition time, Po = 1.0 atm, M = 5.0

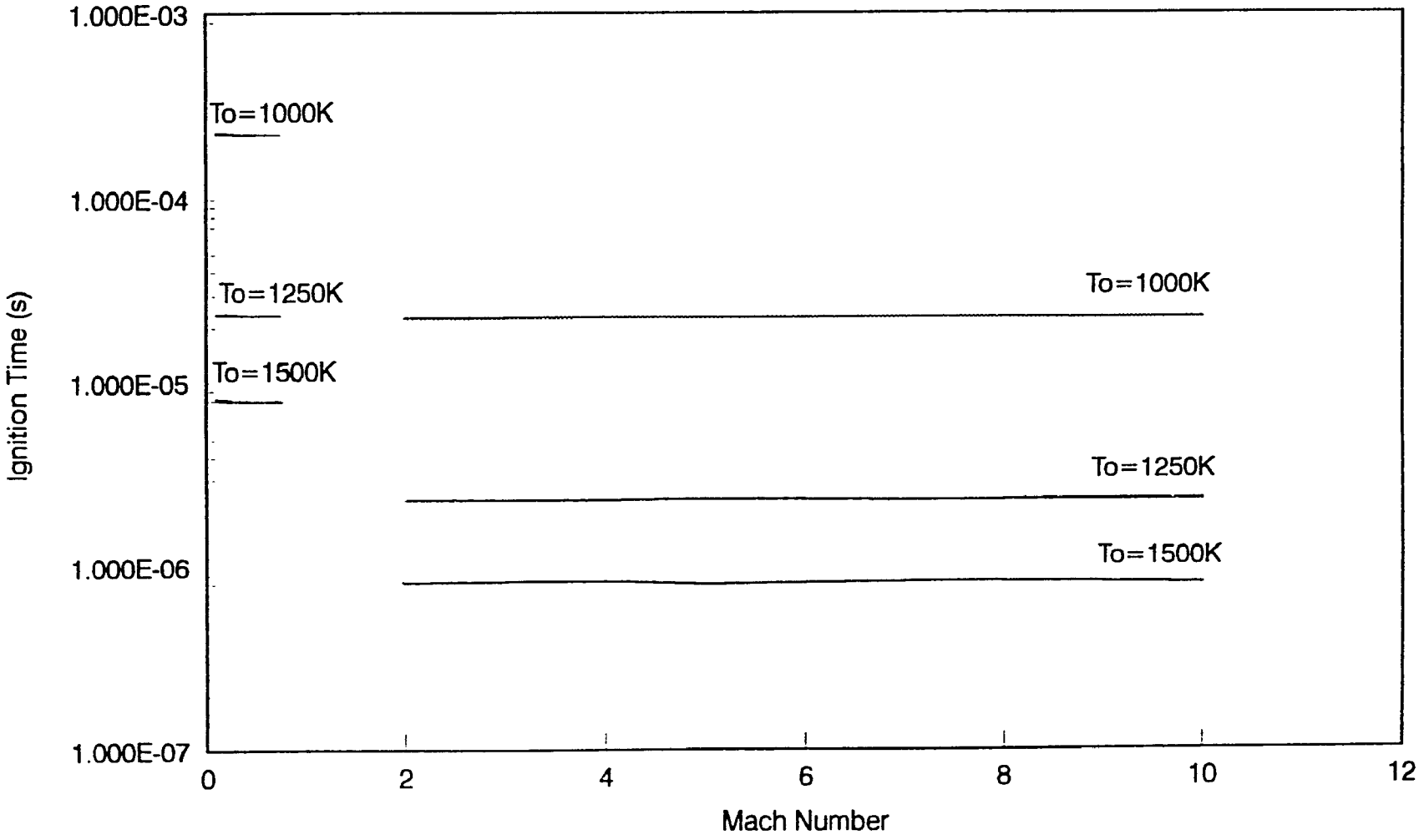

Figure 5.6 The effects of Mach number on ignition time at ϕ = 1.0, Po = 1atm.

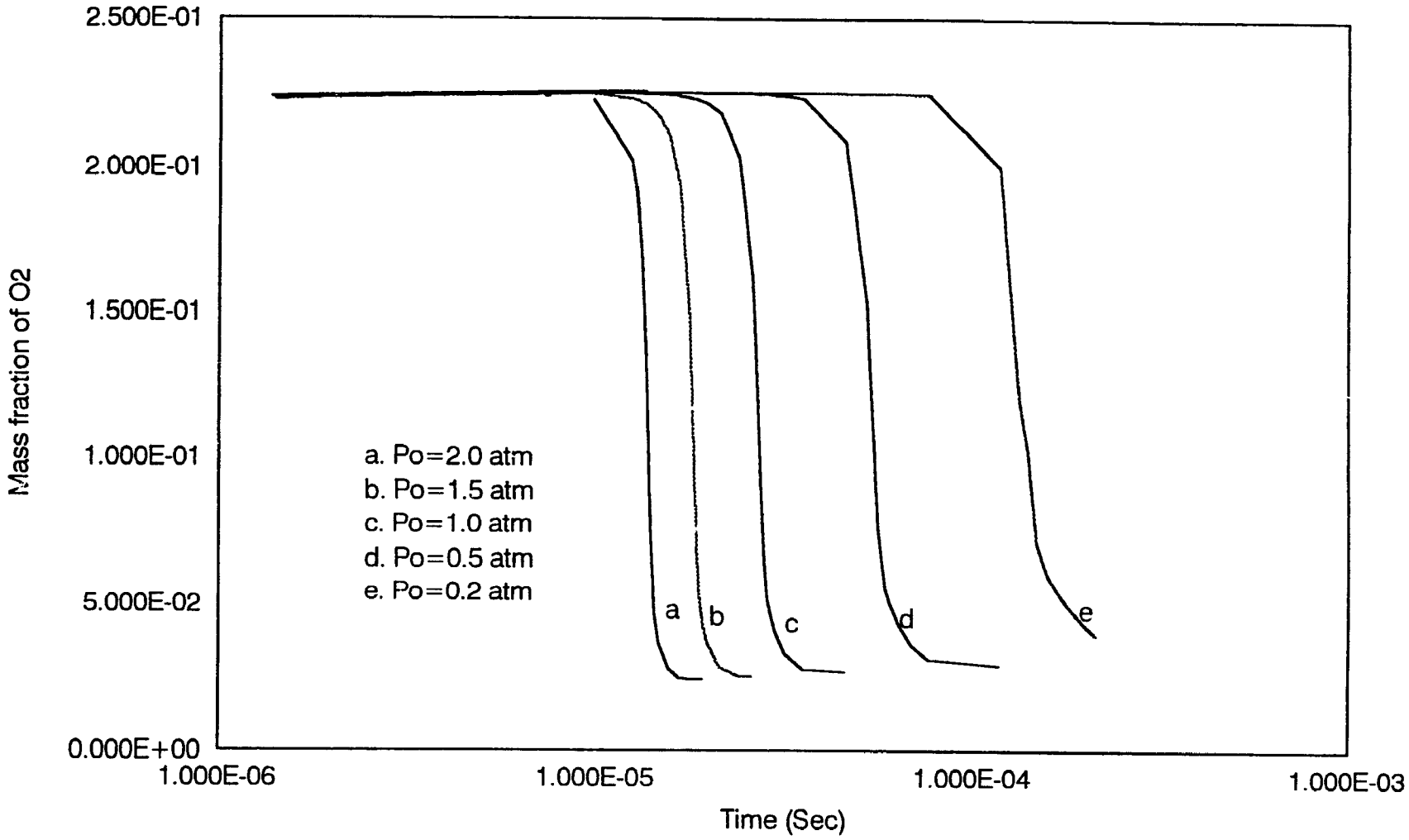

Figure 5.7 (a) Composition - time histories at To=1250K, ϕ=1.0, M= 5.0

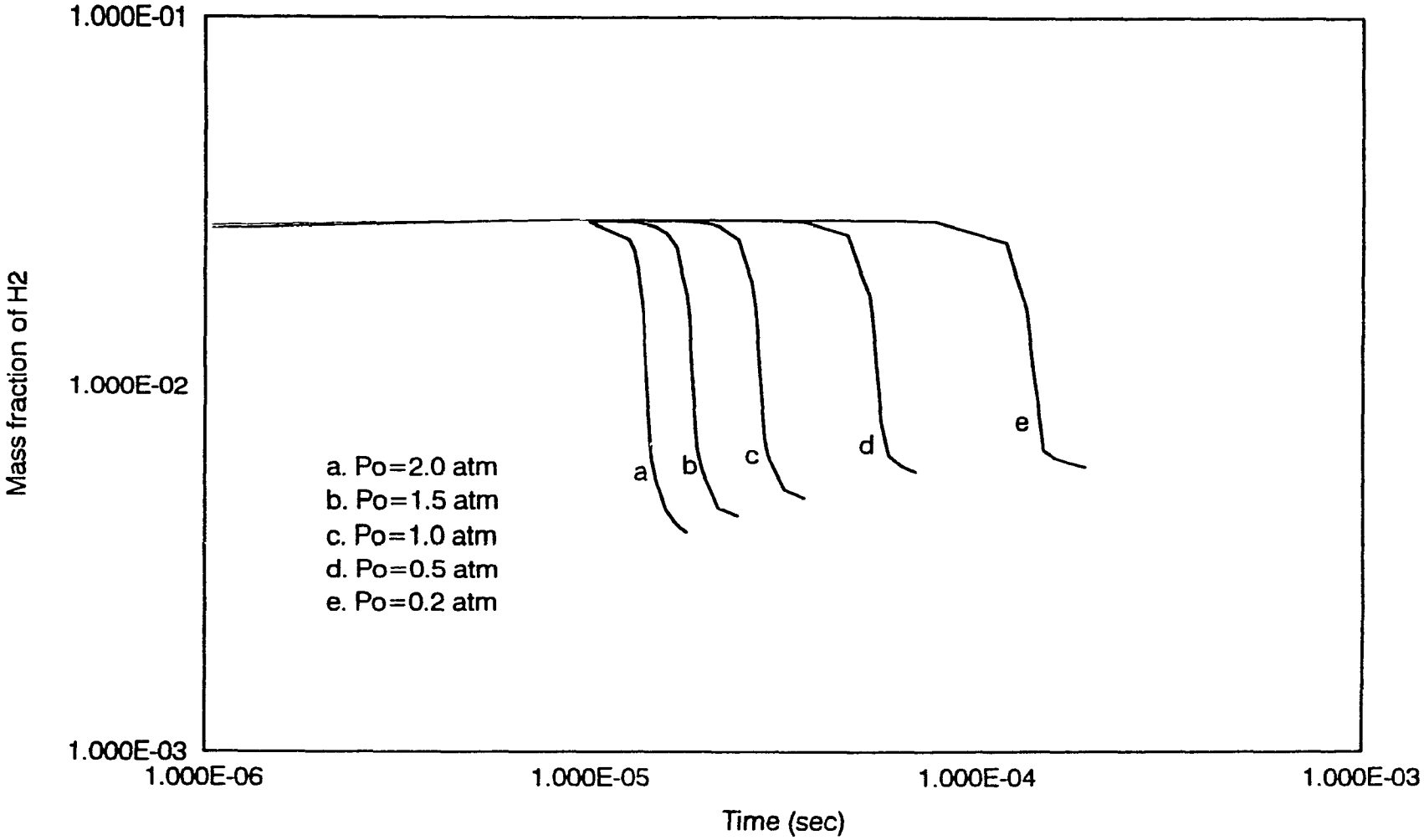

Figure 5.7 (b) Composition - time histories at To=1250K, ϕ=1.0, M=5.0

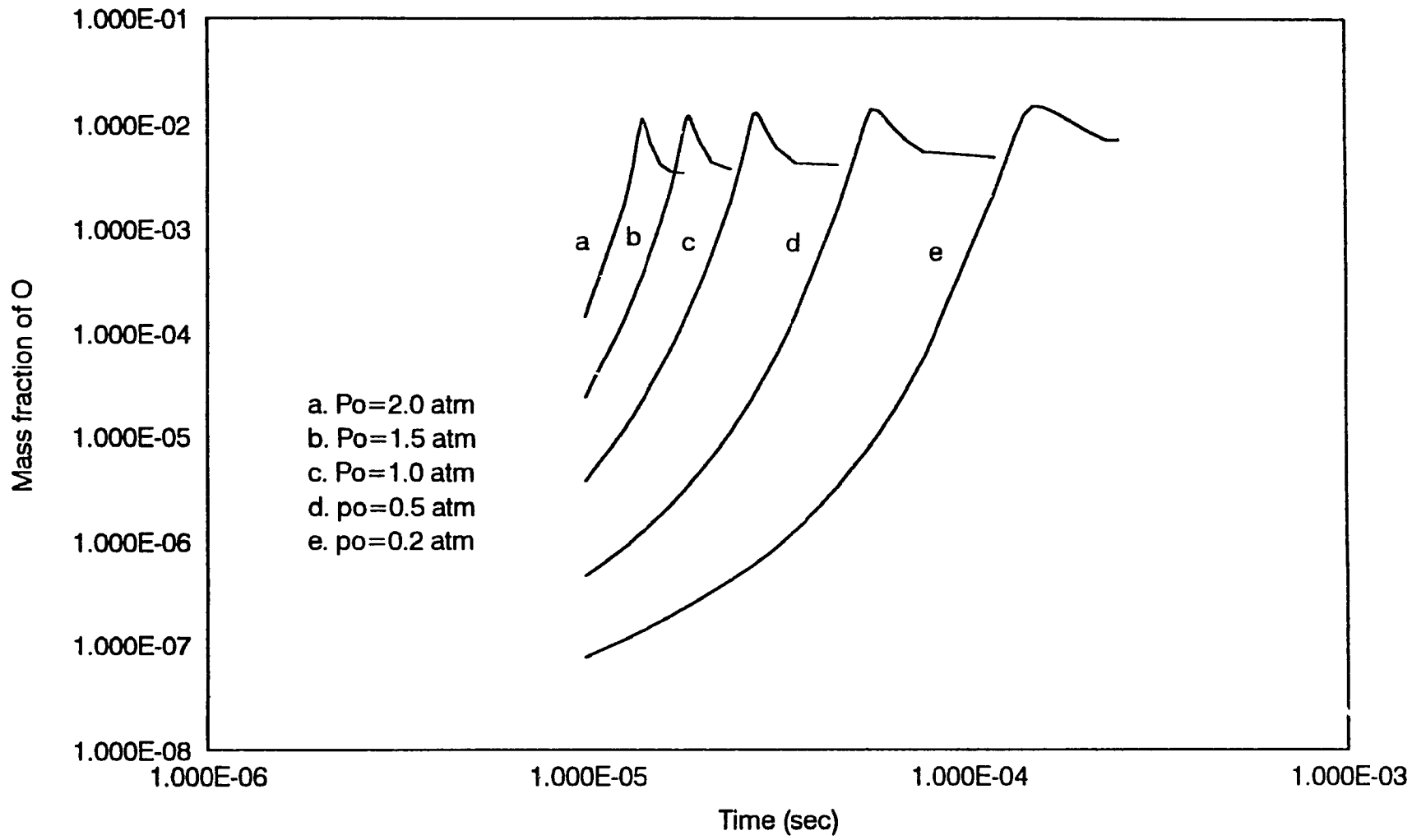

Figure 5.7 (c) Composition - time histories at To=1250K, ϕ=1.0, M = 5.0

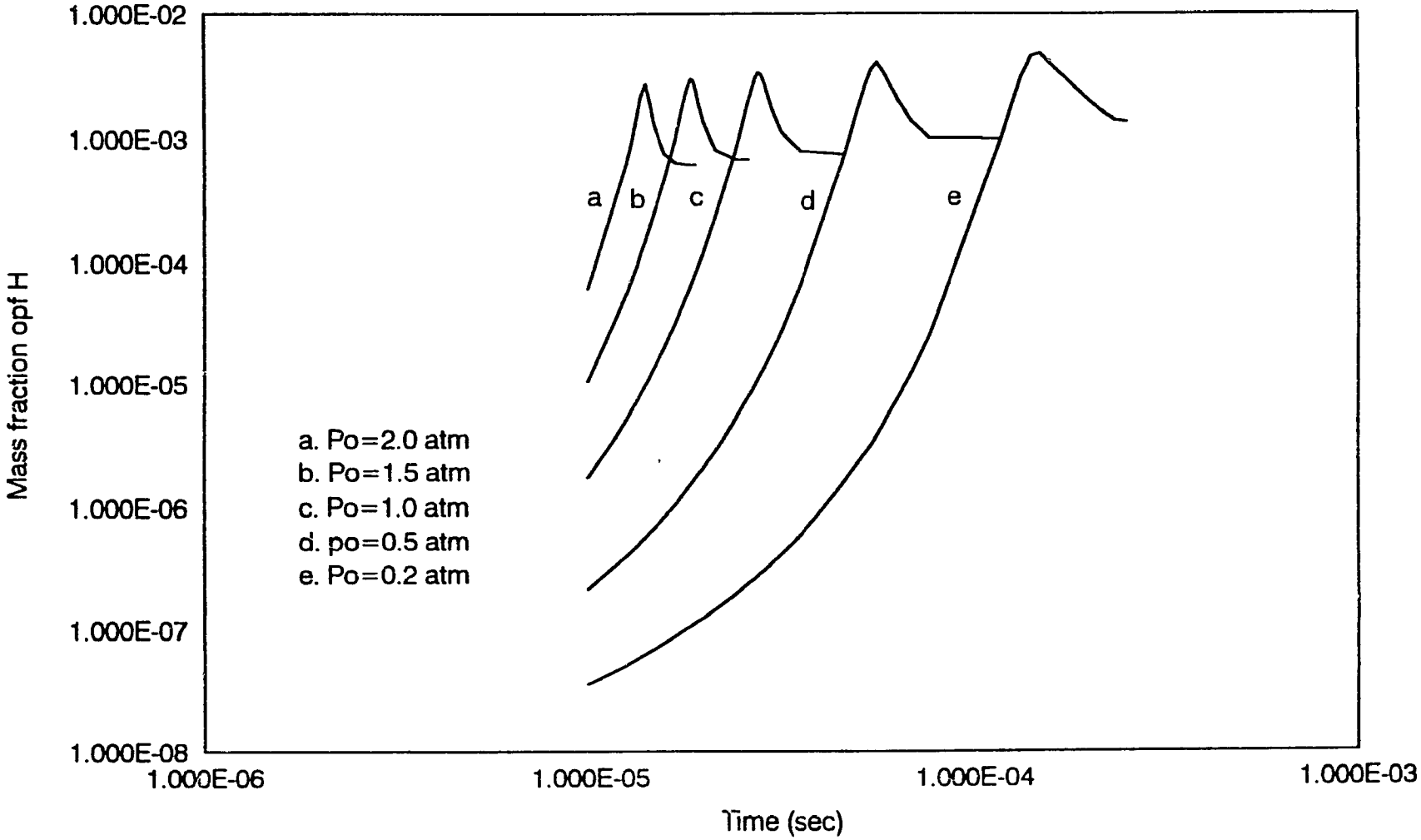

Figure 5.7 (d) Composition - time histories at To=1250K, ϕ=1.0, M= 5.0

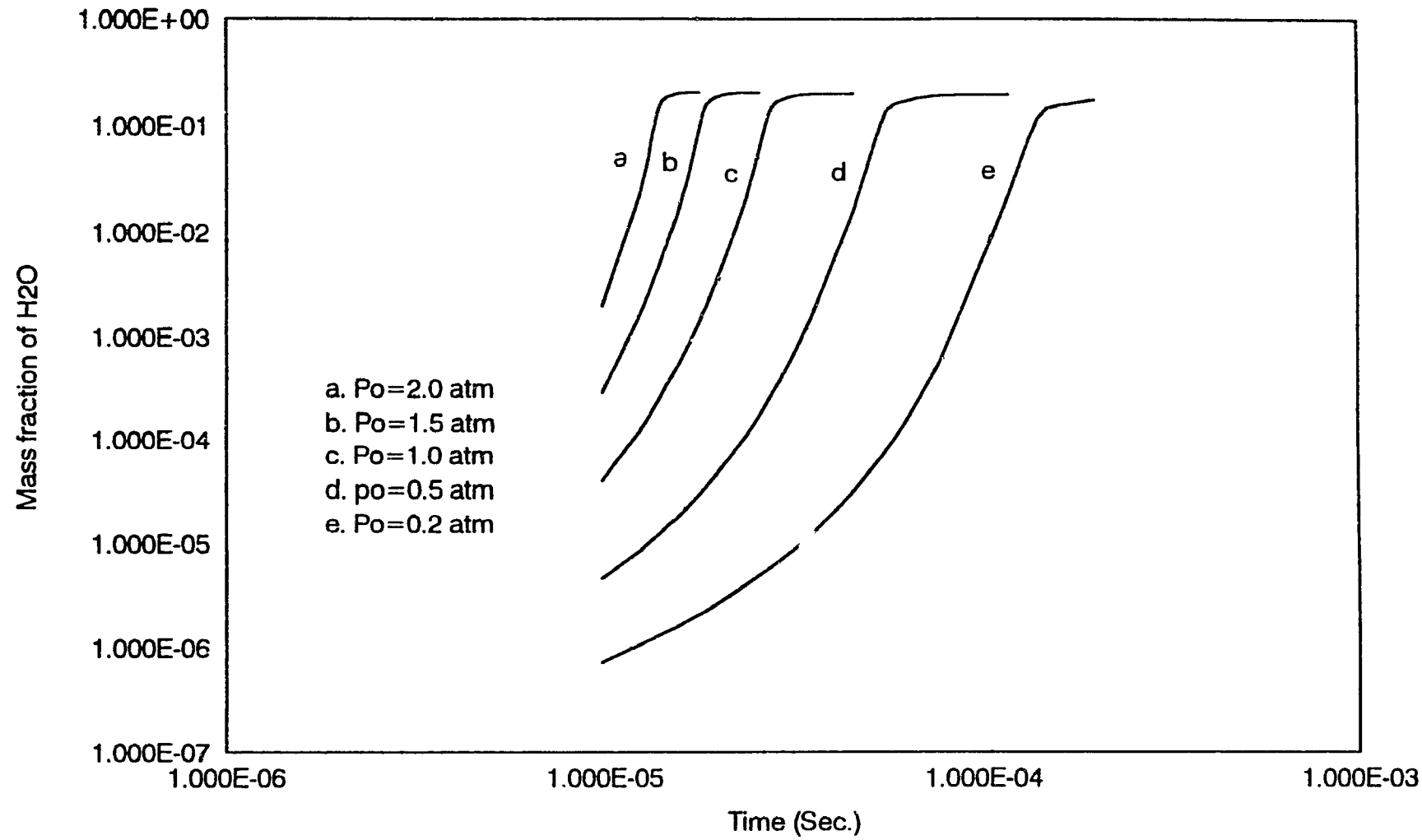

Figure 5.7 (e) Composition - time histories at To=1250K, ϕ=1.0. M = 5.0

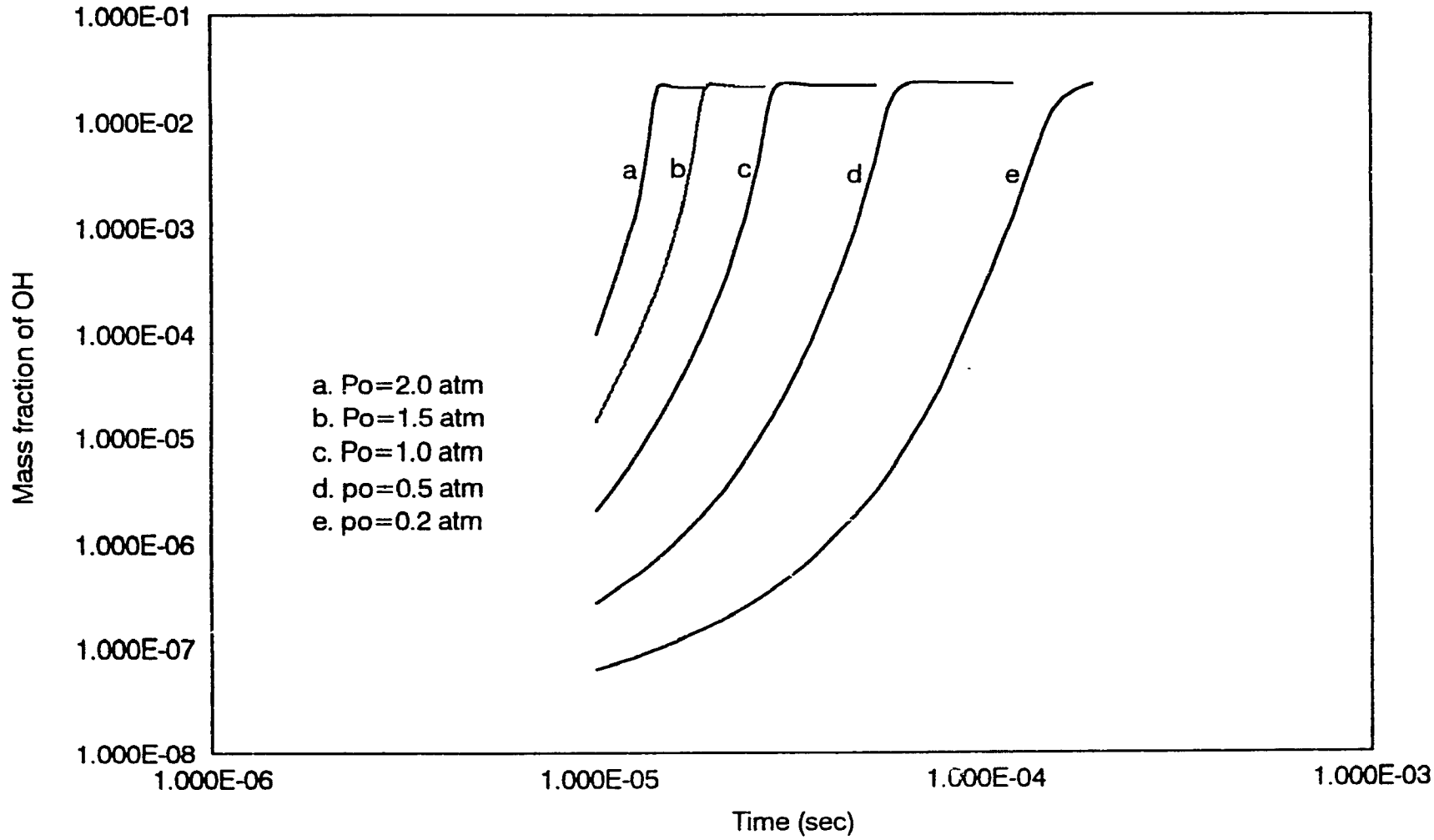

Figure 5.7 (f) Composition - time histories at To=1250K, ϕ=1.0, M = 5.0

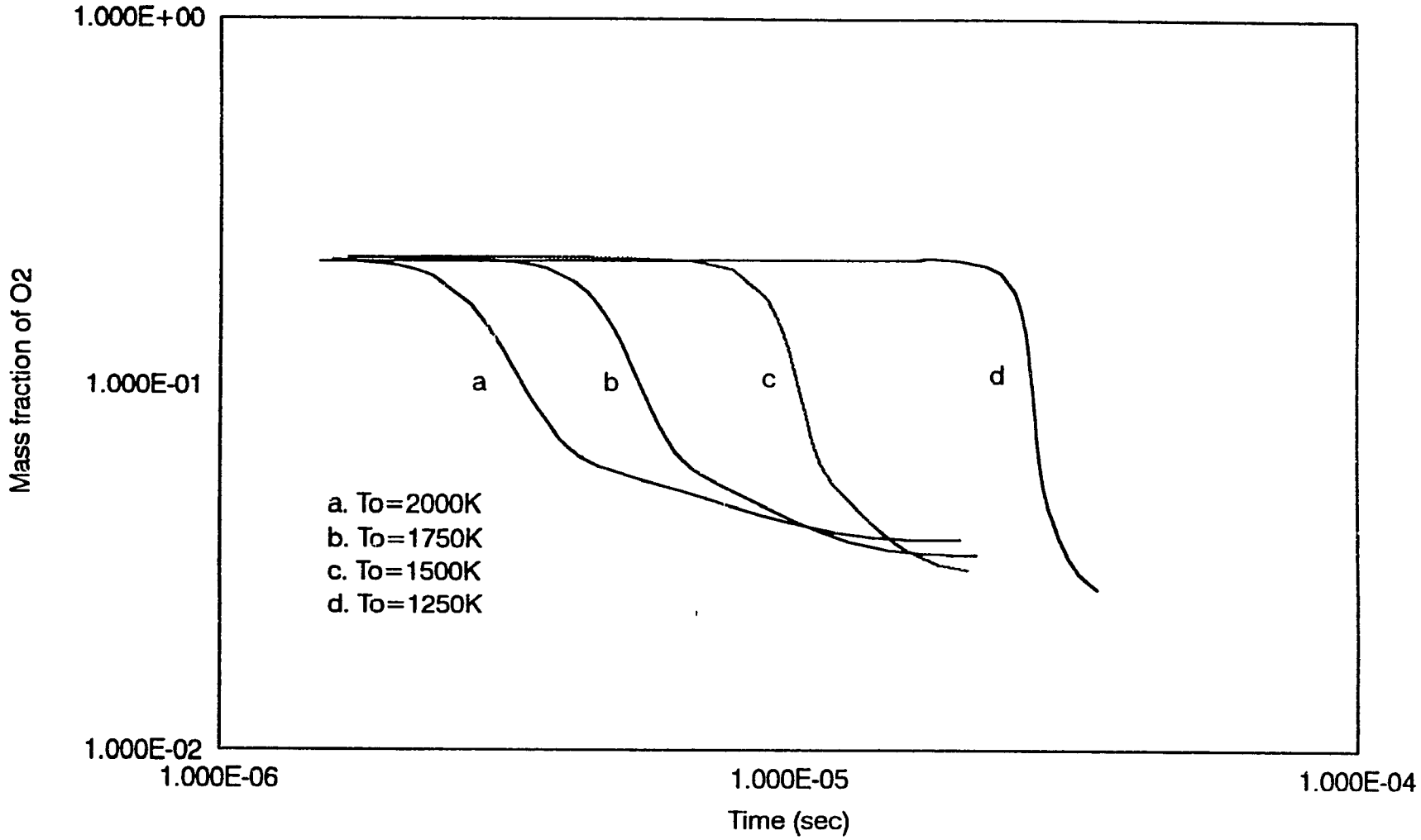

Figure 5.8(a) composition - time histories at Po=1.0 atm, ϕ=1.0, M = 5.0

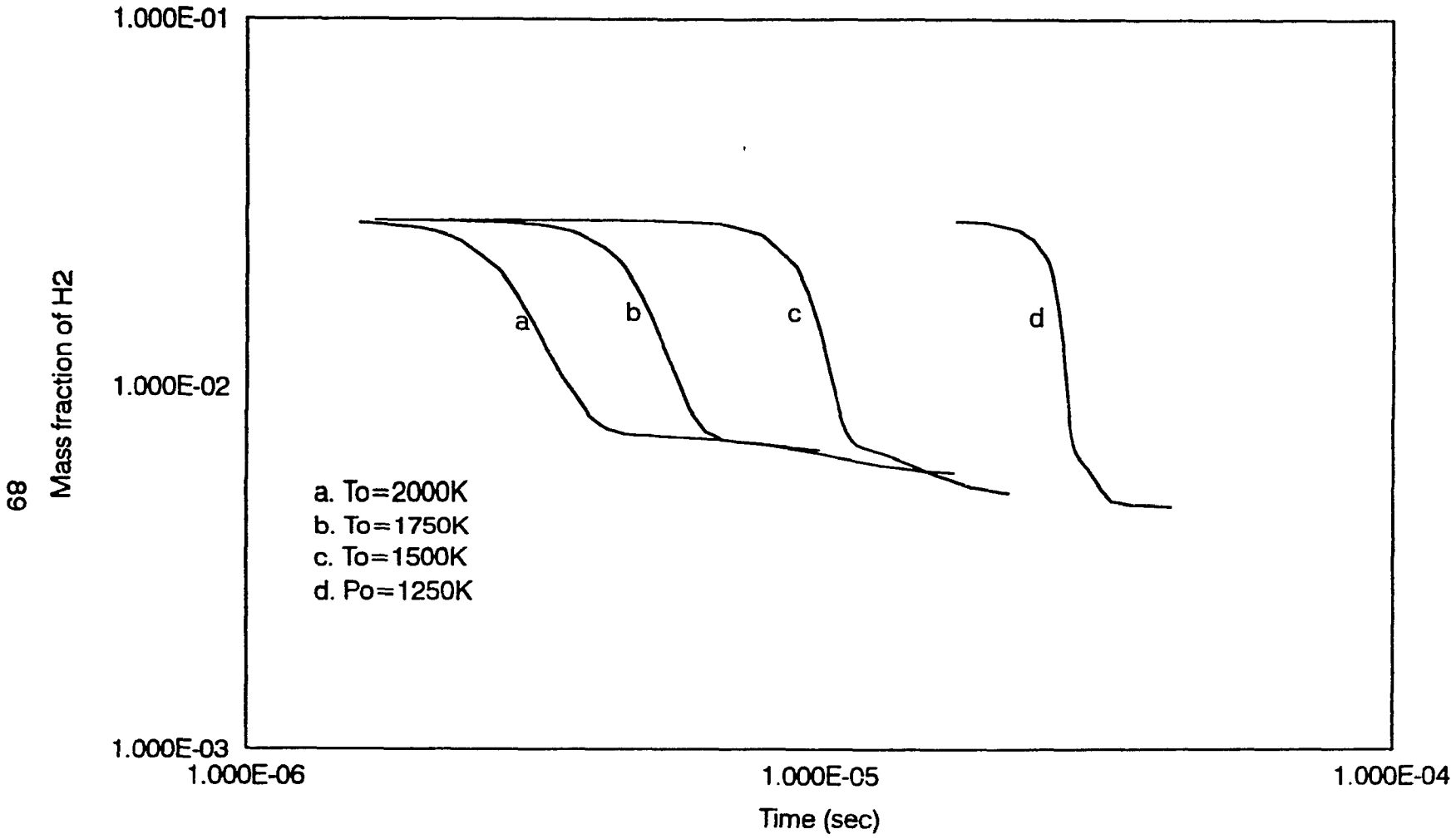

Figure 5.8 (b) Composition - time histories at Po=1.0 atm, ϕ=1.0, M =5.0

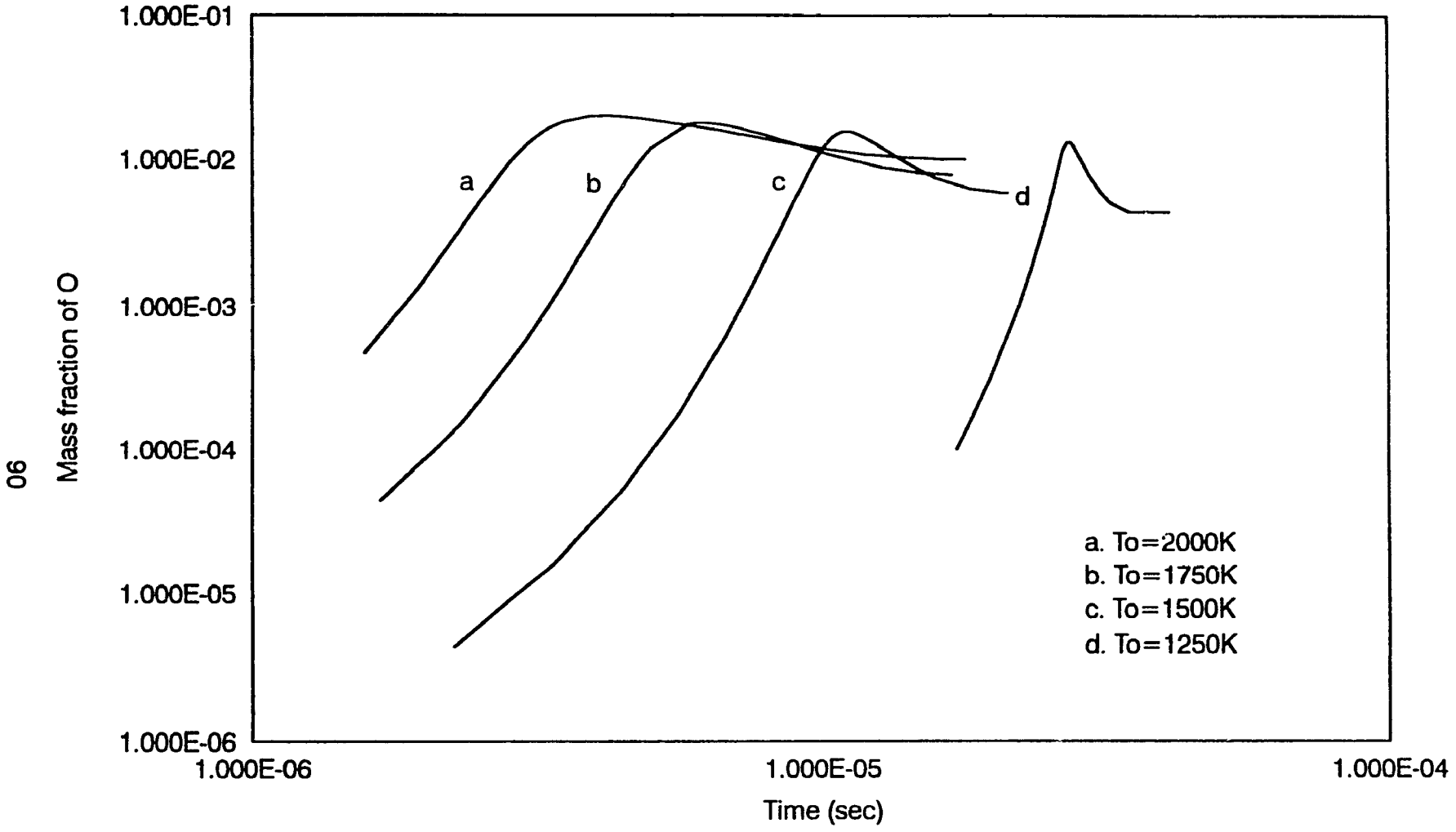

Figure 5.8 (c) Composition - time histories at Po=1.0 atm, ϕ=1.0, M = 5.0

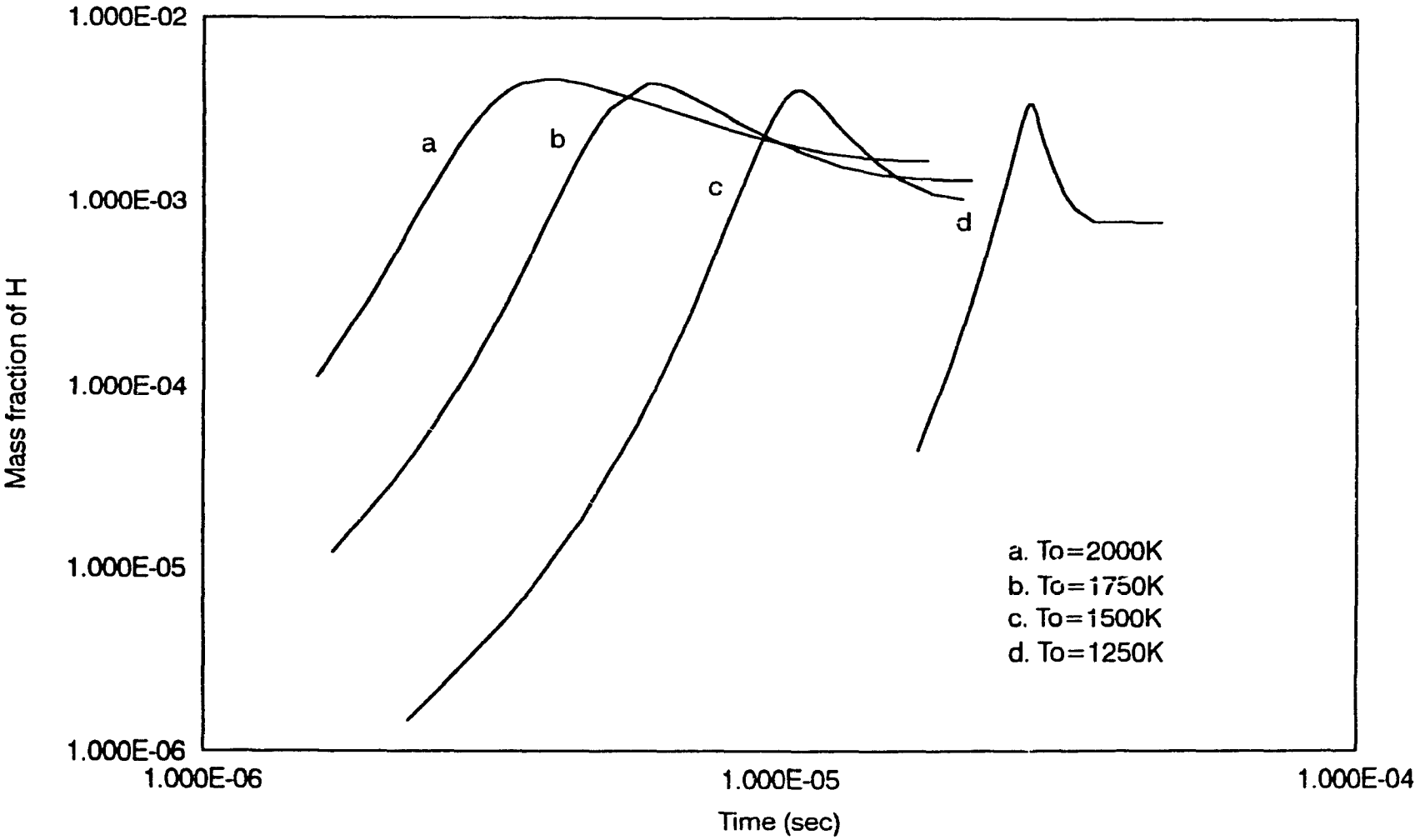

Figure 5.8 (d) Composition - time histories at Po=1.0 atm, ϕ=1.0, M = 5.0

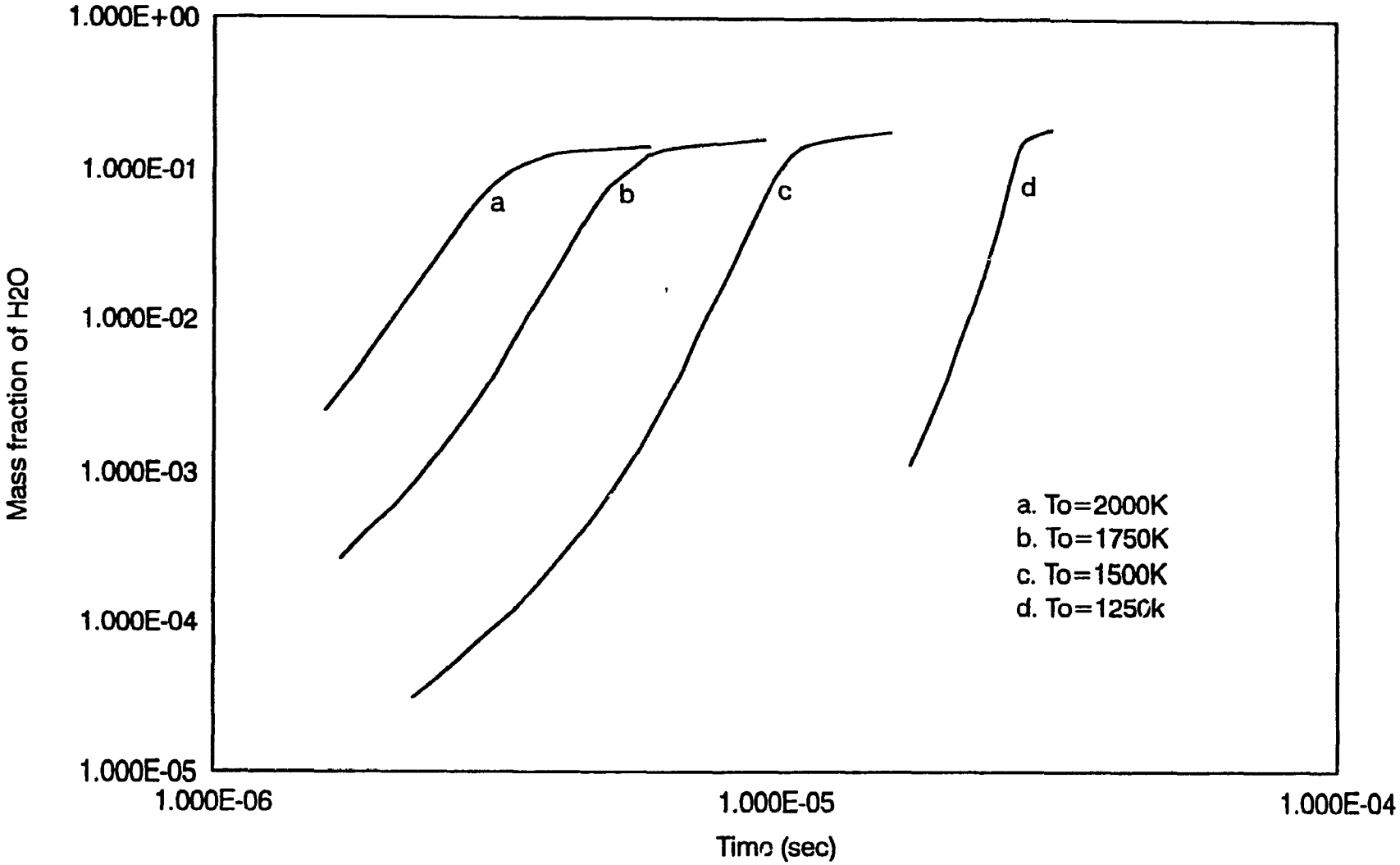

Figure 5.8 (e) Composition - time histories at Po=1.0 atm, ϕ=1.0, M = 5.0

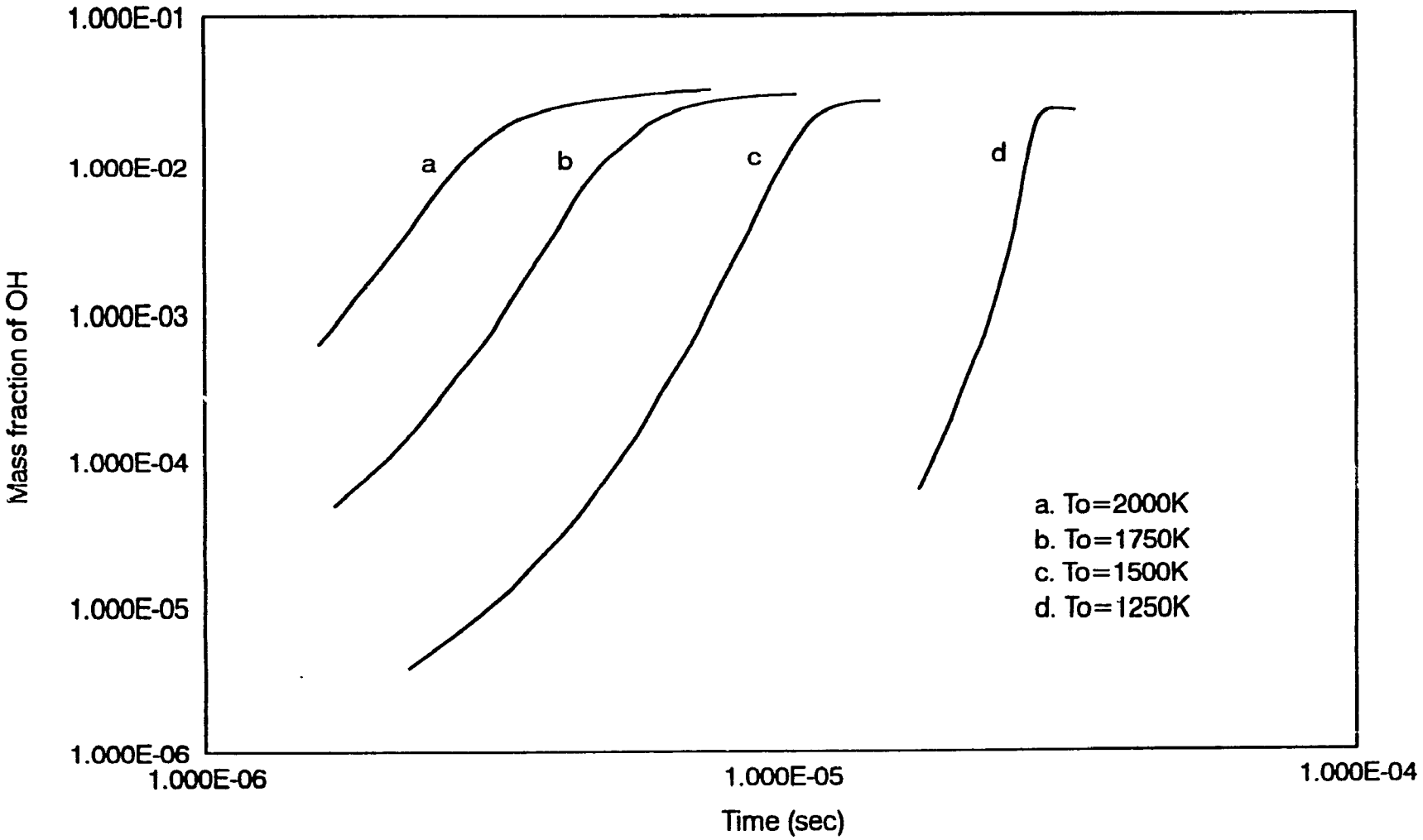

Figure 5.8 (f) Composition - time histories at Po=1.0 atm, ϕ=1.0, M = 5.0

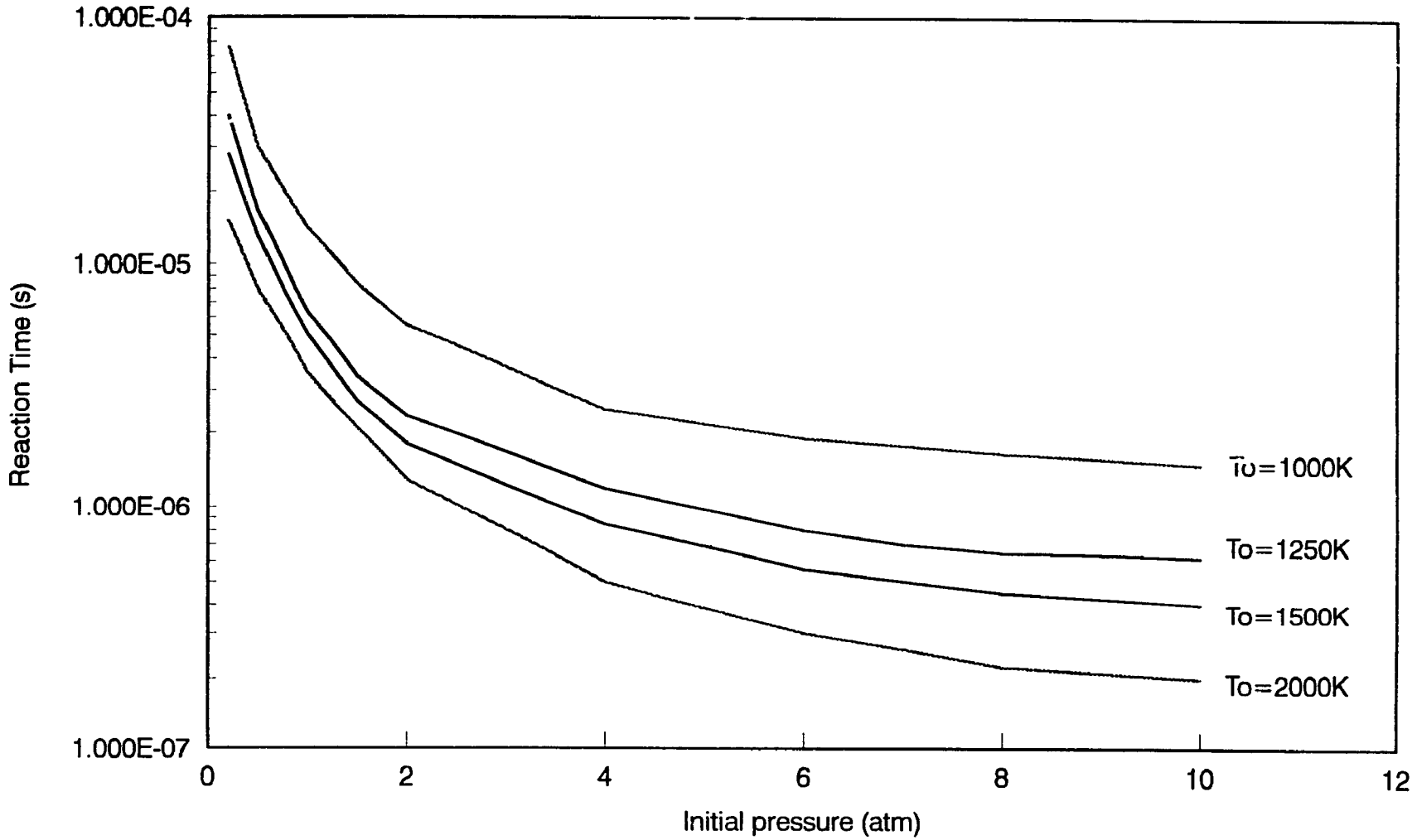

Figure 5.9 The effects of initial pressure on reaction time with initial temperature as parameter at M = 5.0, ϕ = 1.0

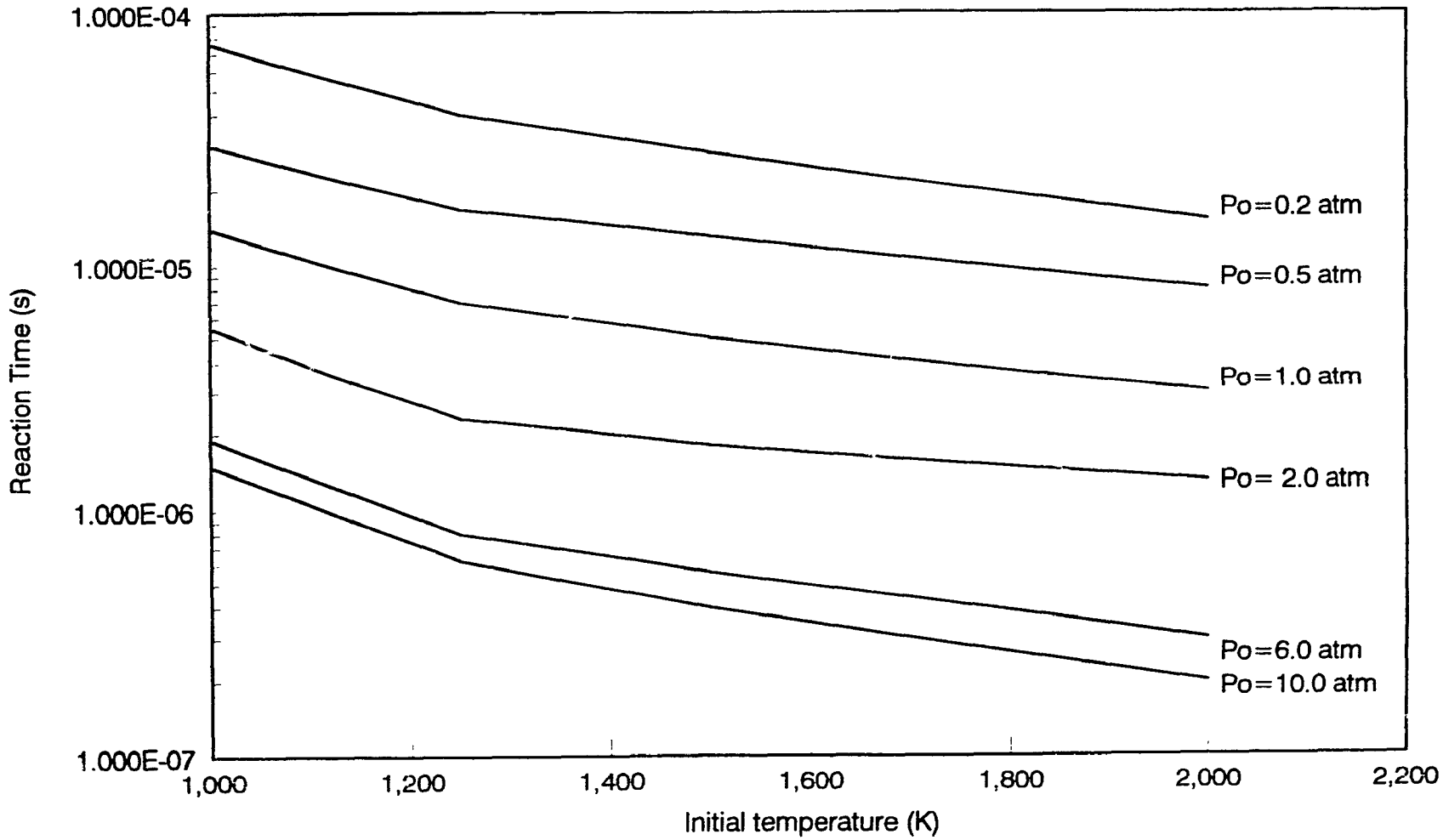

Figure 5.10 The effects of initial temperature on reaction time with initial pressure as parameter at M = 5.0, ϕ = 1.0

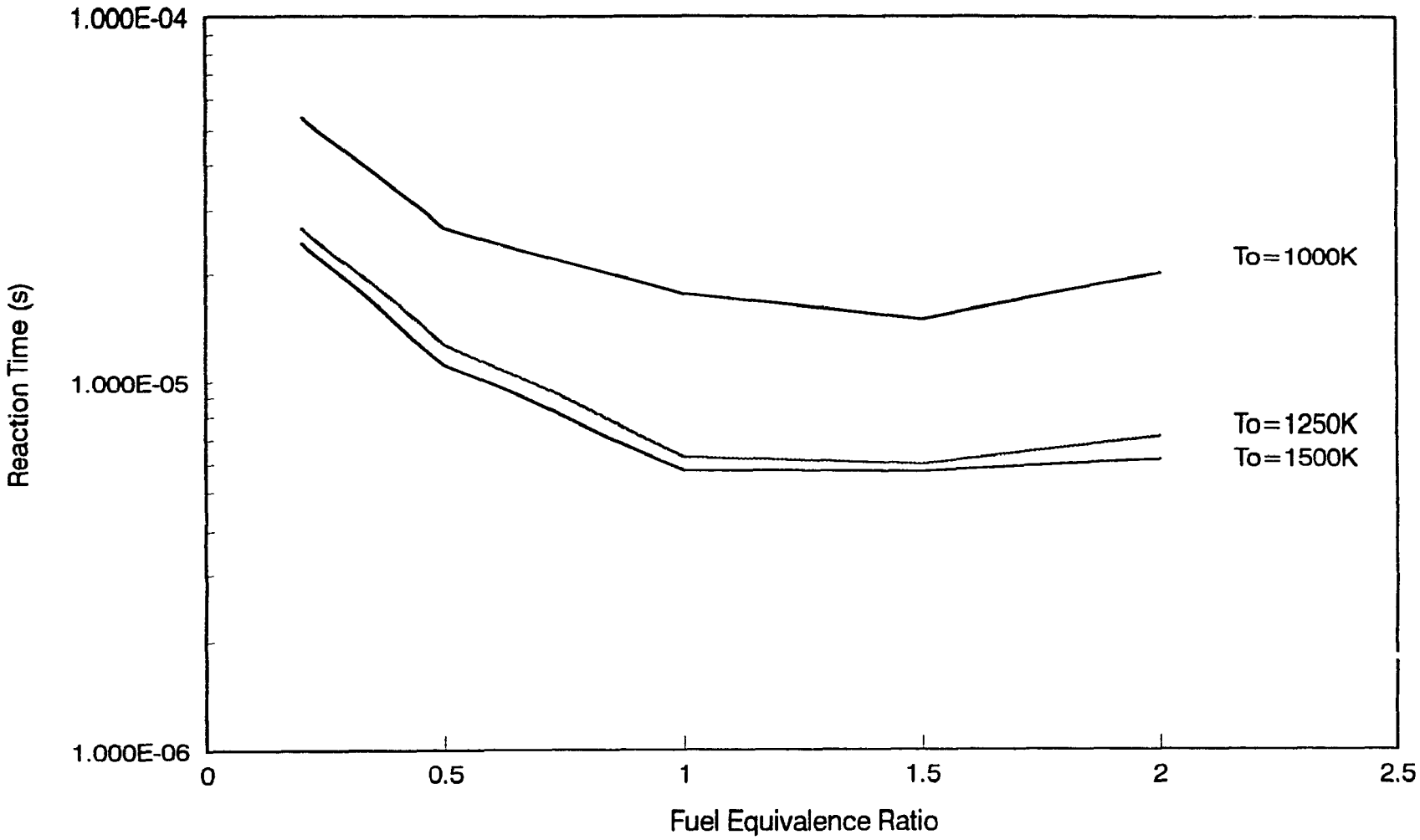

Figure 5.11 The effects of fuel equivalence ratio on reaction time with initial temperature as parameter at Po =1.0 atm, M = 5.0

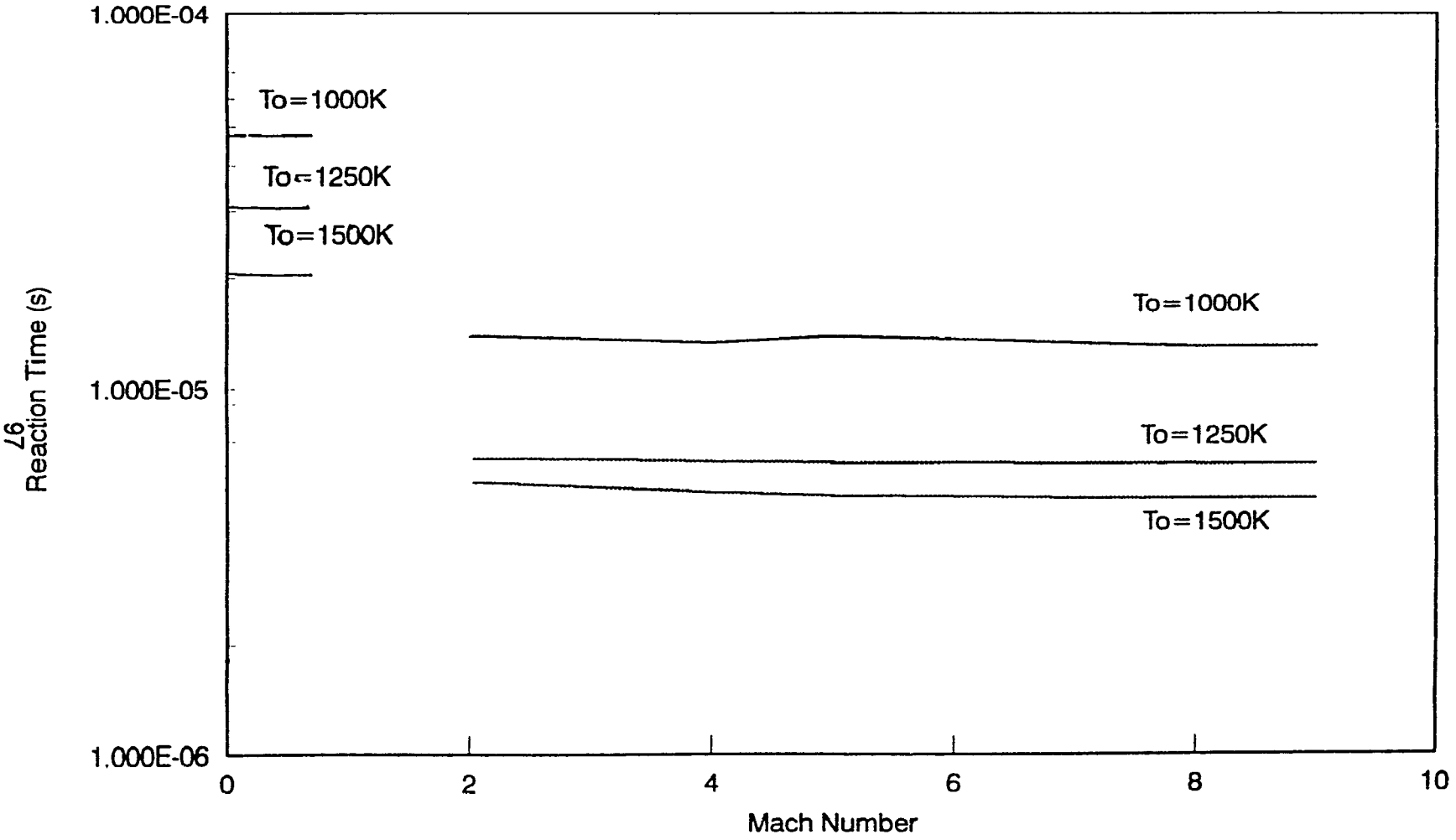

Figure 5-12 The effects of Mach number on reaction time with initial temperature as parameter at Po =1 atm, ϕ = 1.0

CHAPTER 6 QUASI-GLOBAL CHEMICAL KINETIC MECHANISM OF H_2/AIR SUPERSONIC COMBUSTION SYSTEM

6.1 INTRODUCTION

Usually detailed chemical kinetics mechanisms contain a large number of reactions and the species that they possibly happen in the multiple processes. The modelling becomes very complex and usually has computational prohibited. It is very important if one can reduce the number of reactions and species in reaction net work that it will still remaining the predictive capabilities of the mechanism potentially large problem could be solved by using existing technology. In addition the current large scale problem could be moved to the smaller work station computers.

This chapter describes the simplification of the detailed chemical kinetics model of H_2/air supersonic combustion system described in chapter 5 by using sensitivity analysis. The model that we obtain in this chapter is called quasi-global kinetic mechanism of H_2/air supersonic combustion. The comparison of the results obtained from chemical kinetics analysis between the detailed model and the quasi-global model is conducted, in order to indicate the disparities and identities between the two models. Explanations for differential and identical results of the two models are also reported.

6.2 DETAILED SENSITIVITY ANALYSIS

How Does Sensitivity Analysis

In a detailed kinetic scheme not all reactions "contribute" equally to the chemical history. On the contrary, some of them may contribute significantly, some marginally, and some not at all (Frenklach, 1984) Given an overly large full mechanism, one should begin to simplify it immediately by discarding the irrelevant reactions and to identify those which contribute the most The basic concept of sensitivity analysis is already given in Chapter 3, here we take "brute force" method (see Eq (3.32)).

Mention in Chapter 3, the set of the data of the response sensitivities for all rate constant is referred to as a sensitivity spectrum (see Fig.6.1). The highest absolute values of the sensitivities in the spectrum pinpoint the most important reactions in the kinetic scheme for determining the chosen set of responses The lowest absolute values of the sensitivities, however, do not necessarily identify unimportant reactions But for the chemical scheme have more than one important process (or step), such as H_2/O_2 combustion, because there exist ignition step and reaction step, some reactions may not important for first step but good for the second. This principle has been already mentioned in Chapter 5 For multi-step process, the set of data in each step needs to be calculated or a research on chemical mechanism needs to be conducted to for the important reactions. When the reactions having smallest absolute values are removed from the scheme, and the new responses needs to compute and compared to the initial ones If no change is detected, further reactions are removed and the procedure is repeated until the difference in responses becomes larger than the computational errors The removed reactions constitute the least important ones, within the range of the sensitivity test

The Sensitivity Spectrum

In the discussion of Chapter 3, each reaction's rate is determined by the rate constants. Discussions also have been made in Chapter 5, that the effects of the initial pressure, the initial temperature and others on the ignition and the reaction time, actually are since the initial pressure and temperature affect the reaction rate, then it made different ignition and reaction time. If a reaction is sensitive to the system mechanism, the change of the reaction rate must vary the ignition and reaction time dramatically to the system. The method used for making the spectrum, is enlarging one reaction rate at certain time, then put it back to the original scheme. A comparison of the ignition and the reaction times between the enlarging's and original scheme and the enlarging one show the sensitivity of this reaction Repeating this procedure for the reactions, the sensitivity spectrums for the ignition and the reaction time are brought out.

Arranging the set of the rate constants for the reactions from Table 5.1, and then varying their values once at a time by chosen enlargement factor by 5 (typically from 2 to 10). The Figures 6.1 and 6.2 indicate the sensitivities of the ignition-time and the reaction-time for the scheme of 41 reactions For the slowest reactions in both spectrums, which are the most probable candidates for removal, the variations in rate constants should preferably reach the conceivable upper and lower limit values. If no change detected, further reactions that are next level slowest reactions are removed and procedure continued until the difference in response becomes larger than the computational errors (about 15%). The remaining reactions consist a new chemistry scheme that present the mechanism of H_2/O_2 combustion system. It is called reduced mechanism or quasi-global model.Figures 6.1 and 6.2 show the sensitivity of the ignition and reaction times with the following initial conditions: the initial static temperature is 1000K, the initial static pressure is 1 atm, the Mach

number is 5 and the mass fraction of the H_2, O_2, N_2, A_R, CO_2 are stoichiometric (ϕ = 1). From the study of Chapter 5, the initial operation conditions do effect the sensitivities of the reactions in differential range. The initial conditions selected for the sensitivity analysis, is considered to be suitable as the initial operation conditions variation in this range.

Reactions Selected

General discussions have been made in chapter 5 for the detail scheme (8 species, 41 relevant elementary steps), it is possible to give here more mechanism pictures of each reaction involved in this system Since complete reviews have been given by Baulch et al. [1972] and Warnatz [1984], in this section only results are discussed The chemical reaction ($H + O_2 \rightarrow OH + O$) is the number 4 reaction in this scheme (Table 5 1) This is the one of the most sensitivity reactions shown in Fig. 6.1 This is the basic chain-branching process in high-temperature combustion. About 80% of the O_2 is consumed by this step in typical hydrocarbon-air stoichiometric flames at atmospheric pressure. Due to its relatively large activation energy, it is one of the rate-controlling elementary reactions. Therefore, the ignition time is very sensitive to the value of this rate coefficient (Fig.6.1).

Because of the parallel occurrence of the reaction $H + O_2 + M \rightarrow HO_2 + M$ (see Fig. 6.1, No.15 reaction) there is a pressure- and temperature-dependent competition with the reaction $H + O_2 \rightarrow OH + O$. At a high temperature and low pressure the reaction $H + O_2 \rightarrow OH + O$ lead to O atoms as a further chain-branching agent. Formation of O and OH is followed by H-atom regeneration in H_2/O_2 flames by $O + H_2 \rightarrow OH + H$ and $OH + H_2 \rightarrow H_2O + H$. On the other hand, for low temperature and high pressure, the reaction $H + O_2 + M$ - $HO_2 + M$ (small activation energy, high reaction order) produces HO_2 as a second (relatively non-

reactive) chain carrier, leading back to H atoms less efficiently via $H + HO_2$ - OH + OH and $OH + H_2 \rightarrow H_2O + H$. $OH + O \rightarrow H + O_2$ is number 5 reaction in the detailed scheme. Since this reaction is the reverse of $H + O_2$ - OH + O, it distinctly inhibits high-temperature combustion, and there is lower sensitive ignition response.

The reaction $O + H_2 \rightarrow OH + H$ is number 6 reaction in the detailed scheme. After $H + O_2$ - OH + O, this slightly endothermic reaction is the second important chain-branching step in the H_2/O_2 system governing high-temperature combustion chemistry The sensitivity of ignition to its rate coefficient is not very large because of its coupling to the rate-determining step $H + O_2$. The reaction of No.7 of the detailed scheme, $H + OH \rightarrow O + H_2$, is the reverse reaction of NO.6. It shows small sensitivity of ignition to its coefficient. The No.8 reaction, $OH + H_2 \rightarrow H_2O + H$, shows a moderate sensitivity to the rate coefficient of this exothermic chain-propagation reaction. Together with $OH + OH \rightarrow H_2O + O$, this step is the main source of water in the system.

$H + H_2O \rightarrow OH + H_2$ is No.9 reaction. This reaction has an inhibiting effect on combustion. Even it doesn't show the sensitive for the ignition-time, it can't be taken out easily. Together with No.8 reaction, it is mainly responsible for the water-gas equilibration. For recombination reactions of H, O, and OH, because of their third-body behaviour, recombination reactions are of minor important at normal or reduced pressure but it may be relevant at elevated pressure or in the ignition process, such as reaction No.13, $H + OH \rightarrow H_2O + M$ Dissociation reactions of H_2, O_2, and H_2O, can play a part rolw only in the ignition processes at very high temperature. The No.15 reaction, $H + O_2 + M \rightarrow HO_2 + M$, is a chain-propagating step competing with the chain-branching reaction No.4. As No.4 reaction, this

reaction is very sensitive to its rate coefficient. However, because of the low reactivity of HO_2, this reaction behaves effectively as a chain-terminating step, especially at high temperature. Furthermore, this reaction is important because a considerable part of heat of combustion may be released in this step. The reaction of No.17, $H + HO_2 \rightarrow OH + OH$, is rather sensitive to the rate coefficient because of the competition of the chain-branching reaction leading to OH + OH.

The Quasi-Global Chemical Kinetic Model

The reactions having lowest sensitivity of the ignition and reaction to its rate coefficient should be removed from the scheme. From the sensitivity spectrum (Figures 6.1 and 6.2), there are 33 reactions and one species have been removed. So the new reducing scheme, called quasi-global chemical kinetic mechanism, remains 8 reactions and 7 species. Table 6.1 illustrates this scheme.

Table 6.1 Quasi-Global Chemical Kinetic Mechanism

No	Reaction	A	N	E
1	$H + OH \rightarrow H_2O + M$	1.40E+23	-2.	0.
2	$H + O_2 \rightarrow OH + O$	2.00E+14	0.	16859
3	$H_2 + O \rightarrow OH + H$	1.80E+10	1.	8826
4	$H + O_2 \rightarrow HO_2 + M$	1.50E+15	0.	-985
5	$H + HO_2 \rightarrow OH + OH$	2.50E+14	0.	1872
6	$H_2 + O_2 \rightarrow OH + OH$	1.00E+13	0.	43000
7	$H_2 = OH \rightarrow H_2O + H$	2.20E+13	0.	5102
8	$OH + O \rightarrow H + O_2$	2.30E+13	0.	0.

6.3 COMPARISON BETWEEN DETAILED AND QUASI-GLOBAL MECHANISMS AND CONCLUSIONS

To evaluate the quasi-global mechanism, the comparisons between the reducing and detailed schemes calculations under certain range conditions are suitable.

The quasi-global mechanism has 8 reactions and 7 species. Figure 6.3 shows the comparison of composition-time histories between the detailed mechanism and the quasi-global model. The second line from the top of the fig indicates that the consumption of H_2 for the quasi-global model is about 20.0% more than for the detailed mechanism. It is correspond to first line, that the consumption of O_2 for the quasi-global model is increased too comparing the detailed mechanism. The profile of the production of H_2O is shown in third line. It indicates the production of H_2O for quasi-global model is more than that the detailed mechanism. This is because of more H_2 and O_2 consumed in the quasi-global model. Therefore, the combustion process presented by the quasi-global model is more completely than the one presented by the detailed mechanism. Furthermore the consumption of H_2 and O_2 also produces more H.

Comparisons of the temperature-time histories of the quasi-global scheme with those of the detailed mechanism, under the fuel equivalence ratio equal to 1, Mach number equal to 5, are presented in figure 6.4. For each pressure level the results for the quasi-global mechanism (broken lines) are close to those for the detailed mechanism (solid lines). Figure 6.4 also shows that the equilibrium temperatures

of the quasi-global scheme are higher or lower than those of the detailed scheme for pressure less or more than 1 atm, respectively. The difference of the equilibrium temperature between the two schemes about 15%.

Figure 6.4 indicates that the temperature profiles between the two schemes are in good agreement. It is expected that the ignition and reaction times of the detailed mechanism and the quasi-global model are also in a good agreement as shown in Figures 6.5 and 6.6.

CONCLUSIONS

From the comparisons presented in Figures 6.3, 6.4, 6.5, and 6.6, the quasi-global model would be adequate for the calculation of the ignition-time and reaction-time of hydrogen-air reaction in a constant pressure stream (about 0.5 to 6 atm for this calculation). The errors caused by using this scheme to calculate the ignition and the reaction times are about 10% in comparison with the results of the detailed mechanism.

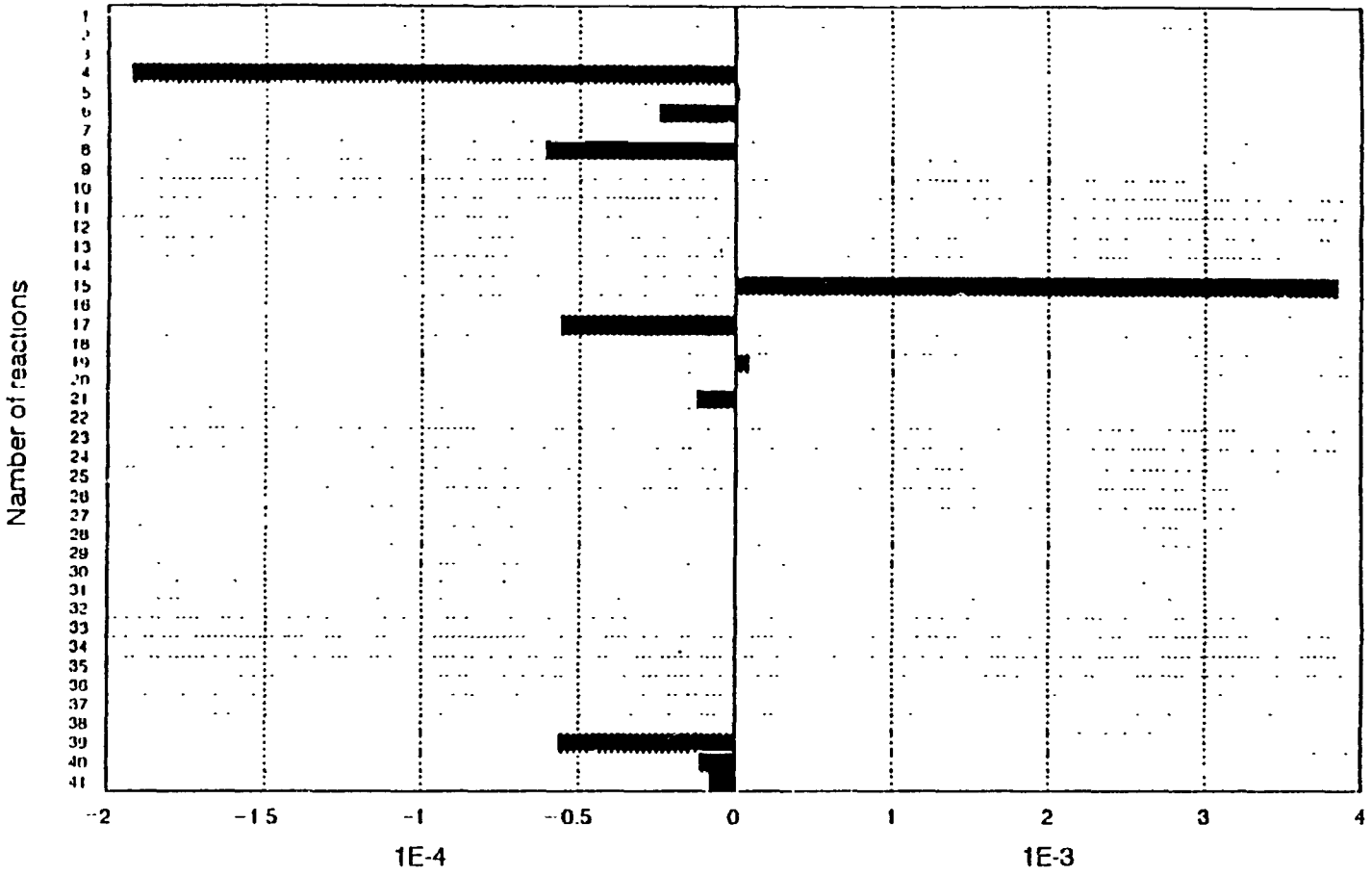

Figure 6-1 The sensitivity spectrum of 41 reactions

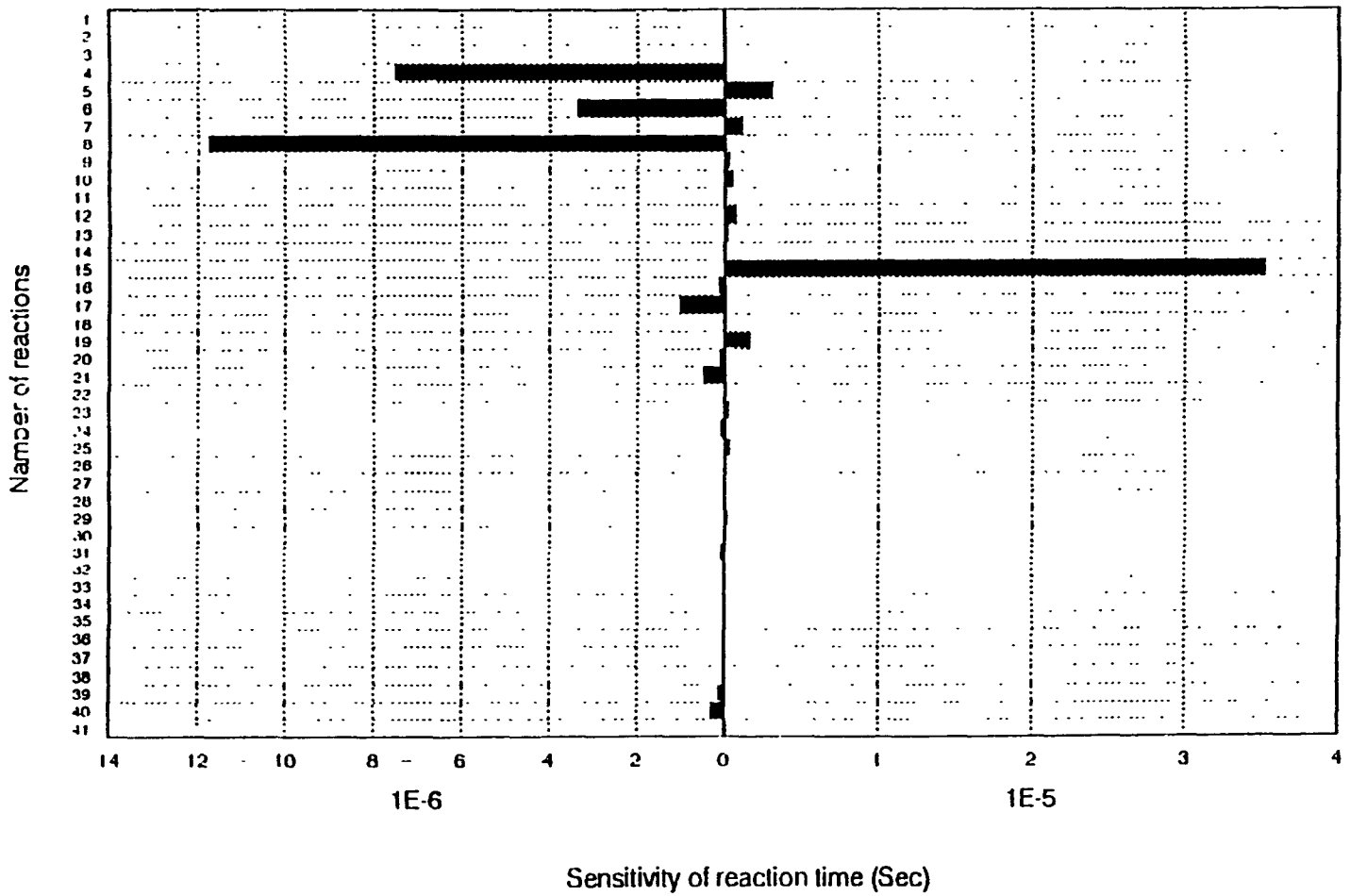

Figure 6.2 The sensitivity spectrum of 41 reactions

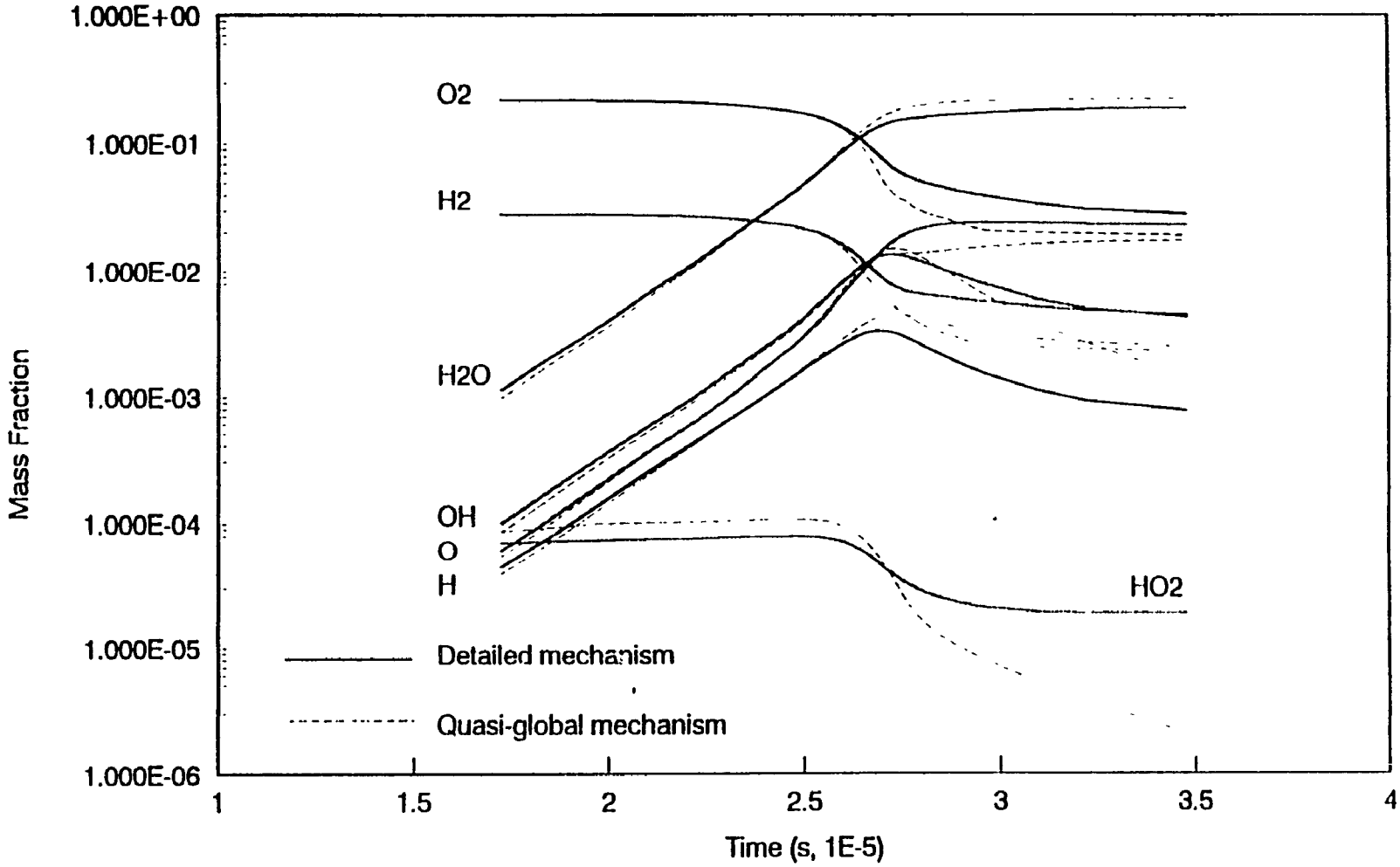

Figure 6.3 Comparison of detailed and quasi-global mechanism.
Po = 1.0 atm, To = 1250K, M = 5.0, ϕ = 1.0

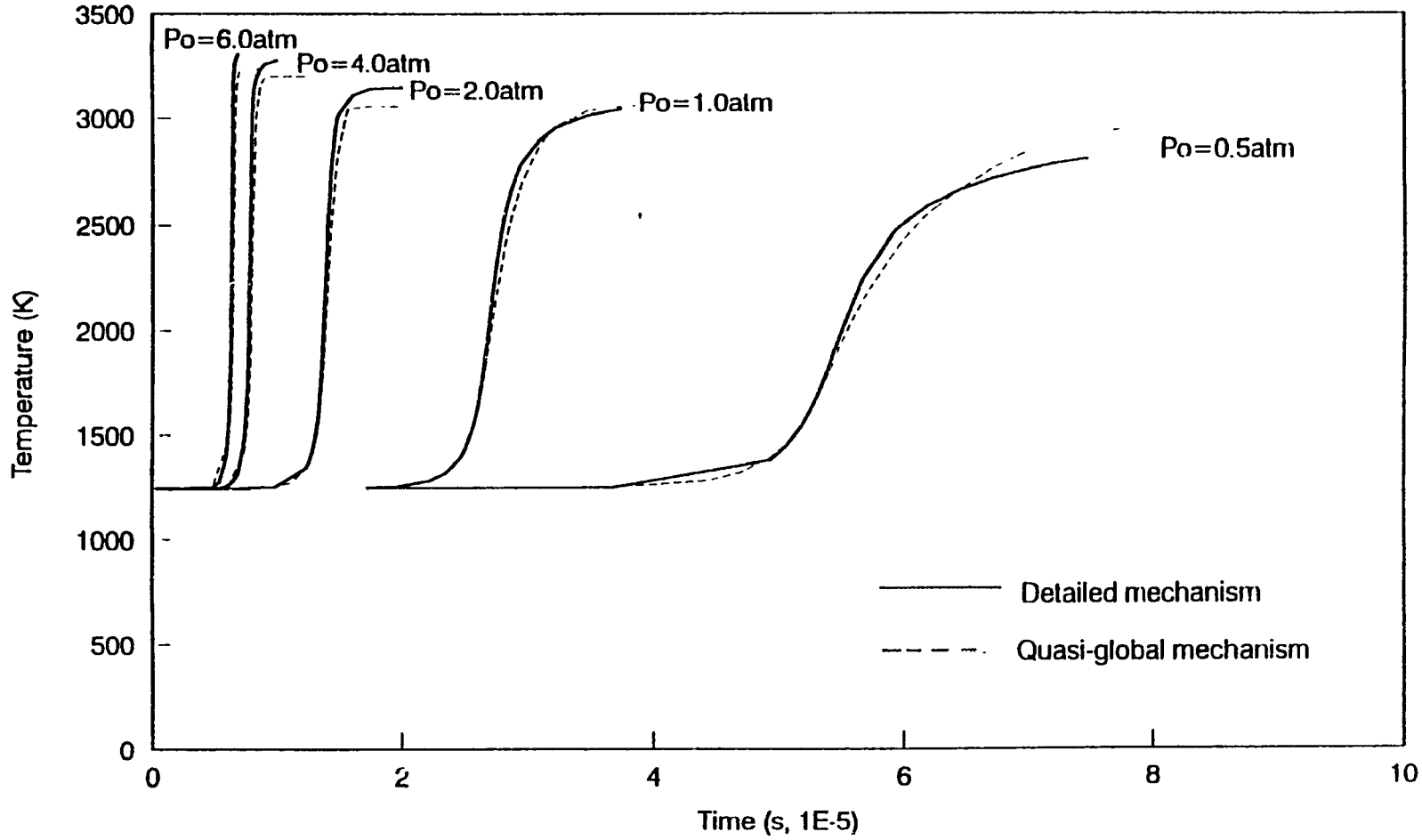

Figure 6.4 Comparison of detailed and quasi-global mechanism on temperature-time histories at $M = 5.0, \phi = 1.0$

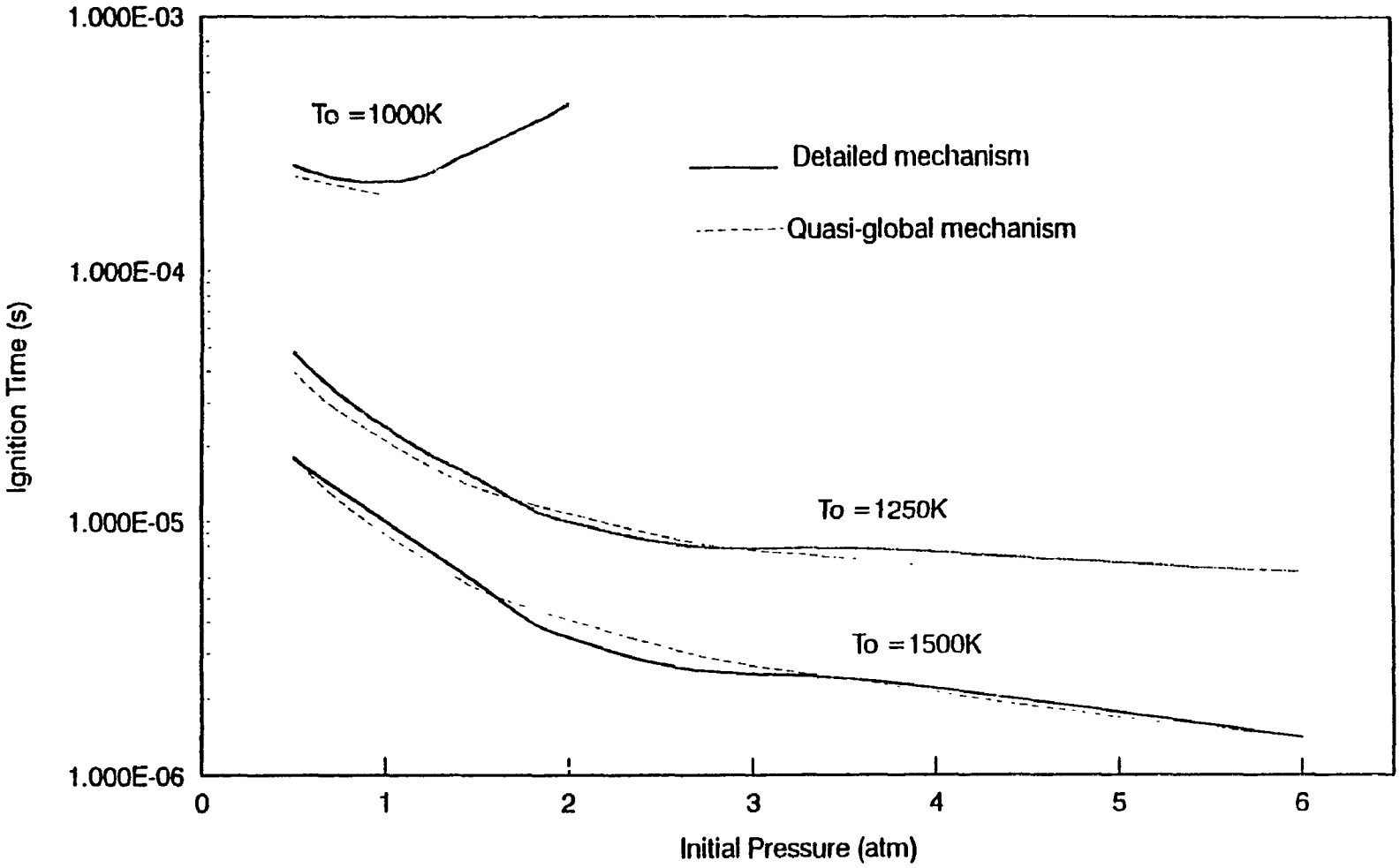

Figure 6.5 Comparison of detailed and quasi-global mechanism on ignition time at ϕ=1.0, M = 5.0

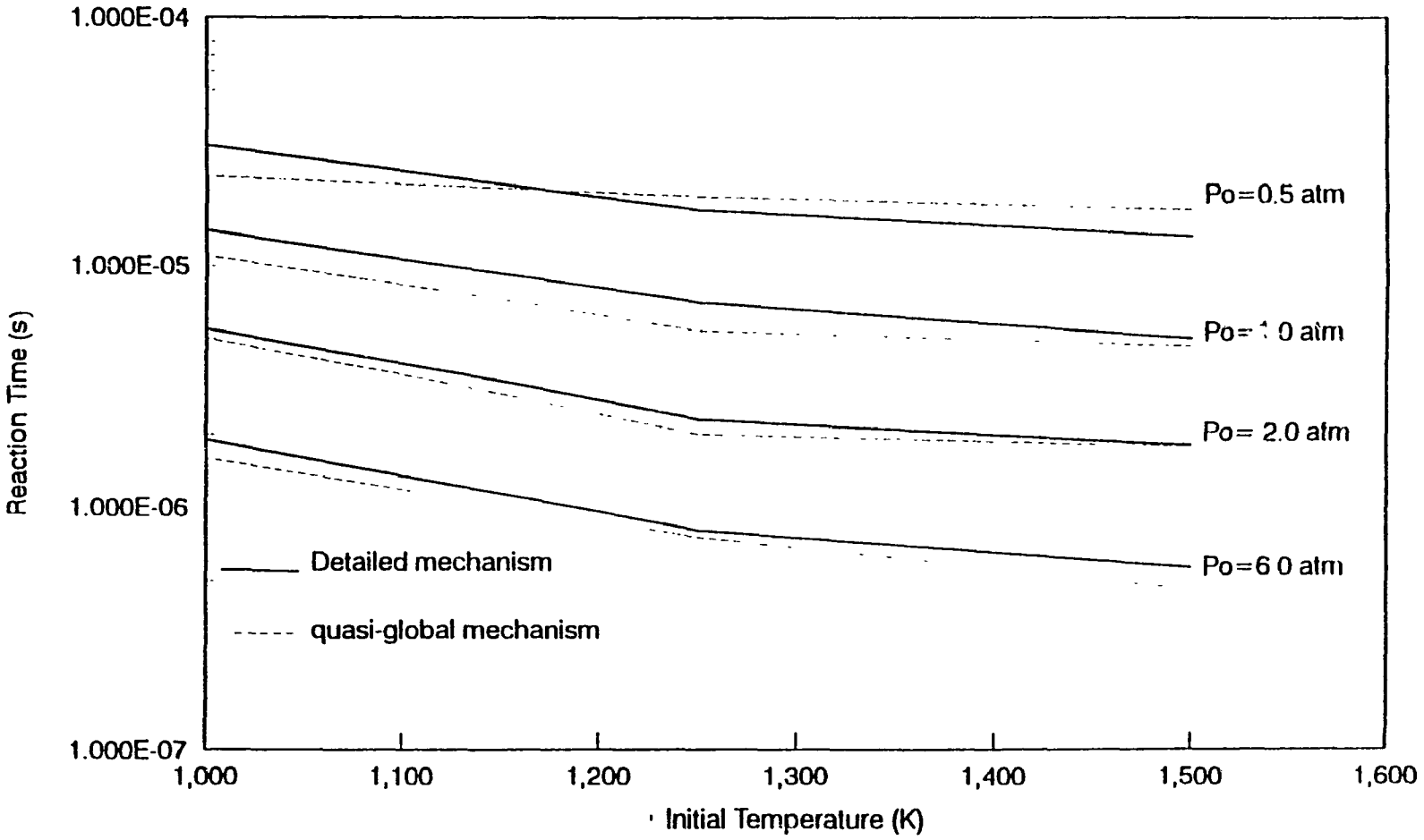

Figure 6.6 Comparison of detailed and quasi-global mechanism on reaction time
M = 5.0, ϕ = 1.0

CHAPTER 7 GLOBAL CHEMICAL KINETIC MECHANISM OF H_2/AIR SUPERSONIC COMBUSTION

7.1 INTRODUCTION

We already know that combustion is a three-dimensional, highly complex physic-chemical process of transient nature. Models are therefore needed to simplify a given combustion problem to such a degree that it becomes amenable to theoretical or numerical analysis but it is not restrictive as to distort the underlying physics or chemistry.

In this chapter, the steady-state approximation method has been chosen to reduce the quasi-global scheme. The basic concept about steady-state reducing has been described in Chapter 3. Here under the appropriate assumptions, a two steps scheme has been derived from the 8 reaction scheme. The comparison of three level mechanisms have been brought out for making a conclusion about the global chemical model at the end of this chapter.

7.2 STARTING MECHANISM

The first step in deriving a global scheme is to define a suitable starting mechanism. This may be viewed as an already reduced scheme from a large detailed mechanism. For the specific problem considered, a numerical solution must be obtained using the full mechanism and a sensitivity analysis must be carried out to identify the influence of each individual reaction on the solution. These are the studies have been done in the passed two chapters.

The starting mechanism should contain only those elementary reactions that are necessary to reproduce a characteristic quantity such as the ignition and reaction times. The quasi-global scheme that we obtained by using sensitivity analysis in Chapter 6 is considered as a starting mechanism listed in Table 6.1.

7.3 THE STEADY-STATE APPROXIMATION

The second step of this procedure is to identify steady-state species. For the 8 reactions of the starting mechanism, besides the fuel H_2, oxygen O_2, and N_2 (assumed inert), this mechanism involves the main product H_2O, the members of hydrogen-oxygen radical pool H, O, and OH, and the hydroperoxyl radical HO_2. In the following, w_i represents the reaction rate of ith reaction listed in Table 6.1. For the seven reacting species, the following system of balance equations is divided

$$L([H]) = -w_1 - w_2 + w_3 - w_4 - w_5 + w_7 + w_8 \quad (7.1)$$

$$0 = L([OH]) = -w_1 + w_2 + w_3 + 2w_5 + 2w_6 - w_7 - w_8 \quad (7.2)$$

$$0 = L([O]) = w_2 - w_3 - w_8 \quad (7.3)$$

$$L([H_2]) = -w_3 - w_6 - w_7 \quad (7.4)$$

$$L([O_2]) = -w_2 - w_4 - w_6 + w_8 \quad (7.5)$$

$$L([H_2O]) = w_1 + w_7 \quad (7.6)$$

$$0 = L([HO_2]) = w_4 - w_5 \quad (7.7)$$

Here, L([Xi]) represents a linear differential operator in the balance equations From the study of Peters [1993], the steady-state approximations introduced3 species, intermediate O, OH, HO_2. With these three steady-states and 2 atom-

conservation conditions (for H and O) among the 7 reacting species, a total number of two global steps should describe the chemistry. The following system of balance equations is derived by eliminating the reaction rates w_3 for O, w_5 for HO_2 and w_7 for OH as those which are the fastest to be consumed, respectively. By the procedure described below, one obtains the following system of balance equations for the remaining non-steady-state species H, H_2, O_2 and H_2O:

$H + \{OH + 2O + HO_2\}$

$= -w_1 - w_2 + w_3 - w_4 - w_5 + w_7 + w_8 - w_1 + w_2 + w_3 + 2w_5 + 2w_6 - w_7 - w_8 + 2w_2$

$- 2w_3 - 2w_8 + w_4 - w_5$

$= -2w_1 + 2w_2 + 2w_6 - 2w_8$

$= \mathbf{2(w_2 + w_4 + w_6 - w_8) - 2(w_1 + w_4)}$

$H_2 + \{-OH - 2O\}$

$= -w_3 - w_6 - w_7 + w_1 - w_2 - w_3 - 2w_5 - 2w_6 + w_7 + w_8 - 2w_2 + 2w_3 + 2w_8$

$= w_1 - 3w_2 - 2w_5 - 3w_6 + 3w_8$

$= \mathbf{-3\ (w_2 + w_4 + w_6 - w_8) + (w_1 + w_4)}$

$O_2 + HO_2$

$= -w_2 - w_4 - w_6 = w_8 + w_4 - w_5$

$= \mathbf{-(w_2 + w_4 + w_6 - w_8)}$

$H_2O + \{OH + O\}$

$= w_1 + w_7 + w_2 - w_3 - w_8 - w_1 + w_2 + w_3 + 2w_5 + 2w_6 - w_7 - w_8 + w_2 - w_3 - w_8$

$= \mathbf{2(w_2 + w_4 + w_6 - w_8)}$

The operates in the curly brackets correspond to those of steady state species and can be neglected. Grouping rates equal stoichiometric coefficient one obtain

$$L([H]) = 2(w_2 + w_4 + w_6 - w_8) - 2(w_1 + w_4)$$

$$L([H_2]) = -3(w_2 + w_4 + w_6 - w_8) + (w_1 + w_4)$$

$$L([O_2]) = -(w_2 + w_4 + w_6 - w_8)$$

$$L([H_2O]) = 2(w_2 + w_4 + w_6 - w_8)$$

This lead to the two steps global mechanism

(I) $3H_2 + O_2 = 2H + 2H_2O$

(II) $2H + M = H_2 + M$

with the global rates

$$w_I = w_2 + w_4 + w_6 - w_8 \qquad (7.8)$$

$$w_{II} = w_1 + w_4 \qquad (7.9)$$

In the second global reaction the inert body M has been added as a reminder of the third body that appears in reactions 1 and 4 of the quasi-global scheme in Table 6.1, Chapter 6. This shall illustrate the role of reaction II as a chain breaking global reaction where the only remaining radical, namely H, is being consumed. The role of the first global reaction is that of an overall chain-branching step.

The steady state assumptions for O, OH and HO_2, i.e. Eqs.(7.2), (7.3) and (7.7)can be used to derive algebraic relations for the species, namely

$$[O] = \frac{k_{1b}[H_2O][M] - (k_{2f} - k_{8b})[H][O_2] - 2k_{5f}[H][HO_2] - 2k_{6f}[H_2][O_2] + k_{7b}[H_2O][H]}{k_{3f}[H_2]} \qquad (7.10)$$

$$[HO_2] = \frac{k_{1b}[H][O_2] - (k_{2f} - k_{8b})[H][O_2] - k_{3f}[H_2][O] - 2k_{6f}[H_2][O_2] + K_{7b}[H_2O][H]}{2k_{5f}[H]} \qquad (7.11)$$

$$[OH] = \frac{k_{2f}[H][O_2] - k_{8b}[H][O_2]}{k_{3b}[H]} \qquad (7.12)$$

These equations are explicit, they are coupled and must be solved iteratively. Now entering into the evaluation of global mechanism by comparing the three level mechanisms.

7.4 COMPARISON BETWEEN DETAILED, QUASI-GLOBAL, AND GLOBAL MECHANISM

The explicit algebraic relations derived above have been used in a numerical calculation. Three different chemical kinetic mechanisms were taken to compare:
(1) detailed chemical scheme, 41 reactions and 8 species,
(2) quasi-global chemical scheme, 8 reactions and 7 species,
(3) global chemical scheme, 2 reactions and 4 species.
In all the figures of this Chapter, solid line is the detail model, broken line is the quasi-global model, and dot-dash line is for global model scheme.

The mass fractions of the non-steady-state species of a stoichiometric flame at 1 atm, Mach number at 5, initial temperature is 1250K, are plotted in Fig.7.1. It is seen, that except the detailed scheme, the agreement of the reduced schemes is quite good, but not as good as ignition and reaction times. The differences of the species are expected since the steady state assumptions enter their balance

equations directly. It is seen that by neglecting the steady state equations, the chemical interaction focusses on the principal rates and not on side reactions.

Comparisons of the temperature-time history under variation of the initial pressure are illustrated in Figure 7.2. The results obtained from the three schemes are agreeable satisfaction to each other, except for equilibrium temperature. The ignition and reaction times are in a good agreements.

In Fig.7.3 the ignition-time at ϕ = 1.0 and M = 5, with the initial temperature as a parameter is plotted as a function of the initial pressure and the three cases are studied (T=1000K, 1250K, 1500K). The global model seems to match the other two models resonably. In Fig.7.4 the reaction-time at ϕ = 1.0 and M = 5, with the initial pressure as a parameter is plotted as a function of the initial temperature. The differences between the results obtained by the global model is about 15%.

7.5 COMPARISON BETWEEN PRESENT RESULTS WITH THE EXISTING DATA

In order to test the accuracy of the ignition time predicted by the present chemistry model, the results are compared with stoichiometric H_2-air shock tube data from Slack et al (1977) and the theoretical results of chemistry model of H_2-air from Laster et al (1988). Fig 7-5 presents the ignition time vs the initial temperature at initial pressure 0.5 atm and Fig.6 presents the ignition time vs initial temperature at initial presure 1.0 atm. The present ignition times agree reasonably well with the referenced results.

7.6 CONCLUSIONS

A 2-step mechanism has been derived for premixed hydrogen flames, with the initial pressure between 0.2 to 6.0 atm, the initial temperature up to 1500K, Mach number equal to 5.0, and various equivalence ratio. This mechanism involves only the reactants H_2 and O_2, the product H_2O and radical H. The steady state assumption for the other species considered here, namely O, OH, and HO_2, was well justified. Numerical calculations of the flame structures, employing this mechanism as well as a 41 reactions mechanism, and an 8 reactions mechanism, were performed to investigate the accuracies of the reduced mechanisms. The good agreements are in ignition and reaction time prediction. The additional effect of an element mass fraction defect, which is implicitly associated with the steady state assumptions, causes the concentration of some of the non-steady-state species to be too large Detailed considerations are necessary in order to derive the corrective parameters for the global mechanism. Also the experimental study is necessary to be carried out.

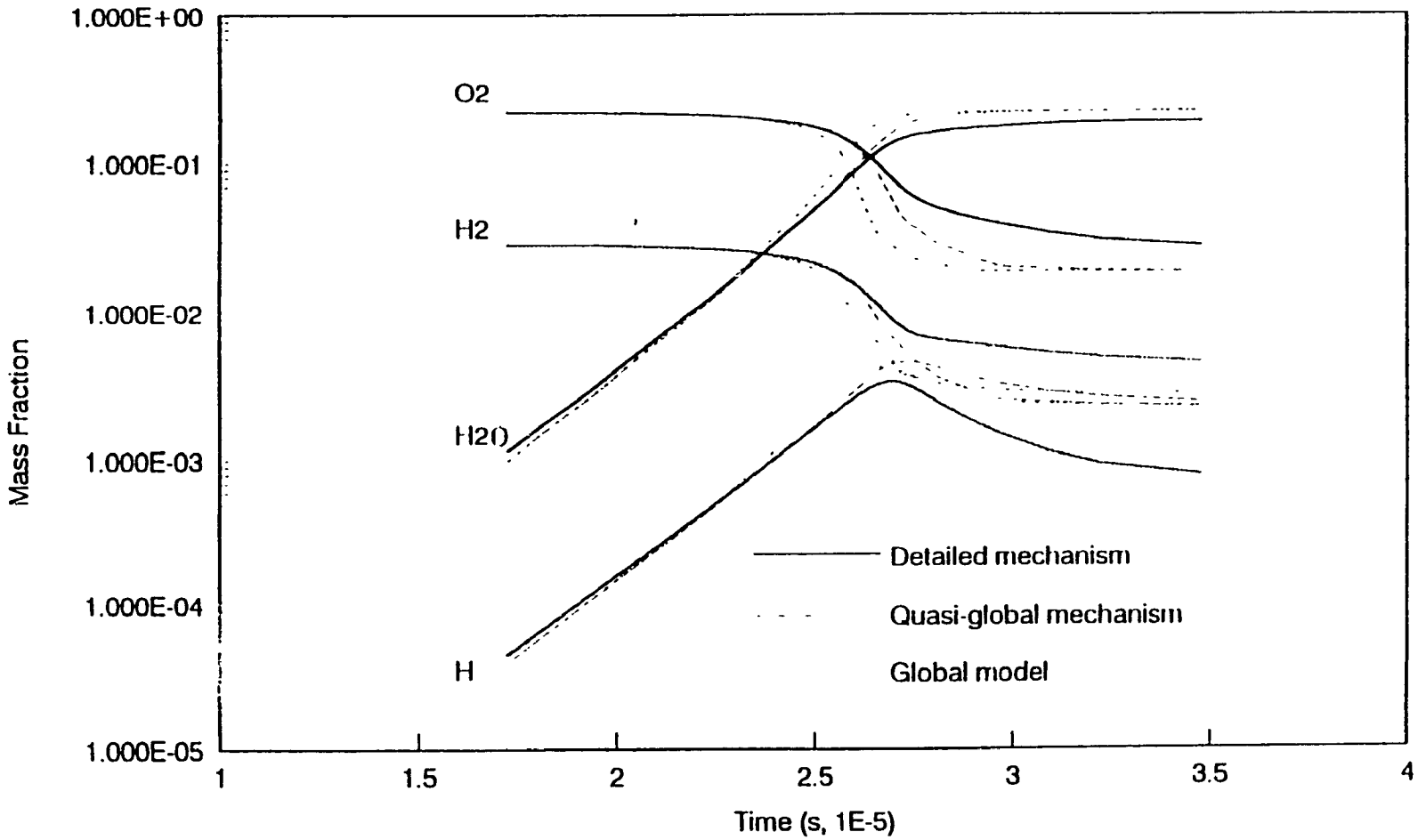

Figure 7.1 Comparison of detailed, quasi-global and global mechanism.
Po = 1.0 atm, To = 1250K, M = 5.0, ϕ = 1.0

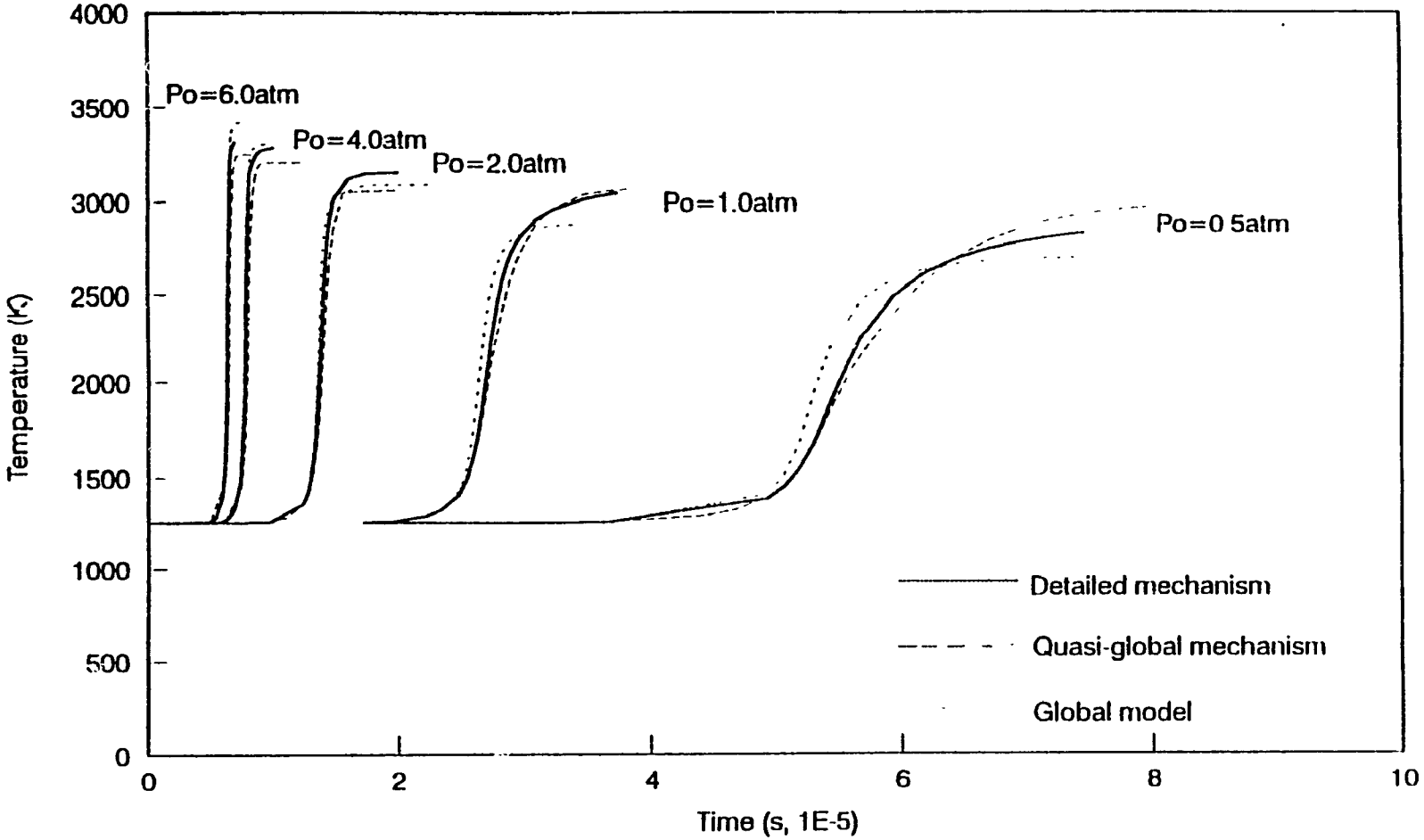

Figure 7.2 Comparison of detailed, quasi-global and global mechanism on temperature-time histories at $M = 5.0, \phi = 1.0$

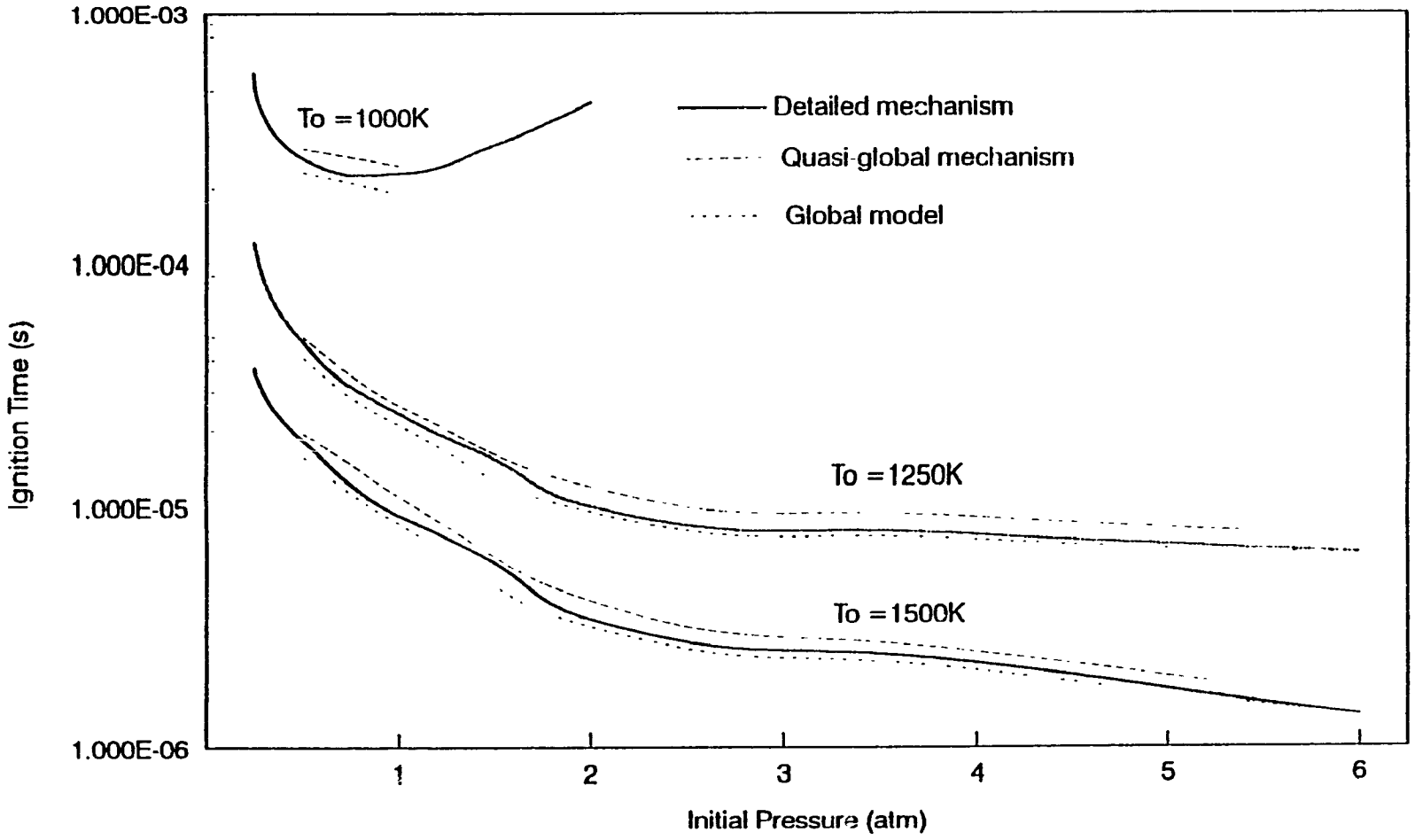

Figure 7.3 Comparison of detailed, quasi-global and global mechanism on ignition time at ϕ=1.0, M = 5.0

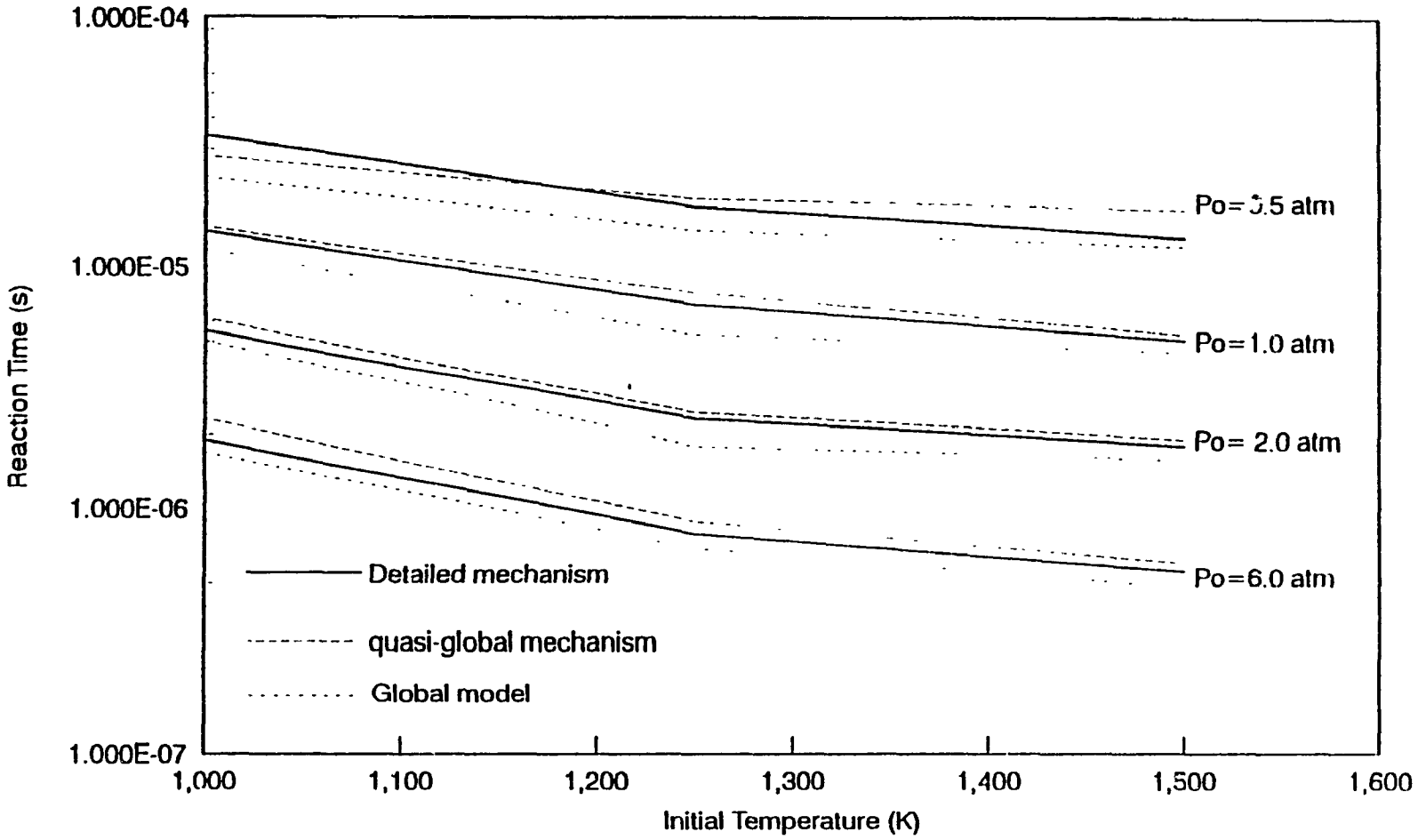

Figure 7.4 Comparison of detailed, quasi-global and global mechanism on reaction time
$M = 5.0, \phi = 1.0$

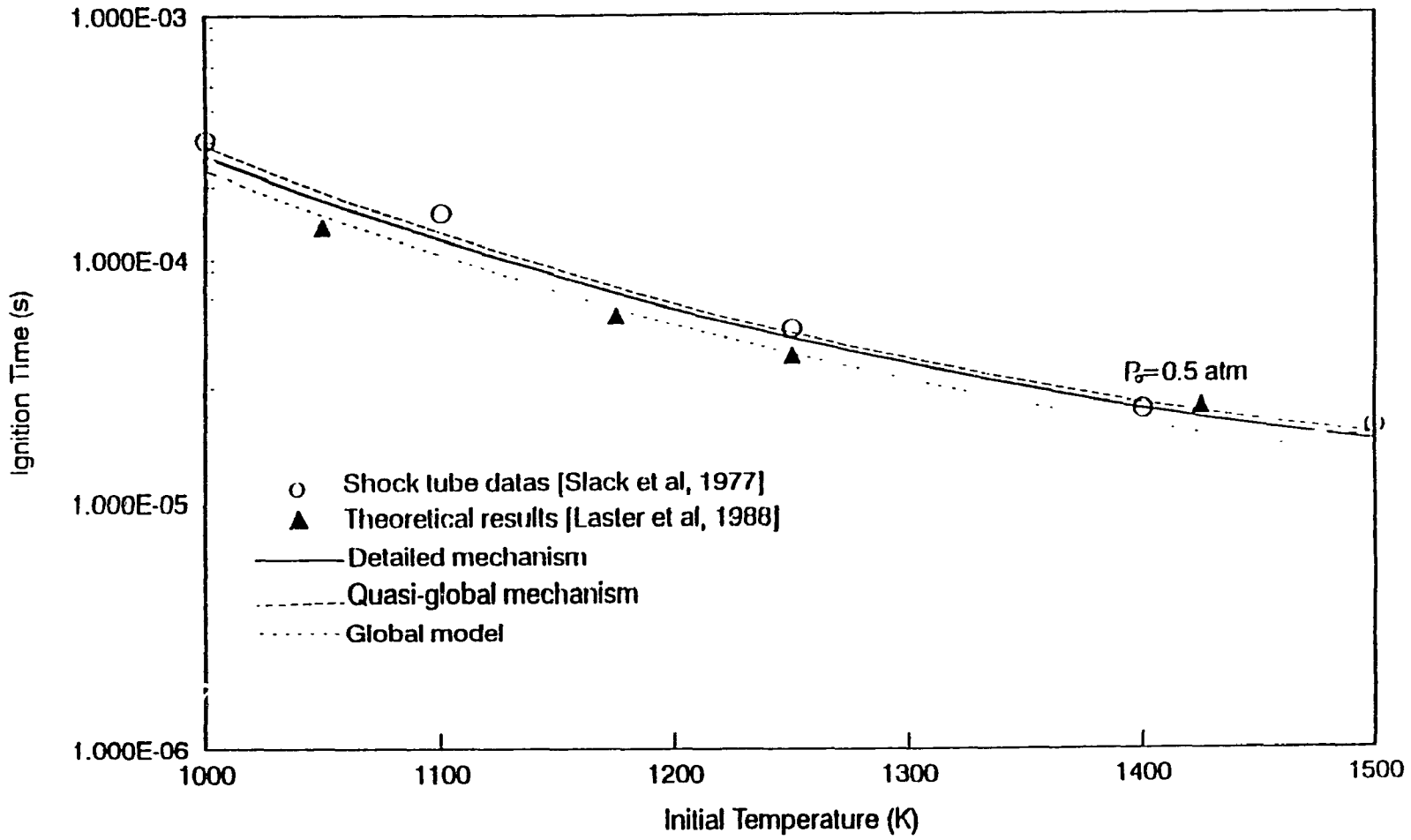

Figure 7.5 Comparison of ignition time at $\phi = 1.0$, M = 5.0

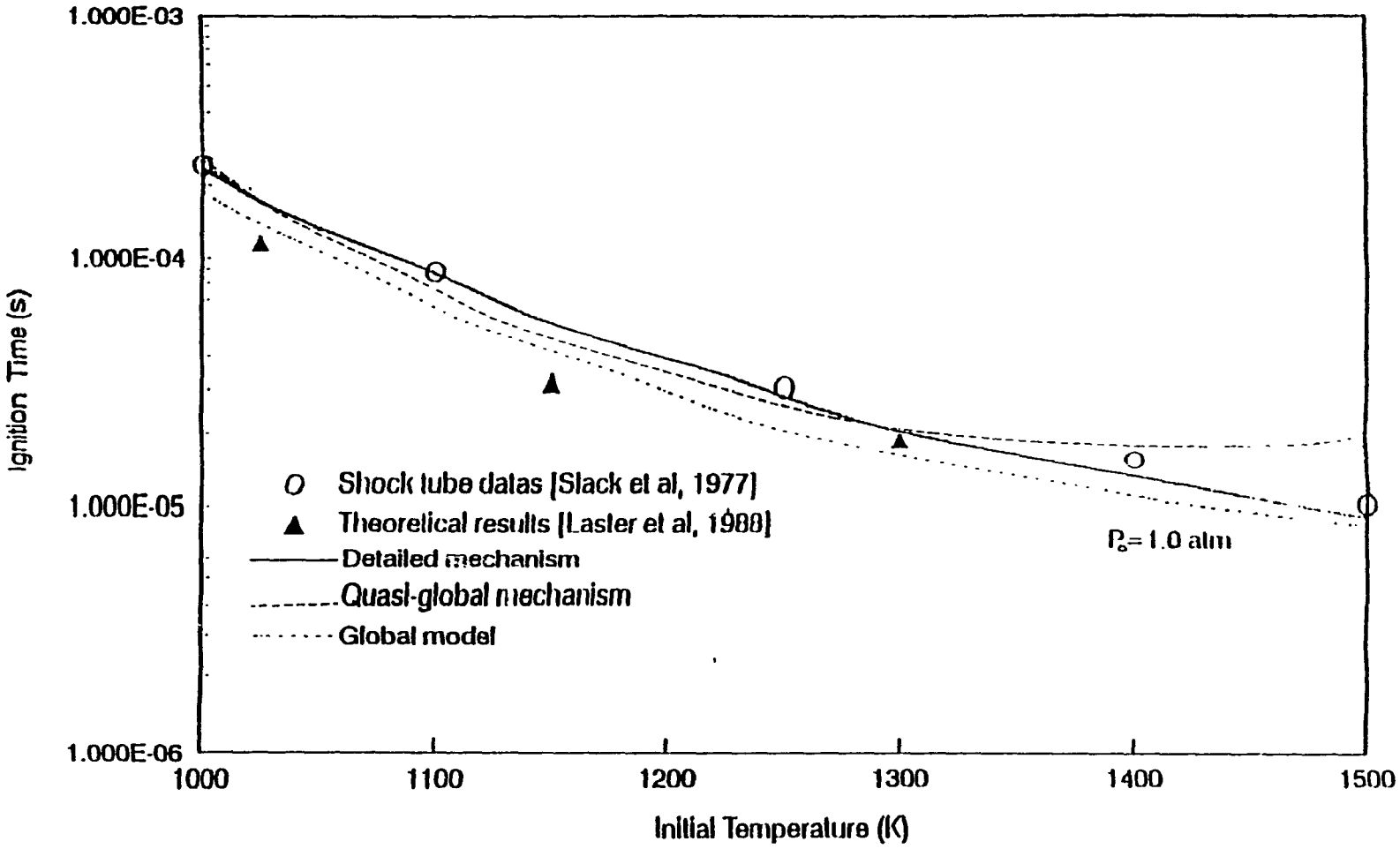

Figure 7.6 Comparison of ignition time at ϕ= 1.0, M = 5.0

CHAPTER 8 CONCLUSIONS

An analytical study of the chemical mechanism involving in the ignition and reaction of the H_2/Air system has been performed with conditions representative of the scramjet combustor. The calculation was made with an one-dimensional kinetic program with H_2-O_2 (N_2 is considered as an inert) finite-rate chemistry model.

Three level kinetic schemes have been investigated. The first one is the detailed chemistry model with 41-step elementary reactions and 8 species. The second one is the quasi-global mechanism with 8-step elementary reactions and 7 species, which is derived from the detailed model by using the sensitivity analysis The third one is the global model with 2-step elementary reactions and 4 species, which is obtained from the quasi-global model by using the steady state approximations.

The calculation objective of the detailed mechanism is to provide the information for an assessment of the conditions at which kinetics are important in the scramjet combustor. Specifically, the study considers how the ignition and reaction times are affected by the initial temperature, initial pressure, fuel equivalence ratio and Mach number. Results of the detailed model calculations indicate that, within a 15% percent error, the ignition-time is nearly constant over a range of the equivalence ratio from 0.5 to 2.0. The Mach number change makes the temperature-time history fall into two groups, one for supersonic combustion and the other for subsonic combustion. In each group, the ignition-time is independent of Mach number. The effects of the initial temperature and initial pressure on the ignition-time are indicated as a non-linear relation. However, the variation of the reaction-time with the initial temperature is nearly linear, and with the initial pressure shows an

exponential manner.

Calculations from the quasi-global model indicate that the model is adequate for prediction the ignition and reaction times of the hydrogen-air reactions. The errors obtained from this model is about 10% in comparison with the results obtained from the detailed mechanism.

The most interest of the reducing scheme for engineering calculation purpose is the global model which is able to predict the ignition and reaction time with about 15% error in comparison with the results obtained from the detailed model.

Numerical modelling of combustion processes in scramjets has become an important element of the computational program. An essential component in any combustion modelling is the chemical kinetic reaction mechanism which describes the oxidation of the fuel The numerical models which attempt to combine the description of the chemistry with other processes, such as turbulence, mass transfer, and fuel vaporization, encounter serious computational difficulties when the detailed mechanism is used. The global modelling of the overall fuel-air reaction can be provide a practical substitute for the detailed kinetic model.

Future Work

Since the present study is the modelling of H_2/air supersonic combustion process combining with one-dimensional fluid dynamics while N_2 is considered as an inert, the future work may focus on the modelling of H_2/air supersonic combustion system with N_2 as a reactive. If it is possible, an experiment work should be performed. A study on two or three dimensional fluid dynamics combining with

REFERENCES

Ashmore P. G. and Tyler B. J., " The Nature and Cause of Ignition of Hydrogen and Oxygen Sensitized by Nitrogen Dioxide," Proceedings of the Ninth Symposium (International) on Combustion, Academic Press, New York, 1963, pp. 201-209.

Bahn, G. S., "Calculations on the Autoignition of Mixtures of Hydrogen and Air." NASA CR-112067, 1972.

Baulch D.L. et al., "Evaluated Kinetics Data for High Temperature Reactions, Vol. 1, Homogeneous Gas Reactions of the H_2-O_2 System", Butterworths, London, 1972.

Baulch D.L. et al., "Evaluated Kinetics Data for High Temperature Reactions, Vol. II, Homogeneous Gas Reactions of the H_2-O_2-N_2 System", 1972.

Bilger, R. W., Starner, S. H. and Kee, R. J., "On Reduced Mechanisms for Methane-Air Combustion in Premixed Flames", Comb. Flame 80, 1990, pp. 135.

Billig, F. S., " Ramjets With supersonic Combustion" Laurel, Maryland, The Johns Hopkins U., 1971.

Bittker D.A.and Scullin V.J.: General Chemical Kinetics Code for Gas-Phase Flow and Batch Processes Including Heat transfer Effects. NASA TP-2320, 1984.

Bittker, D. A., and Scullin, V. J., " General Chemical Kinetics Computer Program For Static and Flow Reactions, With Application to Combustion and Shock-Tube Kinetics." NASA TN D-6586, 1971

Brokaw, R. S., "Rate of Reaction Between Molecular Hydrogen and Molecular Oxygen." NASA TM-2707, 1973.

Bukhman, F.A., "Primenenie Vycheslite'noi Matematikiv Khimicheskoji Fizicheskoi Kinetike", Edited by L.S. Polak, Nauka, Moskow, Chap.1, 1969.

Correa S.M. and Mani R., "None Equilibrium Model For Hydrogen Combustion in Supersonic Flow", J. of Propulsion, pp.523, 1980.

David A. Bittker and Vincent J. Scullin, "GCKP84 - General Chemical Kinetics Code For Gas-phase Flow and Batch Processes Including Heat Transfer", 1984.

Dickinson, R. P., Gelinas, R. J., J. Comp. Phys., 21, pp. 123-143, 1976.

Dixon-Lewis, G., Goldworthy, F.A. and Greenberg, J.B., Proc. Roy. Soc. Lond. A346, pp.261, 1975.

Dixon-Lewis, G., Phil. Trans. Roy. Soc. Lond. A292, pp.45, 1979.

Drummond, P., "Supersonic Reacting Internal Flowfields" AIAA J. Vol. 20, 1982

Erickson, W.D. and Klieb, G.F., "Analytical Chemical Kinetics Study of the Effect of Carbon Dioxide and Water Vapor on Hydrogen-Air Constant-Pressure Combustion", NASA Technical Note, NASA TND_5768, 1970.

Evans. J and Schexnaydv, "Critical Influence of Finite Rate Chemistry and Unmixedness on Ignition and Combustion of Supersonic Hydrogen-Air Streams", 1980.

Ferri, Antonio, "Review of problems in application of supersonic combustion" presented at the seventh Lanchester Memorial Lecture, Royal Aeronautical Society, May 1964, London, England.

Frenklach, M., "Combustion Chemistry", Edited by Gardiner, W. C. Jr, Chapter 7, pp. 438-452, 1984, Springer-Verlag.

Frank P. M., Inter. J. Chem. Kinet. 11, pp. 1237-1248, 1978.

Gardiner W. C., Jr. "Combustion Chemistry" published by Springer-Verlag, New York Inc. 1984.

Gardiner, W.C., Jr. J. Phys. Chem. 81, pp. 2367-2371, 1977.

Gear C.W.: Numerical Initial Value Programs in Ordinary Differential Equations. Prentice Hall, 1971.

Gutheil, E., Williams, F. A., Twenty-Third Symposium (International) on Combustion, The Combustion Institute, Pittsburgh, 1991.

Hill P. and Peterson C., "Mechanics and Thermodynamics of Propulsion." ADDISON-WESLEY Publishing Company, Second Edition, 1992.

Hindmarsh A.C.: Linear Multistep Methods for Ordinary Differential Equations: Method Formulations, Stability, and the Methods of Nordsieck and Gear. UCRL-51186-Rev.1, Lawrence Livermore Lab., 1972.

Jensen, D. E., and Jones, G. A., "Reaction Rate Coefficients for Flame

Calculation." Comb. & Flame, Vol. 32, no. 1, pp. 1-34, May 1978.

Kanury, A. M., "Introduction to Combustion Phenomena", Gordon & Breach, New York, 1982, pp. 363-371.

Laster W. R. and Sojka P. E., "Autoignition of H2-Air: The effect of NOx Addition," Propulsion, Vol.5, No.4, (1989)

Law C. K., "A Compilation of Recent Experimental Data of Premixed Laminar Flames",Lecture Notes in Physics, Vol. m15, pp. 15-29, 1992.

Lloyd, A. C., "Evaluated and Estimeated Kinetic Data for Phase Reactions of the Hydroperoxyl Radical." Int. J. Chem. Kinet., Vol. 6, pp. 169-228, May. 1974.

McBride J., Heimel S., Ehlers G., and Gordon S., "Thermodynamic Properties to 6000 K for 210 Substances Involuing the First 18 Elements. NASA SP-3001, 1963

Momtchiloff, I. N., Taback, E. D., and Buswell, R. F., "An Analytical Method of computing Reaction Rates For Hydrogen-Air Mixtures", Paper presented at the Ninth International Meeting of the Combustion Institute, Cornell University, August, 1962

Oran E. S. and Boris J. P. "Detailed modelling of combustion systems" pro. Energy Combust. Sci. Vol. 7, pp 1-72, Pergamon Press Ltd., 1981. (Printed in Great Britain)

Paczko, G., Lefdal, p. M., Peters, N., Twentyfirst Symposium (International) on Combustion, The Combustion Institute, pp. 739-748, 1988.

Pergament, Harolds S. "A theretical Analysis of Non-Equilibrium Hydrogen-air Reaction in Flow Systems", AIAA-ASME Hypersonic Ramjet Conference, 1963.

Perters, N. " Reduced Kinetic Mechanisms ans Asymptotic Approximations for Methane-Air Flames", Lecture Notes in Physics, 1991.

Peters, N., Kee, R. J., "The Computation of Stretched laminar methane-air diffusion flames using a reduced four-step mechanism", Comb. and Flame, 68, 1987.

Russin R. W. ,"Performance of A Hydrogen Burner To Simulate Air Entering Scramjet Combustors," NASA TN D-7567, February 1974.

Saber A.J., Chen, X, and M. Gorman, "H_2/air subsystem combustion kinetics in aerospaceplane powerplants", 43rd Congress of the Internation Astronautical Federation, 1992, IAF-92-0660.

Saber A.J., Chen, X, and M. Gorman, "Kinetics of H_2/air with reactive nitrogen combustion in aerospaceplane powerplants", 42nd Congress of the Internation Astronautical Federation, 1992, IAF-91-267.

Schott Garry L., "Kinetic studies of Hydroxyl Radical in Shock Waves. III. The OH Concentration Maximum in the Hydrogen-Oxygen Reaction", Journal of Chemical Physics, Vol. 32, No. 3, March 1960.

Slack M. W. and Grillo A. R., "Investigation of Hydrogen-Air Ignition Sensitized by Nitric Oxide and Nitrogen Dioxide," NASA, CR-2896, Oct. 1977.

Slack M. W. and Grillo A. R., "Rate Coefficient for H2+NO2=HNO2+H Derived

from Shock Tube Investigation of H2-O2-NO2 Ignition," Combustion and Flame, Vol. 31, 1978, pp. 275-283.

Smooke, M. D., "Reduced Kinetic Mechanisms and Asymptotic Approximations for Methane-Air Flames", 1991.

Warnatz, J., Ber. Bunsenges. Phys. Chem. 83, pp. 950, 1979.

Warnatz, J., Enghteenth Symposium (International) on Combustion, pp. 369-384, The Combustion Institute, 1981.

Warnatz, J., "Combustion Science & Technology", 26, pp. 203, 1981.

Warnatz, J., "Combustion Chemistry" Edited by Gardiner, W.C. Jr, 1984.

Williams, F. A., "Combustion Theory" Addison-Wesley, Reading, MA, 1978.

Williams, F. A., "Combustion Theory" 2nd Ed., Addison-Wesley, Menlo Park, CA, pp.178, 1985.

Williams, F. A., "Influences of Detailed Chemisty on Asymptotic Approximations for Flame Structure", Martinus Nijhoff Publishers, Dordrecht, The Netherlands, 1988, pp. 315.

Zeleznik F.J. and McBride B.J.: Modeling the internal Combustion Engine. NASA RP-1094, 1984.

APPENDIX 1
[Baulch et al. scheme tables]

Table I Evaluated Kinetic Data For High Temperature Reactions: Homogeneous Gas Phase Reactions Of The $H_2 - O_2$ System

	Reaction	Rate Constant k (cm³ mole⁻¹ sec⁻¹)	Temperature Range (K)	Error in log k	Page	Notes
H atom reactions						
1	$H + H + M \rightarrow H_2 + M$	$6.4 \times 10^{17} T^{-1.0}$ (M=Ar)	1700 - 5000	± 0.3	261	a
2	$HO_2 + H \rightarrow H_2 + O_2$	$2.5 \times 10^{13} \exp(-350/T)$	290 - 800	± 0.4	161	
3	$HO_2 + H \rightarrow H_2O + O$	No recommendation	-	-	173	
4	$HO_2 + H \rightarrow OH + OH$	$2.5 \times 10^{14} \exp(-950/T)$	290 - 800	± 0.3	165	b
5	$H_2O + H \rightarrow H_2 + OH$	$9.3 \times 10^{13} \exp(-10\ 250/T)$	300 - 2500	± 0.06	181	
6	$H_2O_2 + H \rightarrow H_2 + HO_2$	$1.7 \times 10^{12} \exp(-1000/T)$	300 - 800	± 0.3	209	
7	$H_2O_2 + H \rightarrow H_2O + OH$	No recommendation	-	-	229	
8	$O + H + M \rightarrow OH + M$	No recommendation	-	-	417	
9	$OH + H \rightarrow H_2 + O$	$6.3 \times 10^{9} T \exp(-3500/T)$	400 - 2000	± 0.1	69	c
10	$OH + H + M \rightarrow H_2O + M$	$1.6 \times 10^{23} T^{-2.0}$ ($M=H_2O$)	1000 - 5000	± 0.2	327	c
11	$O_2 + H \rightarrow O + OH$	$2.2 \times 10^{14} \exp(-8450/T)$	700 - 2500	± 0.1	9	
12	$O_2 + H + M \rightarrow HO_2 + M$	$1.8 \times 10^{18} \exp(-1000/T)$ (M=Ar)	300 - 2000	± 0.2	377	a
HO_2 radical reactions (see also reactions 2,3 and 4)						
13	$HO_2 + HO_2 \rightarrow H_2O_2 + O_2$	$(2.0 \pm 0.4) \times 10^{12}$	300	-	181	b
14	$H_2 + HO_2 \rightarrow H_2O_2 + H$	$7.3 \times 10^{11} \exp(-9400/T)$	300 - 800	± 0.3	217	c
15	$H_2O + HO_2 \rightarrow H_2O_2 + OH$	$1.8 \times 10^{13} \exp(-16\ 500/T)$	300 - 800	± 0.1	293	c
16	$OH + HO_2 \rightarrow H_2O + O_2$	No recommendation	-	-	251	
17	$OH + HO_2 \rightarrow H_2O_2 + O$	No recommendation	-	-	267	
18	$HO_2 + H \rightarrow O_2 + H + H$	$2.1 \times 10^{15} \exp(-23\ 000/T)$ (M=Ar)	300 - 2000	± 0.2	407	a
19	$HO_2 + H \rightarrow O + OH + H$	No recommendation	-	-	415	
O atom reactions (see also reaction 8)						
20	$H_2 + O \rightarrow H + OH$	$1.8 \times 10^{10} T \exp(-4480/T)$	400 - 2000	± 0.1	49	
21	$H_2O + O \rightarrow H + H + O_2$	No recommendation	-	-	129	
22	$H_2O + O \rightarrow OH + OH$	$6.8 \times 10^{13} \exp(-9240/T)$	300 - 2000	± 0.2	189	b
23	$H_2O_2 + O \rightarrow HO_2 + OH$	No recommendation	-	-	241	
24	$OH + O \rightarrow O_2 + H$	$(2.3 \pm 1.8) \times 10^{13}$	300	-	37	c
25	$OH + O + M \rightarrow HO_2 + M$	No recommendation	-	-	411	
OH radical reactions (see also reactions 9,10,24 and 25)						
26	$H_2 + OH \rightarrow H_2O + H$	$2.2 \times 10^{13} \exp(-2590/T)$	300 - 2500	± 0.06	77	
27	$H_2O + OH \rightarrow H_2O_2 + H$	No recommendation	-	-	237	
28	$H_2O_2 + OH \rightarrow H_2O + HO_2$	$1.0 \times 10^{13} \exp(-910/T)$	300 - 800	± 0.1	193	
29	$OH + OH \rightarrow H + HO_2$	$1.2 \times 10^{12} \exp(-70\ 200/T)$	290 - 800	± 0.3	157	b,d
30	$OH + OH \rightarrow O + H_2O$	No recommendation	-	-	461	
31	$OH + OH \rightarrow H_2O + O$	$6.3 \times 10^{12} \exp(-550/T)$	300 - 2000	± 0.2	119	b
32	$OH + OH + M \rightarrow H_2O_2 + M$	$9.1 \times 10^{30} \exp(2150/T)$ ($M=H_2$)	700 - 1500	± 0.1	357	b,c,e
33	$OH + H + H \rightarrow H + O + H$	No recommendation	-	-	485	
Molecular reactions						
34	$H_2 + O_2 \rightarrow H + HO_2$	$5.5 \times 10^{12} \exp(-29\ 100/T)$	290 - 800	± 0.4	169	d
35	$H_2 + O_2 \rightarrow OH + OH$	No recommendation	- -	-	131	
36	$H_2O + O_2 \rightarrow HO_2 + OH$	No recommendation	-	-	257	
37	$H_2O_2 + O_2 \rightarrow HO_2 + HO_2$	No recommendation	-	-	181	
38	$H_2 + H + M \rightarrow H + H + M$	$2.2 \times 10^{14} \exp(-48\ 380/T)$ (M=Ar)	2500 - 5000	± 0.3	309	a,b
39	$H_2O + H + M \rightarrow OH + H + M$	$2.2 \times 10^{16} \exp(-52\ 960/T)$ ($M=H_2O$)	2000 - 6000	± 0.2	349	a
40	$H_2O_2 + H \rightarrow OH + OH + M$	$1.2 \times 10^{17} \exp(-22\ 900/T)$ ($M=H_2$)	700 - 1500	± 0.1	361	b,a

a. Rate constants for other collision partners (M) are given in main text.
b. The rate constant for the elementary reaction $aA + bB + ... \rightarrow cC + dD + ...$ is defined by the relation
$$-\frac{1}{a}\frac{d[A]}{dt} = -\frac{1}{b}\frac{d[B]}{dt} = ... = k[A]^a[B]^b = \frac{1}{c}\frac{d[C]}{dt} = \frac{1}{d}\frac{d[D]}{dt} = ...$$
c. Rate constant k_f calculated from k_r using $k_f = k_r k_c$.
d. Not compatible with reverse rate constant, see text, p 65
e. Error in log k increases to ± 0.3 at 1500 K.

Table II Evaluated Kinetic Data For High Temperature Reactions: Homogeneous Gas Phase Reactions Of The $H_2 - N_2 - O_2$ System

	Reaction	Rate Constant k (cm-mol-s units)	Temperature Range (K)	Error in log k	Page	Notes
H ATOM REACTIONS						
1	$NNO + H \rightarrow N_2 + NO$	4.8×10^{12}	2000	± 0.2	399	
2	$NNO_2 + H \rightarrow N_2 + HO_2$	No recommendation	-	-	420	
3	$HNO_3 + H \rightarrow$ products	No recommendation	-	-	437	
4	$NH_2 + H + M \rightarrow NH_3 + M$	$4.8 \times 10^{14} \exp(+4330/T)$ (M=Ar)	1900 - 3900	± 0.3	471	a
5	$NH_3 + H \rightarrow N_2 + NH_2$	No recommendation	-	-	475	b
6	$NO + H + M \rightarrow HNO + M$	$5.4 \times 10^{15} \exp(+300/T)$ ($M=N_2$)	230 - 700	± 0.2	389	c
7	$NO_2 + H \rightarrow NO + OH$	$3.5 \times 10^{14} \exp(-740/T)$	298 - 630	± 0.2	445	d
8	$N_2H_4 + H \rightarrow N_2 + N_2H_3$	$1.3 \times 10^{13} \exp(-1260/T)$	250 - 500	± 0.3	519	
9	$N_2O + H \rightarrow N_2 + OH$	$7.6 \times 10^{13} \exp(-7600/T)$	700 - 2500	± 0.2	463	
HNO MOLECULE REACTIONS (see also reaction 1)						
10	$HNO + HNO \rightarrow N_2O + H_2O$	No recommendation	-	-	413	e
11	$HNO + H \rightarrow NO + H + H$	No recommendation	-	-	396	
12	$OH + HNO \rightarrow N_2O + HO$	3.6×10^{13}	2000	± 0.2	407	
HNO_2 MOLECULE REACTIONS (see also reaction 2)						
13	$O + HNO_2 \rightarrow HO_2 + OH$	No recommendation	-	-	420	
14	$OH + HNO_2 \rightarrow H_2O + NO_2$	No recommendation	-	-	420	
HNO_3 MOLECULE REACTIONS (see also reaction 3)						
15	$HNO_3 + M \rightarrow HO_2 + OH + M$	$1.6 \times 10^{15} \exp(-15\,400/T)$ (M=Ar)	800 - 1200	± 0.4	421	c
16	$O + HNO_3 \rightarrow HO_2 + OH$	No recommendation	-	-	437	
17	$OH + HNO_3 \rightarrow H_2O + NO_3$	8×10^{10}	300	± 0.3	439	
HO_2 RADICAL REACTION						
18	$NO + HO_2 \rightarrow NO_2 + OH$	No recommendation	-	-	386	
N_2 MOLECULE REACTIONS						
19	$NH_2 + N_2 \rightarrow NH_3 + H$	No recommendation	-	-	481	
20	$NO + N_2 \rightarrow NNO + N$	No recommendation	-	-	405	
21	$N_2H_3 + N_2 \rightarrow N_2H_4 + H$	No recommendation	-	-	525	
H_2O MOLECULE REACTIONS						
22	$NH_2 + H_2O \rightarrow NH_3 + OH$	No recommendation	-	-	495	
23	$NO + H_2O \rightarrow HNO + OH$	No recommendation	-	-	411	
24	$HO_2 + H_2O \rightarrow HNO_3 + OH$	No recommendation	-	-	444	
25	$N_2H_2 + H_2O \rightarrow N_2H_4 + O$	No recommendation	-	-	531	
26	$N_2O + H_2O \rightarrow HNO + HNO$	No recommendation	-	-	416	
N ATOM REACTIONS						
27	$N + N \rightarrow N_2 + h\nu$	No recommendation	-	-	55	
28	$N + N + M \rightarrow N_2 + M$	$3.0 \times 10^{14} \exp(+500/T)$ ($M=N_2$)	300 - 600	± 0.2	25	c,f
29	$NO + N \rightarrow N_2 + O$	1.6×10^{13}	300 - 5000	± 0.1	171	d
30	$NO_2 + N \rightarrow NO + NO$	No recommendation	-	-	265	
31	$O + N + M \rightarrow NO + M$	$6.4 \times 10^{16} T^{-0.5}$ ($M=N_2$)	100 - 400	± 0.2	187	c
32	$OH + N \rightarrow NO + H$	No recommendation	-	-	385	
33	$O_2 + N \rightarrow NO + O$	$6.4 \times 10^9 T \exp(-3150/T)$	300 - 3000	± 0.15	193	d
34	$O_3 + N \rightarrow NO + O_2$	No recommendation	-	-	386	

NH RADICAL REACTION															
35	NH_3	+	NH		=	NH_2	+	NH_2		No recommendation		-		-	166	
NH_2 RADICAL REACTIONS (see also reactions 4, 19 and 22)															
36	NH_2	+	NH_2		=	NH_3	+	NH		No recommendation		-		-	161	
37	NH_2	+	NH_2	+ M	=	N_2H_4		+ M		No recommendation		-		-	113	
38	N_2H_4	+	NH_2		=	NH_3	+	N_2H_3		No recommendation		-		-	133	
39	OH	+	NH_2		=	NH_3	+	O		No recommendation		-		-	489	b
NH_3 MOLECULE REACTIONS (see also reactions 5 and 35)															
40			NH_3	+ M	=	H	+	NH_2	+ M	$9.2 \times 10^{15} \exp(-42\,480/T)$	(M=Ar)	2000 - 3000		± 0.3	461	
41	N_2H_2	+	NH_2		=	N_2H_4	+	NH_2		No recommendation		-		-	138	
42	O	+	NH_3		=	NH_2	+	OH		$1.5 \times 10^{12} \exp(-1820/T)$		298 - 1000		± 0.2	483	
43	OH	+	NH_3		=	H_2O	+	NH_2		No recommendation		-		-	491	b,e
NO MOLECULE REACTIONS (see also reactions 6, 18, 20, 23 and 29)															
44			NO	+ M	=	N	+	O	+ M	No recommendation		-		-	99	
45	NO	+	NO		=	NO_2	+	N		No recommendation		-		-	269	
46	NO	+	NO		=	N_2	+	O_2		No recommendation		-		-	227	
47	NO	+	NO		=	N_2O	+	O		$1.3 \times 10^{12} \exp(-32\,180/T)$		1200 - 2000		± 0.3	249	f
48	NO	+	NO	+ O_2	=	NO_2	+	NO_2		$1.2 \times 10^{9} \exp(-530/T)$		273 - 660		± 0.2	285	f
49	NO_2	+	NO	+ O_2	=	NO_2	+	NO_3		$2.9 \times 10^{7} \exp(-400/T)$		300 - 500		± 0.4	245	
50	NO_3	+	NO		=	NO_2	+	NO_2		No recommendation		-		-	245	
51	O	+	NO		=	NO_2	+	hν		$4.4 \times 10^{7} (T/300)^{-2.3}$	(M=O_2)	220 - 3750		± 0.15	147	c,d
52	O	+	NO		=	O_2	+	N		$1.5 \times 10^{9} T \exp(-19\,500/T)$		1000 - 3000		± 0.15	211	c,d
53	O	+	NO	+ M	=	NO_2		+ M		$1.1 \times 10^{-15} \exp(+540/T)$	(M=O_2,Ar)	200 - 300		± 0.1	129	c
54	OH	+	NO		=	NO_2	+	H		No recommendation		-		-	458	
55	OH	+	NO	+ M	=	HNO_2		+ M		No recommendation		-		-	419	c
56	O_2	+	NO		=	NO_2	+	O		$1.7 \times 10^{12} \exp(-23\,400/T)$		300 - 550		± 0.1	286	c,g
57	O_2	+	NO	+ M	=	NO_3		+ M		No recommendation		-		-	283	
58	O_3	+	NO		=	NO_2	+	O_2		$8.9 \times 10^{11} \exp(-1220/T)$		200 - 350		± 0.2	359	h
NO_2 MOLECULE REACTIONS (see also reactions 7, 28 and 49)															
59			NO_2	+ M	=	NO	+	O	+ M	$1.1 \times 10^{16} \exp(-33\,000/T)$	(M=Ar)	1400 - 2400		± 0.1	119	c
60	NO_2	+	NO_2		=	NO	+	NO_3		No recommendation		-		-	257	
61	NO_2	+	NO_2		=	NO	+	NO	+ O_2	$2.3 \times 10^{12} \exp(-13\,500/T)$		600 - 2000		± 0.15	201	d,f
62	NO_2	+	NO_2	+ M	=	N_2O_4		+ M		$1.7 \times 10^{13} \exp(-460/T)$	(M=N_2)	250 - 350		± 0.15	321	a,f
63	NO_3	+	NO_2		=	NO	+	NO_2	+ O_2	$1.4 \times 10^{11} \exp(-1600/T)$		300 - 650		± 0.4	227	
64	NO_3	+	NO_2	+ M	=	N_2O_5		+ M		1.0×10^{12}	($M=N_2O_5$ + NO)	300		± 0.3	234	i,i
65	O	+	NO_2		=	NO	+	O_2		$1.0 \times 10^{13} \exp(-300/T)$		300 - 550		± 0.1	271	
66	O	+	NO_2	+ M	=	NO_3		+ M		2.3×10^{16}	(M=N_2)	295		± 0.4	375	i
67	OH	+	NO_2	+ M	=	HNO_3		+ M		5.0×10^{17}		300		± 0.25	427	c,e
68	O_2	+	NO_2		=	NO	+	O_3		No recommendation		-		-	367	
69	O_3	+	NO_2		=	NO_3	+	O_2		$5.9 \times 10^{12} \exp(-2500/T)$		255 - 350		± 0.3	369	
NO_3 RADICAL REACTIONS (see also reactions 24, 50, 63 and 64)															
70			NO_3	+ M	=	NO_2	+	O	+ M	No recommendation		-		-	381	
71	NO_3	+	NO_3		=	NO_2	+	NO_2	+ O_2	No recommendation		-		-	383	
72	O_2	+	NO_3		=	NO_2	+	O_3		No recommendation		-		-	373	
N_2 MOLECULE REACTIONS															
73			N_2	+ M	=	N	+	N	+ M	$3.7 \times 10^{21-1.6} \exp(-113\,200/T)$	(M=N_2)	6000 - 15 000		± 0.5	11	c
74	O	+	N_2		=	NO	+	N		$7.6 \times 10^{13} \exp(-38\,000/T)$		2000 - 5000		± 0.3	183	c
75	O	+	N_2	+ M	=	N_2O		+ M		$1.4 \times 10^{13} \exp(-16\,400/T)$	(M=Ar)	1300 - 2500		± 0.2	95	c,d,i
76	OH	+	N_2		=	N_2O	+	H		No recommendation		-		-	459	
77	O_2	+	N_2		=	NO	+	NO		No recommendation		-		-	221	
78	O_2	+	N_2		=	N_2O	+	O		$6.3 \times 10^{12} \exp(-35\,200/T)$		1700 - 2000		± 0.4	263	c

	Reaction	Rate Constant k (cm-mol-s units)	Temperature Range (K)	Error in log k	Page	Notes
N_2H_2 MOLECULE REACTION (see reaction 25)						
N_2H_3 RADICAL REACTIONS (see reactions 27 and 61)						
N_2H_4 MOLECULE REACTIONS (see also reactions 8 and 38)						
79	$N_2H_4 + M \rightarrow NH_2 + NH_2 + M$	$4 \times 10^{15} \exp(-20\,600/T)$ (M=Ar)	1250 - 1400	± 0.5	497	i
80 O + N_2H_4	$\rightarrow N_2O + N_2H_2$	No recommendation	-	-	527	
81 OH + N_2H_4	$\rightarrow$ products	No recommendation	-	-	532	
N_2O MOLECULE REACTIONS (see also reactions 9 and 26)						
82	$N_2O + M \rightarrow N_2 + O + M$	$5.0 \times 10^{14} \exp(-29\,000/T)$ (M=Ar)	1300 - 2500	± 0.2	69	c,i
83 O + N_2O	$\rightarrow NO + NO$	$1.0 \times 10^{14} \exp(-14\,100/T)$	1200 - 2000	± 0.3	235	f
84 O + N_2O	$\rightarrow N_2 + O_2$	$1.0 \times 10^{14} \exp(-14\,100/T)$	1200 - 2000	± 0.4	259	
N_2O_4 MOLECULE REACTION						
85	$N_2O_4 + M \rightarrow NO_2 + NO_2 + M$	$2.5 \times 10^{17} \exp(-5550/T)$ (M=N_2)	250 - 350	± 0.15	311	f
N_2O_5 MOLECULE REACTION						
86	$N_2O_5 + M \rightarrow NO_2 + NO_3 + M$	$1.3 \times 10^{19} \exp(-9700/T)$ (M=N_2O_5 + NO)	300 - 340	± 0.3	325	i
O ATOM REACTIONS (see reactions 13, 16, 31, 42, 51-53, 65, 66, 74, 75, 80, 83 and 84)						
OH RADICAL REACTIONS (see reactions 12, 14, 17, 32, 39, 43, 54, 55, 67, 76 and 81)						
O_2 MOLECULE REACTIONS (see reactions 33, 48, 49, 56, 57, 68, 72, 77 and 78)						
O_3 MOLECULE REACTIONS (see reactions 34, 58 and 69)						

a. Rate constant k_f calculated from k_r using $k_f = k_r K_c$.

b. The reaction may give alternative products (see Discussion).

c. Relative efficiencies of other collision partners (M) are discussed in the main text.

d. Error in log k is greater at the upper end of the temperature range.

e. See note added in proof to the main text.

f. The rate constant k of the elementary reaction $aA + bB + \cdots \rightarrow aM + gG \cdots$ is defined by the relation

$$-\frac{1}{a}\frac{d[A]}{dt} = -\frac{1}{b}\frac{d[B]}{dt} = \cdots = k[A]^a[B]^b \cdots = \frac{1}{m}\frac{d[M]}{dt} = \frac{1}{n}\frac{d[N]}{dt} = \cdots$$

g. Alternative reaction is important (see Discussion).

h. The emission reaction is discussed on p.365.

i. The high pressure limiting rate constant k^∞ is given in the main text.